



2017

ROLE OF SKELETAL PARACRINE SIGNALS IN THE PROLIFERATION AND CHONDROGENIC DIFFERENTIATION OF INTERZONE CELLS

Parvathy Thampi

University of Kentucky, parvathy.thampi@uky.edu

Digital Object Identifier: <https://doi.org/10.13023/ETD.2017.029>

[Right click to open a feedback form in a new tab to let us know how this document benefits you.](#)

Recommended Citation

Thampi, Parvathy, "ROLE OF SKELETAL PARACRINE SIGNALS IN THE PROLIFERATION AND CHONDROGENIC DIFFERENTIATION OF INTERZONE CELLS" (2017). *Theses and Dissertations--Veterinary Science*. 27.

https://uknowledge.uky.edu/gluck_etds/27

This Doctoral Dissertation is brought to you for free and open access by the Veterinary Science at UKnowledge. It has been accepted for inclusion in Theses and Dissertations--Veterinary Science by an authorized administrator of UKnowledge. For more information, please contact UKnowledge@lsv.uky.edu.

STUDENT AGREEMENT:

I represent that my thesis or dissertation and abstract are my original work. Proper attribution has been given to all outside sources. I understand that I am solely responsible for obtaining any needed copyright permissions. I have obtained needed written permission statement(s) from the owner(s) of each third-party copyrighted matter to be included in my work, allowing electronic distribution (if such use is not permitted by the fair use doctrine) which will be submitted to UKnowledge as Additional File.

I hereby grant to The University of Kentucky and its agents the irrevocable, non-exclusive, and royalty-free license to archive and make accessible my work in whole or in part in all forms of media, now or hereafter known. I agree that the document mentioned above may be made available immediately for worldwide access unless an embargo applies.

I retain all other ownership rights to the copyright of my work. I also retain the right to use in future works (such as articles or books) all or part of my work. I understand that I am free to register the copyright to my work.

REVIEW, APPROVAL AND ACCEPTANCE

The document mentioned above has been reviewed and accepted by the student's advisor, on behalf of the advisory committee, and by the Director of Graduate Studies (DGS), on behalf of the program; we verify that this is the final, approved version of the student's thesis including all changes required by the advisory committee. The undersigned agree to abide by the statements above.

Parvathy Thampi, Student

Dr. James N. MacLeod, Major Professor

Dr. Daniel K. Howe, Director of Graduate Studies

ROLE OF SKELETAL PARACRINE SIGNALS IN THE PROLIFERATION AND CHONDROGENIC
DIFFERENTIATION OF INTERZONE CELLS

DISSERTATION

A dissertation submitted in partial fulfillment of the
requirements for the degree of Doctor of Philosophy in the
College of Agriculture, Food and Environment
at the University of Kentucky

By

Parvathy Thampi
Lexington, Kentucky

Director: Dr. James N. MacLeod, Professor of Veterinary Science
Lexington, Kentucky

2016

Copyright ©Parvathy Thampi 2016

ABSTRACT OF DISSERTATION

ROLE OF SKELETAL PARACRINE SIGNALS IN THE PROLIFERATION AND CHONDROGENIC DIFFERENTIATION OF INTERZONE CELLS

Articular cartilage in mammals has a limited intrinsic capacity to repair structural injuries and defects, a fact that contributes to the chronic and progressive nature of osteoarthritis. Current treatment modalities do not enable articular cartilage to achieve a complete and permanent restoration of normal structure and function with large or partial thickness lesions. In contrast to mammals, Mexican axolotl salamanders (*Ambystoma mexicanum*) have demonstrated the remarkable ability to spontaneously and completely repair even large joint cartilage lesions, an intrinsic healing process that involves interzone cells in the intraarticular space. Further, when interzone tissue is transplanted into critical sized diaphyseal defects, it forms an entirely new diarthrodial joint in these amphibians, demonstrating a multi-differentiation potential. Cellular and molecular mechanisms of this repair process, however, remain unclear. This thesis examined whether paracrine signals are an important variable in the interaction between interzone cells and the skeletal microenvironment. *In vivo* experiments in axolotl salamanders compared the outcomes of interzone tissue transplants placed in either a skeletal or non-skeletal site within the same individual. The hypothesis tested was that the interzone-mediated repair of skeletal defects is regulated by mechanisms that are localized to the skeletal microenvironment. Interzone cell proliferation and differentiation was only observed in skeletal transplant sites, suggesting that local signals from the skeletal microenvironment played a vital role in the interzone-mediated repair process. In a second series of experiments, paracrine regulation of the proliferation and chondrogenic differentiation of equine interzone cells was evaluated in an *in vitro* co-culture system. The results of cellular proliferation studies indicated a mitogenic effect of skeletal paracrine signals on interzone cells. Expression of cartilage

biomarker genes, evaluated at both RNA and protein levels, were used to assess chondrogenic differentiation. The *in vitro* findings suggested that paracrine signals may have a role in the chondrogenic differentiation of interzone cells, but were not compelling. The response may have been limited by levels of paracrine factor accumulation achieved in the co-culture system used for these experiments. Taken together, however, the data support a model that paracrine factors from skeletal tissues are important regulators of interzone cell proliferation and differentiation. This knowledge advances the assessment of interzone cells as a potential cell-based therapy for the repair of articular cartilage injuries.

KEYWORDS: Articular cartilage, Interzone, Paracrine, Equine, Axolotl salamander

Parvathy Thampi

Student's signature

02/17/2017

Date

ROLE OF SKELETAL PARACRINE SIGNALS IN THE PROLIFERATION AND CHONDROGENIC
DIFFERENTIATION OF INTERZONE CELLS

By

Parvathy Thampi

Dr. James N. MacLeod

Director of Dissertation

Dr. Daniel K. Howe

Director of Graduate Studies

02/17/2017

Date

ACKNOWLEDGEMENTS

Undertaking this PhD has been a life-changing experience in all aspects and would not have been possible without the support and guidance from many people. First, a big thanks to my advisor, Dr. James MacLeod for giving me this opportunity and for his encouragement and guidance throughout this memorable journey. I am especially grateful to him for challenging me to go beyond my comfort zone which has driven me to be a better person on both professional and personal levels.

I would also like to thank the members of my dissertation committee. Drs. Nielsen and Howe, I truly appreciate your enthusiasm and willingness to help at each stage of this research project. I am grateful to Dr. Esser for her valuable insights that have guided and challenged me throughout. I greatly appreciate the friendship and assistance of past and present members of the MacLeod lab, particularly Drs. Emma Adam and Jennifer Janes, for all the good memories. Thank you for keeping a sense of humor when I lost mine. I would also like to thank Ellen Wiegand, Rachel Lowney, Dr. Jasmin Bagge, ChanHee Mok, Dr. Scotty DePriest, and Dr. Rashmi Dubey for their immense support and assistance in this research. Thank you to Dr. Fallon Segarra – I really enjoyed the opportunity to work with and learn from you.

I am immensely grateful for the help and support of the faculty, office staff, librarians and students at the Gluck Equine Research Center for their willingness to help whenever I needed it and making me feel at home. I also wish to thank the faculty and staff at the

Veterinary Diagnostic lab in particular Jamie Howard for her expertise and assistance with the histological analyses. I am extremely grateful to the staff at the University Farm, especially Kevin Gallagher and Chad Tucker for their help with the tissue collections. I graciously acknowledge the assistance of Dr. Constance Wood, Sarah Witt Janse and Eric Roemmele in the Department of Statistics in data analysis and their patience with me. I appreciate the financial support of the Geoffrey C. Hughes Foundation and other funding sources that made this research possible.

I thank my lucky stars to have an amazing family, whose support of me throughout this journey is hard to measure. My heartfelt thanks to my parents and in-laws for helping me in whatever way they could. Words cannot express how grateful I am to have these two people in my life – Mahesh, my husband and best friend, without whom I could not have done any of this and Nanda for being the incredible gift that you are to me. I love you both dearly.

TABLE OF CONTENTS

Acknowledgements.....	iii
List of Tables	vii
List of Figures	viii
Chapter 1: Background and literature review	1
Introduction	1
Articular cartilage – composition and ultrastructure	2
Pathology and Therapy	5
Cell signaling in cartilage development	7
Interzone cells in cartilage repair	12
Important knowledge gaps and questions	13
Dissertation overview	14
Chapter 2: Effect of the skeletal microenvironment on interzone mediated repair of skeletal defects	15
Introduction	15
Materials and methods	17
Animals	17
Surgical procedure.....	18
Sample collection and processing	19
Histology and immunohistochemistry	20
Results	21
Skeletal site interzone transplants	21
Non skeletal site interzone transplants.....	25
Discussion.....	25
Chapter 3: Effect of skeletal paracrine signals on the proliferation of interzone cells	29
Introduction	29
Materials and methods	31
Isolation and culture of cells	31
Conditioned medium preparation	36
Co-culture	37
Background proliferation.....	37
Differential production of mitogens.....	38
Differential cellular response to the same level of mitogenic stimuli.....	40
Assessment of cell viability.....	41

Assessment of cell proliferation	42
Statistical analysis	43
Results	43
Background proliferation	43
Differential production of mitogens	45
Differential cellular response to the same level of mitogenic stimuli	51
Discussion	52
Chapter 4: Effect of skeletal paracrine signals on the chondrogenic differentiation of interzone cells	57
Introduction	57
Materials and methods	60
Isolation and culture of cells	60
Co-culture	60
Conditioned medium and Controls	62
Histological examination	63
Proteoglycan staining and quantification	64
Gene expression analysis	65
Statistical analysis.....	67
Results	68
Controls	68
Macroscopic assessment of pellets.....	69
Morphological examination of pellets	69
Proteoglycan staining and quantification	72
Gene expression analysis	75
Discussion	80
Chapter 5: Reflections and looking ahead to future studies	84
Reflections	84
Future studies.....	88
Appendix: List of abbreviations	94
References	95
Vita	104

LIST OF TABLES

Table 2.1: Experimental samples for skeletal and non-skeletal interzone Transplantation study	22
Table 3.1: Percent proliferation values in experimental and control groups (pilot study)	39
Table 3.2: Differential production of mitogens: Description of biological and technical replicates	39
Table 3.3: Differential cellular response to the same level of mitogenic stimuli: Description of biological and technical replicates	41
Table 3.4: Percent proliferation values in experimental and control groups.....	48
Table 3.5: Percent viability values in experimental and control groups	51
Table 4.1: Description of biological and technical replicates for coculture	61
Table 4.2: Composition of defined negative control medium.....	63
Table 4.3: Description of Taqman primer probe sets.....	67
Table 4.4: <i>ACAN</i> p-value table	77
Table 4.5: <i>COL2A1</i> p-value table	78
Table 4.6: <i>COL1A1</i> p-value table	80

LIST OF FIGURES

Figure 1.1: Zonal organization of articular cartilage..... 5

Figure 1.2: Histological appearance of equine interzone 10

Figure 1.3: Model for articular cartilage and joint development 11

Figure 1.4: Interzone mediated repair of critical sized bone defects..... 13

Figure 2.1: Skeletal and non-skeletal sites for interzone transplantation 19

Figure 2.2: Tissue response in the skeletal site to interzone transplants (H&E) 23

Figure 2.3: Tissue response in the skeletal site to interzone transplants (Safranin-O) ... 23

Figure 2.4: Tissue response in the non-skeletal site to interzone transplants – GFP immunohistochemistry..... 24

Figure 2.5: Tissue response in the non-skeletal site to interzone transplants..... 25

Figure 3.1: Time course study to identify point of minimal background proliferation for interzone cells. 44

Figure 3.2: Image series of change in proliferation of interzone cells in response to control and fetal conditioned media 46

Figure 3.3: Line graphs of percent change in proliferation of interzone cells in response to control and fetal conditioned media..... 47

Figure 3.4: Line graphs of percent change in proliferation of interzone cells in response to control and adult conditioned media 47

Figure 3.5: Image series of change in viability of interzone cells in response to control and fetal conditioned media..... 49

Figure 3.6: Line graphs of percent change in viability of interzone cells in response to control and fetal conditioned media 50

Figure 3.7: Line graphs of percent change in viability of interzone cells in response to control and adult conditioned media	50
Figure 3.8: Box and whiskers plot of percent change in proliferation of all cell lines in response to fetal anlage chondrocyte conditioned medium	52
Figure 4.1: Histology of cell pellets in defined negative control media (Safranin-O)	68
Figure 4.2: Gross image of pellets in conditioned and control media.....	69
Figure 4.3: Histology of cell pellets in control media (H&E)	72
Figure 4.4: Histology of cell pellets in conditioned media (H&E)	72
Figure 4.5: Histology of cell pellets in control media (Safranin O)	74
Figure 4.6: Histology of cell pellets in conditioned media (Safranin O)	74
Figure 4.7: Semi-quantitative evaluation of proteoglycan staining	75
Figure 4.8: Box and whiskers plot of <i>ACAN</i> relative expression values.....	76
Figure 4.9: Box and whiskers plot of <i>COL2A1</i> relative expression values	78
Figure 4.10: Box and whiskers plot of <i>COL1A1</i> relative expression values	79

Chapter 1

Background and literature review

Introduction

Articular cartilage covers adjoining bone surfaces in healthy synovial joints. It is an aneural, alymphatic, and avascular tissue composed of a single cell type – articular chondrocytes. The cells synthesize and maintain a collagen- and proteoglycan-rich matrix that is uniquely adapted to resist compressive and shear forces, absorb and redistribute loads, and enable near frictionless movement of the articulating surfaces [1]. However, not all of the characteristics of articular cartilage are positive. One major problem, also seen in other highly specialized tissues, is a severely limited ability to repair or regenerate after structural injury. Whether the lesion is due to physical trauma or disease, articular cartilage structural defects often progress over time [1-10]. Deep cartilage defects that extend into the subchondral bone gain access to mesenchymal cells and a blood supply in the bone marrow facilitating some level of repair. However, the fibrocartilage repair tissue that develops in mammals with full thickness lesions has inferior biochemical and biomechanical characteristics compared to normal hyaline cartilage, compromising long-term function and structural integrity. Chondral defects that remain superficial have even less spontaneous healing capacity, because the intact calcified cartilage layer and subchondral bone acts as a physical barrier to a blood supply and the bone marrow stem cells [1, 8]. For this reason, a fairly common surgical strategy offered to patients with joint surface chondral defects is to extend the structural lesion and penetrate the subchondral bone plate with the goal of

enhancing formation of fibrocartilage repair tissue and articular resurfacing. Unfortunately, the fibrocartilage that forms following surgical intervention often fails over time for the same reasons as the fibrocartilage that develops spontaneously in full thickness articular lesions. As such, these approaches have limited success long-term, especially with lesions of significant dimension or in patients that try to return to a high level of physical activity [4, 11]. In most cases, osteoarthritis and the progressive loss of joint function is the eventual clinical outcome.

The limitations of existing medical and surgical options for articular cartilage repair have led to a search for better therapies in the field of tissue engineering. Novel strategies are aimed at restoring hyaline cartilage by implanting cells co-delivered with growth factors packaged in appropriate biomaterial scaffolds to replicate the native cartilage tissue [8, 12-14]. While some progress has been made in exploring each of the above components, the ultimate therapeutic goal of generating a viable, functional, and durable repair tissue that is biomechanically and structurally identical to normal articular cartilage, remains elusive. A brief overview of the complex architecture of articular cartilage will facilitate an understanding of the challenges associated with restoring the tissue's structure and function after injury.

Articular cartilage – composition and ultrastructure

Articular cartilage is a highly specialized tissue with unique biomechanical properties that are a function of its ultrastructure composition and complex organization. Chondrocytes are the resident cell types in articular cartilage. They

synthesize, maintain, and remodel the extracellular matrix (ECM), but comprise less than 2% of the overall tissue volume. They exist in a physiological state of hypoxia due to the absence of localized vascularization, and have a low turnover rate. However, their viability and unique functional properties are supported by local paracrine signals and biomechanical forces, both of which are crucial to maintaining cartilage health [1, 15-18].

Major molecular components of cartilaginous tissues include water, collagen, and proteoglycans, but there are also many non-collagenous proteins and glycoproteins present in minor quantities [19]. Collagens constitute about 60% of the dry weight of cartilage of which type II collagen represents 90-95% and is considered a traditional biomarker for this tissue. Other collagen types that are present include V, VI, IX and XII. However, they represent a much smaller percentage of the total collagen content of the matrix [1, 15, 16, 19, 20].

Proteoglycans are the second largest group of macromolecules in the ECM and account for 10-15% of its wet weight. They are heavily glycosylated proteins composed of about 95% polysaccharide and 5% protein. Extensive sulfation of the proteoglycan side chains results in a very high electrostatic negative charge density. This causes the proteoglycans to repel each other, but also draws a lot of water molecules into the matrix structure. Interaction of this fluid phase with the ECM components endows cartilage with the ability to resist compressive forces and facilitates the delivery of nutrients and oxygen to this avascular tissue. Aggrecan is the predominant proteoglycan of articular cartilage and represents a second widely accepted biomarker

[20, 21]. The composition and organization of chondrocytes and the ECM, together with the fluid dynamics, are central to the tissue's viscoelastic properties and differs across the thickness of articular cartilage in direct relation to localized biomechanical forces. Broadly, cartilage can be functionally and structurally divided into four zones as illustrated in Figure 1.1. The superficial zone forms the smooth gliding articulating surface that resists shear forces. It is composed of elongated chondrocytes and densely packed, highly ordered collagen fibers arranged parallel to the articular surface. The middle zone acts as a transition between the superficial and deep zone. Here, the chondrocytes are more rounded, collagen fibrils are thicker, loosely packed and aligned obliquely to the surface. In the deep zone, chondrocytes are arranged in a columnar fashion parallel to the thick collagen fibrils which are oriented perpendicular to the subchondral bone to aid in resisting compressive forces. The tidemark is a histological feature separating the deep zone from the calcified cartilage which anchors the cartilage to the subchondral bone. From the superficial to the deep zone, the water content decreases, while the proteoglycan content and diameter of collagen fibers increases. This unique and interdependent organization gives cartilage its superior loading and force dissipation properties, while minimizing the coefficient of friction during movement – all characteristics that are particularly challenging to restore if the tissue is injured and structurally damaged. Injury to any part can impair the biomechanics of the entire complex and lead to degeneration [1, 16, 22].

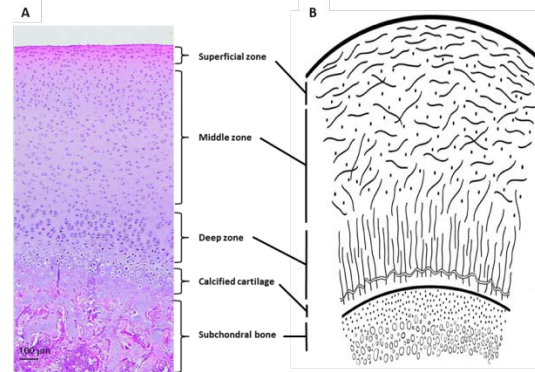


Figure 1.1: Zonal organization of articular cartilage - Histological appearance of articular chondrocytes in a porcine ilium (11 weeks of age) stained with Hematoxylin and Eosin (A) and schematic representation of the distribution of collagen fibers (B) across the thickness of articular cartilage. (Adapted with permission from Shapiro et.al., 2014 and Alford and Cole, 2005).

Pathology and Therapy

Trauma and structural damage to articular cartilage can be the result of normal wear and tear from repeated cycles of loading, acute joint injuries, inflammation, toxic insults to chondrocytes, joint infection, and other causes. Due to the poor intrinsic ability of cartilage to heal, it is common for lesions to progress over time that lead eventually to an irreversible loss of structure and function. This disease process is called osteoarthritis or degenerative joint disease and is a major cause of joint pain and disability affecting an estimated 27 million adults in the United States [12, 23-26]. It is also a significant clinical problem in horses, accounting for up to 60% of lameness and joint pain [27, 28].

Treatment strategies for articular cartilage injuries can be broadly categorized as palliative (medications to relieve joint inflammation and pain, surgical debridement of damaged cartilage, and lavage), reparative (marrow stimulation techniques), or restorative (osteochondral grafting, autologous chondrocyte implantation, other tissue engineering approaches) [1, 8-10]. Recently, restorative approaches have been a focus

of more research efforts, and in some cases achieve a considerable reduction of clinical symptoms [9, 29]. These include reconstruction of the injured articular cartilage with mature intact cartilage along with the underlying subchondral bone (osteochondral grafts) or the *in vitro* expansion of autologous chondrocytes from the patient for implantation at the lesion site (autologous chondrocyte implantation; ACI), a technique first described for humans in 1994 [30]. While successful repair of partial and full thickness defects in humans [9] and horses [31, 32] have been reported with ACI, the need to expand chondrocytes *in vitro* to produce sufficient cell numbers for the procedure and two consecutive surgical interventions has proven to be a disadvantage. An improvement on this technique, matrix-assisted autologous chondrocyte implantation (MACI), involves the use of engineered scaffolds for delivery of chondrocytes into the lesion to improve retention of the transplanted cells [33-37]. However, these chondrocyte-based strategies have been hampered by challenges in achieving a high cell density and maintaining the differentiated state of chondrocytes in culture – problems that have motivated additional research in the field of tissue engineering for improved strategies of cartilage repair.

Key components of tissue engineering are the cells, tissue scaffolds, and biologically active stimulatory molecules. The objective is for the components to work together in a coordinated fashion to achieve successful repair. Numerous natural and synthetic biomaterials have been explored for their ability to mimic the properties of native articular cartilage, including but not limited to, hyaluronan, polylactides, alginate, agarose, and chitosan [12, 38, 39]. While novel biomaterials [3, 40] have been

developed and tested for these attributes, engineering a biocompatible tissue scaffold that achieves the full restoration of articular cartilage has not been accomplished. Considering cells, the optimal source for engineering articular cartilage should be relatively easy to isolate and expand. The cells must retain or be able to achieve the phenotype of articular chondrocytes. The cells or engineered construct must be biologically compatible with the host tissue. In addition to primary chondrocytes, chondroprogenitor cells have also been evaluated. These include cells derived from bone marrow, fat, synovial membrane, placenta, and other tissues [41-46]. However, research results are highly variable and important cell biology parameters of true articular chondrocytes continue to be elucidated [47-49]. The commitment of chondroprogenitor cells to an articular cartilage phenotype is a complex and dynamic process that remains an area of active research [50]. On several levels, therefore, major challenges for widespread clinical applications remain [12].

Cell signaling in cartilage development

Recent studies advocate that the key to engineering a functional and long-lasting articular surface lies in understanding the process of articular cartilage and joint development with the aim of recapitulating the developmental blueprints during repair [3, 12, 51, 52]. Cartilage development occurs during embryogenesis and is a multifaceted and highly organized process [6, 53]. It begins with the formation of precartilaginous condensations of undifferentiated mesenchymal cells termed *anlage* [54]. This process involves cell-cell and cell-matrix interactions which lead to expression

of adhesion molecules such as N-cadherin, Tenascin-C, and fibronectin that facilitate cell aggregation and increased cell packing. This process is orchestrated by a SRY box 9 (*SOX9*) driven transforming growth factor- β (*TGF β*), *WNT*/Beta-catenin signaling pathway. Within the cartilage anlagen, the precartilaginous mesenchymal cells undergo differentiation into chondrocytes, a process that is governed by the *SOX* triad (*SOX 5, 6* and *9*) [55]. This is accompanied by the expression of cartilage specific collagen types II and IX, and aggrecan [56]. The anlage chondrocytes then initiate the processes of hypertrophic differentiation and matrix mineralization starting at primary centers of ossification and later secondary centers of ossification. Terminal hypertrophic chondrocytes die by apoptotic mechanisms in conjunction with neovascularization of the cartilage and the arrival of bone progenitor cells. In mammals, the process of endochondral ossification continues through gestation and the early postnatal period to eventually fully replace cartilage anlagen with bone [57]. The processes of chondrogenesis are regulated by a number of signaling molecules including *TGF β* , bone morphogenetic proteins (*BMPs*), insulin-like growth factors (*IGFs*), fibroblast growth factors (*FGFs*), and *Notch*, which interact with each other to coordinate cell proliferation, differentiation, migration, and synthesis of the extracellular matrix [12]. Several of these factors have been evaluated as chondrogenic inducers *in vitro* (*TGF β 1-3*, *BMP2*, and *IGF1*), while others represent interesting candidates (*WNT*, *Notch*, and *FGF*) based on their role in chondrogenesis *in vivo*. *TGF β* , *BMP7*, and Growth and Differentiation factor 5 (*GDF5*) are important in stimulating chondrogenesis and matrix synthesis while inhibiting cartilage degradation both *in vivo* and *in vitro* [58-65]. In

addition, they can potentiate the mitogenic effects of other growth factors such as *IGF1*, *IGF3*, and basic *FGF* [3, 66-68]. *IGFs* have been demonstrated to be important in proteoglycan production and homeostasis. Used *in vitro*, they promote the stabilization of the chondrogenic phenotype. *WNT* proteins have critical but diverse roles in articular cartilage development which is regulated either by non-canonical or β -catenin mediated canonical signaling pathways [69, 70]. *Notch* signaling plays an important role in postnatal articular cartilage maintenance. Removal of *Notch* signals in postnatal cartilage leads to degeneration and signs of early osteoarthritis [71, 72]. Members of the *FGF* family have been shown to be crucial in patterning of the structures in the developing limb. *FGF2* stimulates cell proliferation and differentiation depending on the time of exposure. *FGF9* and *FGF18* augment cartilage matrix synthesis and inhibit hypertrophic differentiation [73].

Articular chondrocytes, which line the synovial joints, have a separate embryonic origin from the anlage chondrocytes [49, 50]. Joint formation begins in the limb bud early in development, occurring between 35 to 55 days of gestation in equine fetuses [74]. The appearance of interzone cells demarcates the presumptive joint sites within the uninterrupted mesenchymal condensations [7, 49, 75]. The interzone can be appreciated in mammals only *in utero* during early development prior to the process of cavitation that produces the joint space. Figure 1.2 shows the histological appearance of equine interzone tissue in fetal fetlock (metacarpophalangeal) and carpal joints.

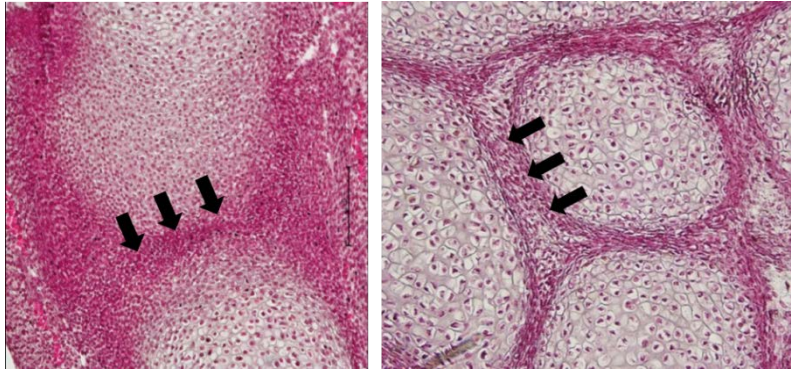


Figure 1.2 showing the interzone (arrows) in equine fetal joints – developing fetlock (A) and cuboidal bones of the carpus (B) stained with Hematoxylin and Eosin. Both images are at 10x (objective lens) magnification.

Much progress has been made in the last few years in understanding the origin, fate, and possible function of interzone cells in joint morphogenesis. Genetic cell lineage tracing studies in mice have demonstrated that interzone cells constitute a progenitor cell cohort giving rise to joint tissues including articular cartilage, synovial membrane, and ligaments [48-50]. Further, these authors isolated interzone cells in culture based on the expression of putative biomarkers such as *GDF5*, *WNT9A*, *CD44*, and *GLI-3* and found that they acquired a round architecture and expressed markers of the chondrocyte phenotype such as type IX collagen and aggrecan. Similar lineage tracing studies using matrilin-1, a molecule expressed by all chondrocytes except articular chondrocytes, suggested that articular cartilage development involves the initial interzone mesenchymal population with concurrent cell migration from flanking regions of the interzone [76]. *In ovo* cellular labeling of chick limbs have shown similar recruitment and migration of cells into the interzone domain from peri-joint sites [49]. More recent lineage tracing experiments provide a better understanding of the role of interzone cells in joint development summarized in recent reviews [47, 50] and

illustrated in Figure 1.3. As per this model, *GDF5* expressing interzone cells constitute the progenitor cell cohort for joint structures including articular cartilage. These *GDF5* positive cells with a history of *SOX9*/type II collagen expression, but negative for matrillin-1, give rise to articular chondrocytes. In addition to the *in situ* based studies using candidate genes summarized above, an unbiased genome-wide expression analysis identified genes differentially expressed in the intermediate and outer layers of the interzone, dissected by laser capture microdissection. The authors reached the conclusion that the cells of the intermediate layer of the interzone form the articular tissues including cartilage [77]. A study by Schwartz et. al. suggests an influx model of cell specification where interzone cells are continuously recruited into the domain of *GDF5* expression and differentially contribute to the development of joint tissues [78]. Taken together, these studies promote the view that interzone cells are the progenitor cells for articular cartilage.

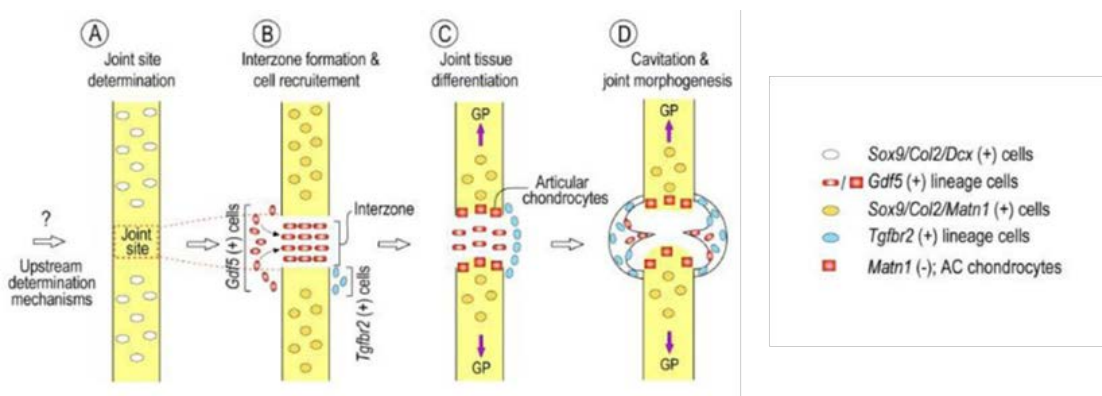


Figure 1.3 depicting the current model for articular cartilage and joint development. During early developmental stages, unknown upstream mechanisms demarcate the presumptive joint site (A) where the initial population of *GDF5* expressing interzone cells appears (B). Along with *TGFBR2* expressing cells from the peri-joint sites, the interzone cells give rise to the *Matrillin*-negative articular chondrocytes and other joint structures (C) and (D). Note that the steps presented as distinct for illustration purposes may be overlapping processes in the biological system (Adapted with permission from Decker et. al., 2014).

Interzone cells in cartilage repair

Experiments from our laboratory have demonstrated a role of interzone cells in the complete and spontaneous repair of large articular cartilage defects in adult axolotl salamanders (*Ambystoma mexicanum*) [79]. The importance of interzone was further emphasized by the failure of joint lesion repair with subsequent joint arthrodesis following surgical ablation of the interzone (unpublished observation). Furthermore, when transplanted into a critical sized bone defect (CSD) in the tibia diaphysis, the defect closed, but with the formation of a new diarthrodial joint rather than diaphyseal bone [80]. The repair tissue that bridges the bone gap is a patterned structure resembling an intact joint with interzone positioned between two cartilaginous layers that are morphologically similar to epiphyseal/articular and metaphyseal chondrocytes. Tracking the interzone cells using green fluorescent protein (GFP) immunostaining revealed that the cells within the accessory joint originate from the transplanted interzone cells as illustrated in Figure 1.4. Interestingly, although the interzone transplant was placed in a random orientation in the skeletal defect, the accessory joints that formed in multiple biological replicates followed correct spatial patterning (discussed in more detail in Chapter 2). These observations suggest that interzone cells play a critical role in the repair of skeletal defects, a process that is likely mediated and organized by intrinsic and extrinsic signaling cues.

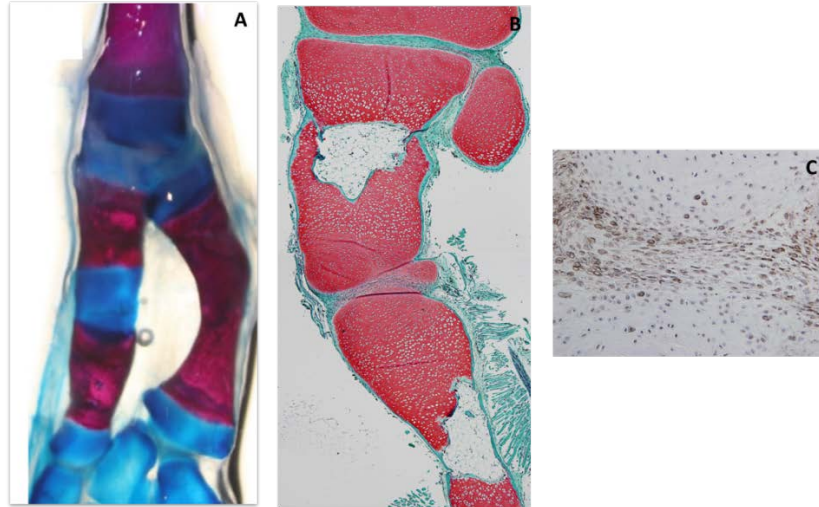


Figure 1.4 showing the repair of the critical sized defect in the tibia with formation of a cartilage-like tissue (A) which histologically exhibits the anatomical organization of an intact joint with an interzone between two cartilaginous columns (B). Cells within the repair tissue appear to be derived from the transplanted interzone cells based on GFP immunostaining (C) (Adapted with permission from Cosden-Decker et. al., 2012). A and B are at 4X and C is at 40x (objective lens) magnification.

Important knowledge gaps and questions

Studies outlined above have demonstrated a central role for interzone cells in diarthrodial joint development, a differentiation commitment that the axolotl studies suggest might also facilitate cell-based therapies to repair articular cartilage lesions. However, many questions remain with regard to interzone cells and cartilage repair. Are interzone cells autonomously regulated, directing their own proliferation and differentiation to form articular cartilage and other synovial joint tissues? Or, are interzone cells regulated by neighboring cells, mechanisms that might be niche-dependent and sensitive to different tissue microenvironments? What are the specific signaling pathways that regulate the interzone-mediated cartilage repair process and *de novo* new joint formation observed in axolotl salamanders? It is possible that many of the signaling molecules that orchestrate synovial joint development during embryogenesis are retained in adult tissues or possibly re-expressed following tissue

injury. If so, adult tissues might have the potential to regulate interzone cell proliferation, migration, and differentiation in a repair context. GFP cell tracing data indicated that interzone tissue transplanted into the diaphyseal bone defect of axolotl salamanders remained localized. Therefore, the major focus of this dissertation is on the proliferation and chondrogenic differentiation of interzone cells in response to environmental stimuli. Unfortunately, further studies in the axolotl model to explore these interactions are significantly impaired by the absence of a reference genome or the ability to culture amphibian cells *in vitro*. For these reasons, tissue culture experiments were conducted with fetal and adult equine cells.

Dissertation overview

The studies presented here are designed to further investigate the biology of interzone cells in a tissue repair context, generating knowledge relevant to emergent cell-based therapies for articular cartilage lesions. Experiments reported in Chapter 2 test the hypothesis that the repair of skeletal defects by interzone cells is regulated by mechanisms that are localized to the microenvironment of skeletal tissues. Chapters 3 and 4 describe experiments conducted with primary equine cell lines, both fetal and adult. They test the hypothesis that paracrine signals derived from the skeletal microenvironment induce the proliferation and chondrogenic differentiation of interzone cells in culture. Finally, chapter 5 will reflect on work performed so far and propose directions for further studies to understand the role of interzone cells in cartilage repair.

Chapter 2

Effect of the skeletal microenvironment on interzone mediated repair of skeletal defects

Introduction

Articular cartilage is a highly specialized tissue that covers adjoining bone surfaces in synovial joints, redistributing the mechanical forces that occur during skeletal loading and facilitating low-friction movement [10, 15, 17, 81]. Cartilage is unique in its matrix structure and biomechanical properties, but like several other highly differentiated tissues has poor regenerative capabilities in mammals after structural injuries. A limited amount of repair can occur in articular cartilage lesions that extend into the subchondral bone (full thickness defects), wherein mesenchymal cells from the bone marrow migrate into the lesion and lay down a fibrocartilaginous repair tissue. However, this repair tissue is structurally and functionally inferior to normal articular cartilage and has low durability over longer terms. Somewhat paradoxically, the repair capacity is even less for partial thickness defects. Without the extension of a lesion into the subchondral bone, marrow-derived mesenchymal cells are blocked from participating in the repair process [8, 10, 11]. There are some data to suggest that repair of partial thickness lesions is possible in fetal and neonatal mammals, but the capacity is not retained in the postnatal period [82, 83]. Numerous and varied treatment approaches ranging from nutritional supplements, medications, surgical debridement, mesenchymal stem cell therapy, and tissue engineering, have been developed and prescribed. However, clinical

outcomes consistently fall short of restoring normal structure and function to synovial joints [4, 8, 11, 84-87]. The ultimate therapeutic goal would be to generate a hyaline cartilage repair tissue that is structurally and biomechanically identical to normal articular cartilage. Unfortunately, incomplete repair often results in progressive cartilage deterioration over time resulting in degenerative joint disease and osteoarthritis. Morbidity of degenerative joint conditions is high in all mammals and it is a leading cause of retirement from athletic careers and even cessation of previously routine activities due to joint pain and decreased mobility [9, 84, 88].

The Mexican axolotl salamander (*Ambystoma mexicanum*) is a promising model system for studies on cartilage repair due to a remarkable ability of these amphibians to regenerate amputated limbs and heal even large joint lesions. Experiments done in our laboratory were the first to demonstrate that axolotls will completely repair large intrinsic articular cartilage defects. This capacity was studied in the femoro-tibio-fibular (knee) joints, which interestingly retain interzone tissue in the intra-articular space and remain non-cavitated even through adulthood. Based on histological assessments of the repair process, interzone cells proliferate and extend into lesions generating a primary repair tissue that then differentiates to restore normal tissue structures [79]. If the interzone tissue is surgically ablated, however, normal tissue structures are not restored and the joint fuses (arthrodesis, unpublished observation).

An additional assessment of interzone tissue's differentiation potential in axolotls was achieved through grafting experiments into critical sized defects created surgically in the tibia diaphysis. Interzone tissue achieved closure of the defect, but rather than

yielding diaphyseal bone, an entirely new joint was formed *de novo* complete with apposing articular surfaces and intervening interzone. In contrast, skin and muscle tissue transplants failed to bridge the skeletal defect in the tibia diaphysis. Cell tracking analysis by GFP immunostaining confirmed that cells within the new diarthrodial joint were indeed derived from the GFP transgenic donor interzone cells [80].

The importance of the interzone as a developmental tissue in synovial joint formation is well established [47-49, 77, 89]. The studies described above, however, suggest that interzone cells also have the potential to spontaneously differentiate into multiple synovial joint tissues in a repair context. Important issues that remain unknown, however, include the cellular and molecular mechanisms regulating this repair process. Are cellular differentiation events orchestrated autonomously by the transplanted interzone cells or are they dependent on the skeletal microenvironment, or perhaps both? The hypothesis tested in this study was that *de novo* joint formation by interzone cells in the tibial CSD is mediated in part by a skeletal microenvironment.

Materials and methods

Animals

A total of 40 axolotl salamanders (1.5 years of age), progeny of a single genetic cross and purchased as fertilized eggs from the Ambystoma Genetic Stock Center (University of Kentucky, Lexington, KY), were maintained at 20-22°C in 25% Holtfreter's solution [90]. Animal care and management was carried out as previously described [79, 80]. All procedures were conducted in accordance with the guidelines of an

approved University of Kentucky Institutional Animal Care and Use Committee protocol (IACUC #2008-0282).

Surgical procedure

Interzone tissue samples were collected immediately postmortem. Donor salamanders (n=20) were deeply anesthetized with 0.01% Benzocaine solution (w/v, Sigma, Cat# E1501, St. Louis, MO) in 25% Holtfreter's solution and euthanized by cervical dislocation. Interzone tissue was dissected from both the right and left femorotibial joints of germline GFP transgenic individuals using a 3 mm micro-sharp blade (Cat# 377513, Beaver-Visitec International, Waltham, MA) under a dissection microscope. Careful attention was paid to avoid inclusion of any attached articular cartilage with the dissected interzone sample.

Harvested interzone tissue samples were immediately transplanted into either skeletal or non-skeletal sites in wild type (non GFP transgenic) recipient individuals (n=20), depicted in Figure 2.1. A surgical plane of anesthesia was achieved by immersing recipient axolotls in 0.01% benzocaine solution and then sustained by keeping them wrapped in paper towels soaked with either the same benzocaine solution or only 25% Holtfreter's solution depending on the depth of anesthesia. Keeping the salamanders moist during surgery also facilitated oxygen exchange and prevented drying of the skin. For the skeletal site transplant, a 5-6 mm skin incision was made over the tibia, which was then exposed by blunt dissection of soft tissues using micro forceps. A 4 mm long centrally positioned fragment of the tibia diaphysis was

then excised and a GFP interzone transplant sample placed into the defect without consideration of orientation. For the non-skeletal site, a pocket was made in the hepatic falciform ligament by folding it upon itself. Harvested interzone tissue was then placed in the falciform ligament pocket with closure secured using nylon 6-0 purse string sutures (Ethicon, Cat# 37098, Somerville, NJ). Finally, skin incisions were closed with 6-0 vicryl suture (Ethicon, Cat# D5890, Somerville, NJ). Following surgery, recipient individuals were recovered in Holtfreter's solution. All salamanders were monitored daily throughout the period of study for post-operative complications and to assess their ability to maintain mobility of the operated limb.

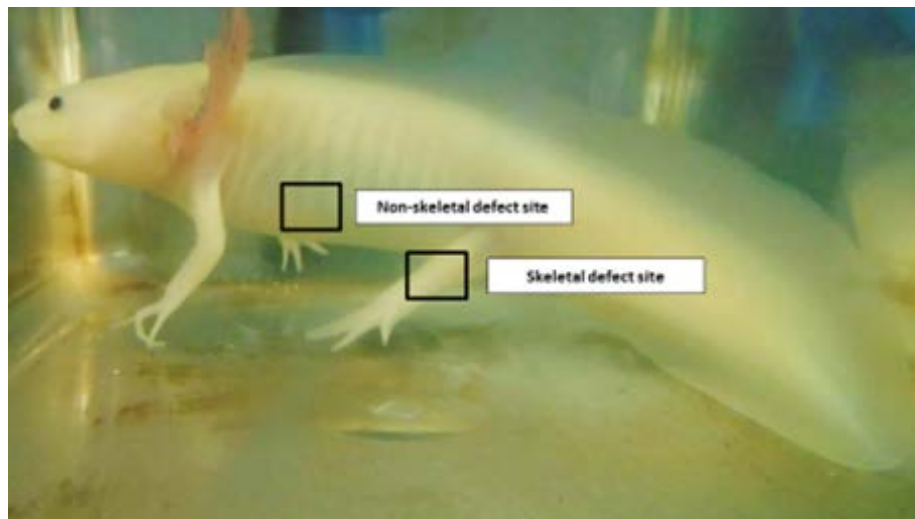


Figure 2.1: Anatomical location of the skeletal and non-skeletal site for interzone transplantation.

Sample collection and processing

Experimental samples were collected from five recipient wild-type salamanders at 2, 6, 18 and 30 weeks after surgery as outlined in Table 2.1. Axolotls were deeply anesthetized with 0.01% Benzocaine solution in 25% Holtfreter's solution and

euthanized by transection of the cervical spinal cord. Interzone transplants and surrounding tissues were collected at each time point and fixed in 4% paraformaldehyde in phosphate buffered saline (PBS) for 48 hours. Samples containing skeletal elements were decalcified in 15-20X volume of Ethylenediaminetetraacetic acid (EDTA) and hydrochloric acid (Cat# 22-050-130, Richard Allen Scientific, Kalamazoo, MI) with periodic testing to assess the progress of decalcification. Decalcification was considered complete by a lack of precipitate formation in the test solution to indicate calcium leaching from the skeletal tissues. The samples were then transferred to 70% ethanol prior to paraffin embedding. All samples were sectioned at 5 μ m.

Histology and immunohistochemistry

Hematoxylin and Eosin (H&E) staining was performed using standard protocols. Safranin-O/Fast Green staining was optimized and standardized for axolotl samples using aqueous 1% Fast Green and 0.05% Safranin-O solutions as previously described [79, 80].

Immunohistochemistry was used to assess the expression of GFP. Immunostaining was performed using standard avidin biotin complex reagents and methods according to the manufacturer's protocol (Santa Cruz Biotechnology, Cat# SC 2051 Santa Cruz, CA). All sections were pretreated with 3% hydrogen peroxide to quench endogenous peroxidase activity. Sections stained for GFP were pretreated to enhance antigen retrieval with a 0.2 M sodium citrate buffer, pH 3.5, for 20 minutes at 37C. For the primary antibody, polyclonal rabbit anti-GFP IgG (Abcam, Cat# AB290,

Cambridge, MA) was diluted at 1:1500. Sections were then incubated for 30 minutes with the supplied pre-diluted biotinylated secondary antibody followed by detection using the HRP-streptavidin system. All sections were counterstained with Gill No. 3 hematoxylin (Sigma, Cat# HS316).

Results

Skeletal site interzone transplants

Transplanted interzone tissues at skeletal sites were successfully recovered from all the individuals at the defined post-surgical time point (Table 2.1). The size and location of the CSD in the tibia diaphysis was confirmed at 2 weeks (Figure 2.2A, 2.3A, 2.4A). By 6 weeks post-surgery, cartilaginous caps were apparent at the transected bone ends of the tibia (Figure 2.2B) that showed positive proteoglycan staining with Safranin O (Figure 2.3B). GFP immunohistochemistry demonstrated an absence of staining in the cartilage outgrowths, but positive staining in the donor interzone tissue within the tibial bone defect (Figure 2.4B). By 18 weeks, columns of proteoglycan expressing tissue were observed at the skeletal site which appeared to progress from the cartilage caps at the both the proximal and distal cut ends of tibia towards the middle of the gap fracture (Figure 2.2C, 2.3C). Cells within this new cartilaginous outgrowth stained positive for GFP by immunohistochemistry (Figure 2.4C) confirming an origin from the interzone transplant. Formation of a *de novo* diarthrodial joint was apparent at 30 weeks and appeared to follow normal spatial patterning. Specifically, the new accessory joints were comprised of an interzone-like tissue between two

proteoglycan expressing cartilaginous structures. In addition, cellular morphological features in the new cartilage appeared similar to normal epiphyseal/articular and metaphyseal chondrocytes (Figure 2.2D, 2.3D). Cells within the newly formed diarthrodial joint stained positive for GFP by immunostaining, including the interzone-like tissue and a subset of the adjacent chondrocytes. In contrast, cells within the repair tissue positioned closer to the original ends of the tibia demonstrated negative GFP staining comparable to controls (Figure 2.4D-H). Regions of GFP positive cells did exhibit asymmetry proximal and distal of the new interzone layer. However, there was no evidence to suggest a migration of the transplanted interzone cells outside the tibial skeletal defect. These observations are broadly consistent with previous findings [80].

Surgical procedure	Collection time point	Biological replicates (n)	Interzone transplant located (n)
Skeletal site transplantation	2 weeks	5	5
	6 weeks	5	5
	18 weeks	5	5
	30 weeks	5	5
Non-skeletal site transplantation	2 weeks	5	0
	6 weeks	5	2
	18 weeks	5	0
	30 weeks	5	0

Table 2.1: Experimental samples - Biological replicates, post-surgical collection time and incidence of recovery of skeletal and non-skeletal interzone tissue transplant.

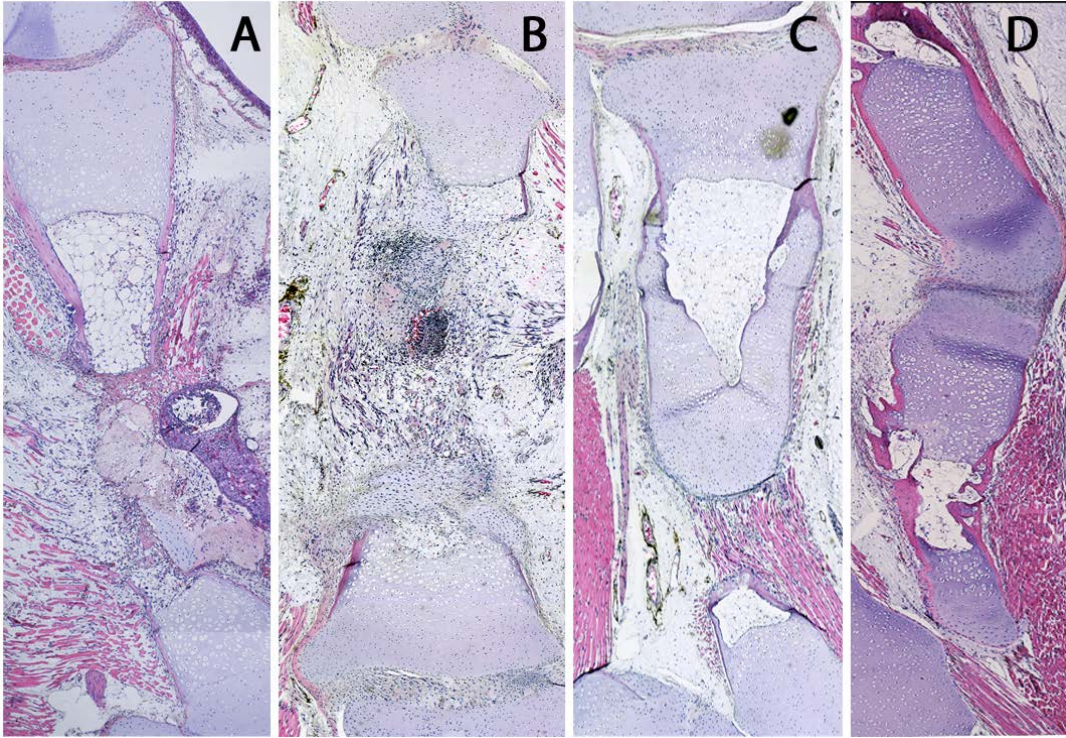


Figure 2.2: Repair of critical sized bone defects (skeletal) with interzone tissue transplants. H&E stained sections at 2,6,18, and 30 weeks post-surgery (A-D, respectively). At 30 weeks (D), the defect is closed with formation of a new joint. All images are at 4x (objective lens) magnification.

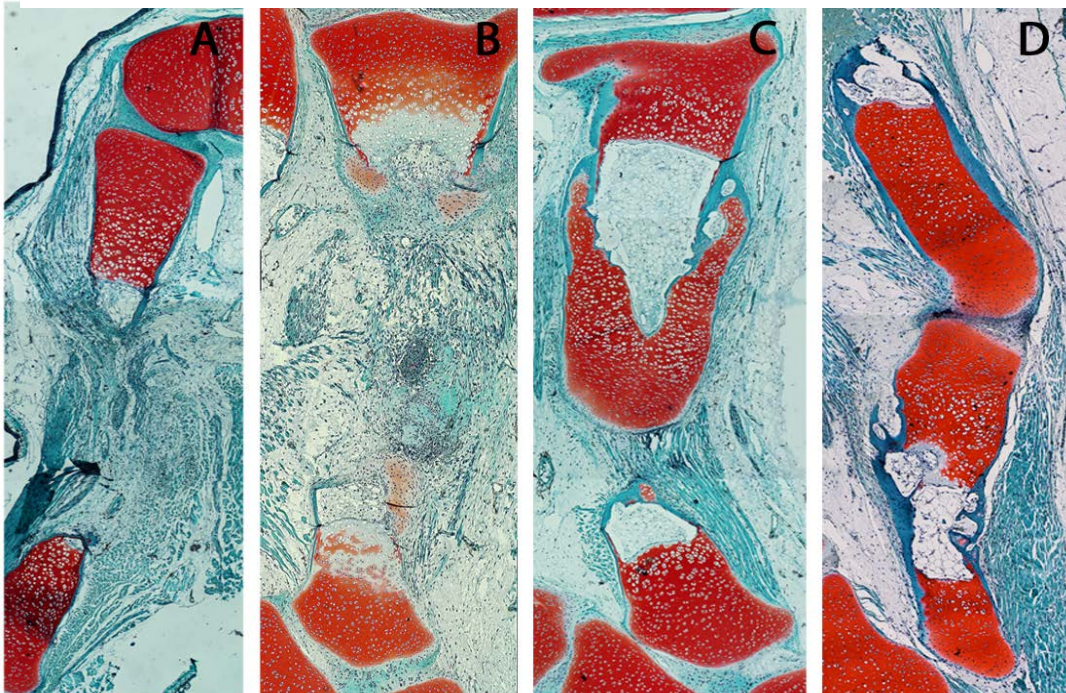


Figure 2.3: Repair of critical sized bone defects (skeletal) with interzone tissue transplants. Safranin-O stained sections are shown at 2,6,18, and 30 weeks post-surgery (A-D, respectively). At 30 weeks (D), the defect is closed with formation of a new joint. All images are at 4x (objective lens) magnification.

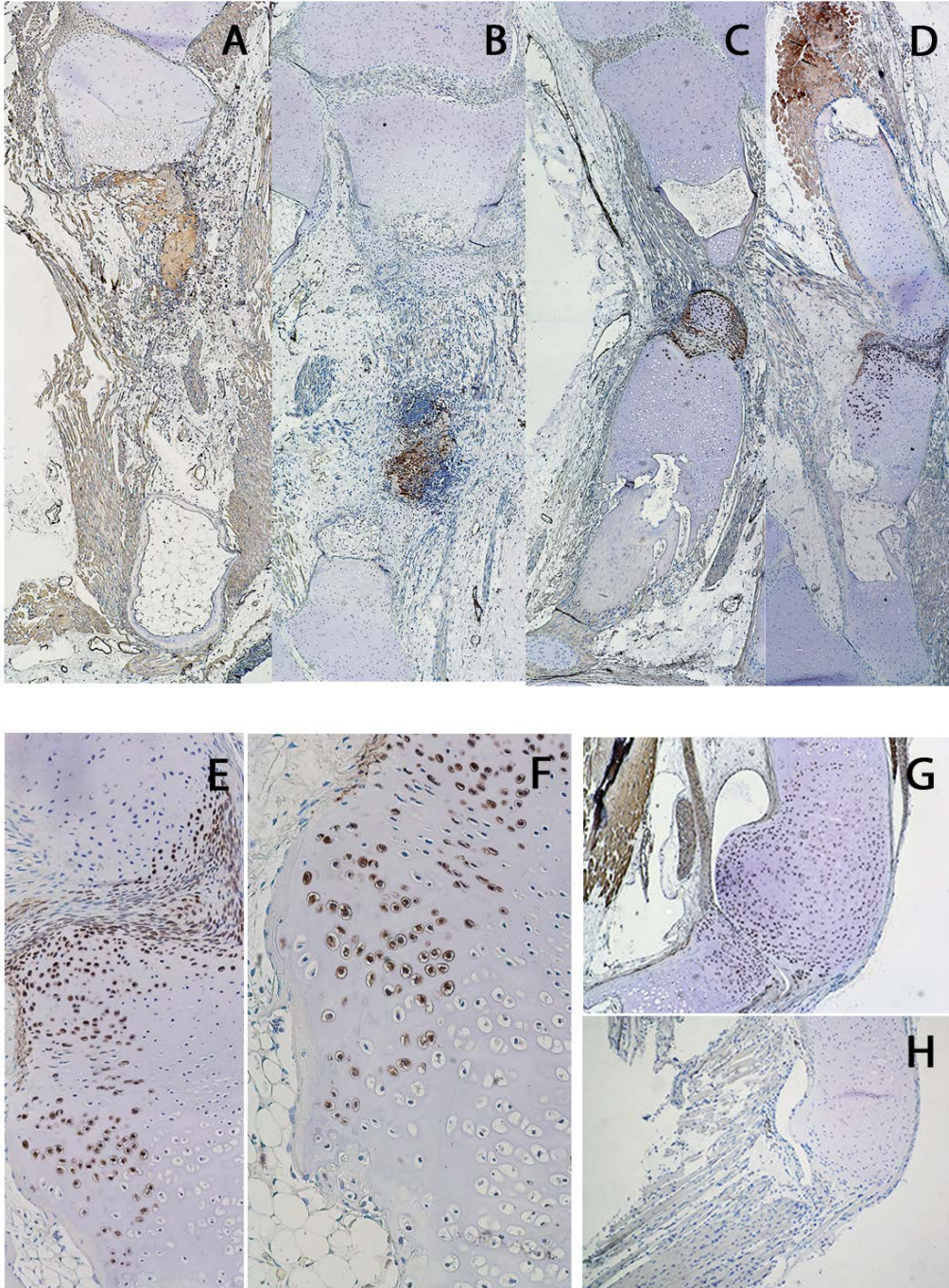


Figure 2.4: Repair of critical size bone defects with interzone tissue transplants. GFP immunostaining at 2,6,18, and 30 weeks post-surgery (A-D, respectively). At 30 weeks (D-F), cells within the accessory joint show positive immunostaining for GFP suggesting their origin from the transplanted interzone cells. Positive (G) and negative (H) controls for GFP immunostaining. A-D and G-H are at 4x, E-20x and F-40x (objective lens) magnification.

Non-skeletal site interzone transplants

In contrast to the tibial surgical site, interzone tissue that was transplanted to the non-skeletal falciform ligament pockets were located post-surgically in only two salamanders (Table 2.1) This occurred even with placement of surgical markers at the transplant site in all recipients and careful assessment of serial sections. For the two exceptions, both at the 6 week time point, the interzone transplant presented as a nondescript area of GFP expressing tissue (Figure 2.5C). There was no evidence of chondrogenic differentiation and minimal proteoglycan expression. However, a zone of basophilic cellular infiltration was apparent around the transplanted interzone tissue suggestive of an immune response against the allograft (Figure 2.5A, B and C (arrows)).

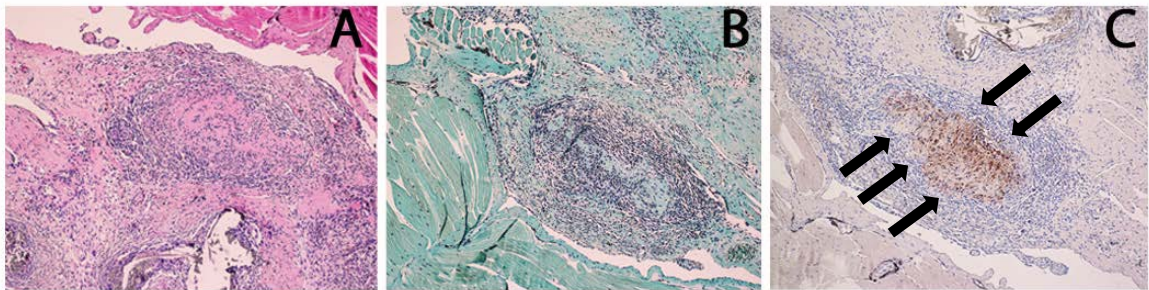


Figure 2.5: Tissue response in the non-skeletal site to interzone tissue transplants. The transplanted interzone tissue remained intact in the non-skeletal site as revealed by H&E (A), Safranin-O (B) and GFP immunostaining (C). Cellular cuffing (arrows) around the transplant suggests an immune response against the allograft. All images are at 10x (objective lens) magnification.

Discussion

The data presented in this chapter support the hypothesis that *de novo* joint formation by interzone cells in tibial CSDs is mediated in part by the skeletal microenvironment. The first sign of repair in the gap fracture was formation of a

cartilaginous callus at the fractured bone ends that showed an absence of GFP immunostaining. This rounding of the proximal and distal ends of the tibia with cartilage was also observed with control (non-interzone) skin and muscle transplants reported previously [80] and appears to mimic the process of host-directed transverse fracture repair in mammals [91, 92]. Histological analysis of the skeletal defect with interzone transplants revealed the *de novo* formation of an accessory joint by 30 weeks. Positive proteoglycan expression and chondrocyte-like cell morphology were observed in the adjoining cartilaginous structures of the accessory joint. Moreover, cells within the repair tissue stained positively for GFP by immunohistochemistry, confirming that they were derived directly from the interzone transplant tissue. However, this GFP expression was limited to the subset of cells within the new layer of interzone and immediately adjacent cartilage. The rest of the cells within the repair tissue that closed the gap fracture stained negative for GFP suggesting that they were derived from the recipient and not the transplant.

The transplanted interzone tissue was placed in a random orientation within the CSD, yet at 30 weeks, the repair tissue had clearly developed a level of structural organization. The neo joint resembled the architecture of the normal diarthrodial joint with a layer of interzone tissue between two cartilaginous structures that displayed cellular morphologies similar to epiphyseal/articular chondrocytes and metaphyseal chondrocytes. The findings suggest a multifaceted role for the interzone cells in skeletal repair – the ability to self-renew to maintain an interzone cell population and the potential to differentiate into cartilaginous cell types. This differentiation profile is

similar to the normal developmental function of interzone cells in mammalian joints [48, 74, 77].

In contrast, the non-skeletal falciform ligament microenvironment did not appear to support the transplanted interzone tissue. One possible explanation for the inability to locate the transplants in a majority of the experimental samples is immune rejection by the recipient. This argument is strengthened by the basophilic cellular cuffing observed around the transplanted tissue and is consistent with previous reports of immune response against allotransplants in related amphibians [93, 94]. In the only two samples where the interzone transplant could be located, there was no evidence of chondrogenic differentiation.

Taken together, these results raise the question as to why interzone cells were able to proliferate and differentiate in the tibial CSD but not in the falciform ligament pocket. One possible reason for this differential response could be qualitative and/or quantitative differences in localized growth factor production between the two sites. The critical sized defect in the tibia diaphysis may have been subjected to more local trauma from the surgical procedure. Such a lesion could be expected to take longer to heal. This provides an extended period of time with localized growth factor production to aid the repair process which could also have a positive trophic effect on the transplanted interzone cells. In contrast, the degree and duration of stimulation by localized growth factors in the non-skeletal site could be limited owing to lower trauma and rapid tissue repair. The possibility that the diaphyseal surgical site is immunologically privileged cannot be ruled out in the current study, but is not reported

in the literature. The data support a model whereby the interzone transplants respond to paracrine inductive signals from the skeletal environment to proliferate and differentiate into multiple cell types. Further investigation of paracrine mechanisms that regulate interzone cell proliferation and differentiation in a skeletal microenvironment may provide new insight into the potential of interzone for cell-based therapy for the repair of synovial joint defects involving the articular surface.

Chapter 3

Effect of skeletal paracrine signals on the proliferation of interzone cells

Introduction

Interzone cells demarcate the presumptive site of synovial joint development in mammalian and avian embryos, initially appearing as a compact layer of mesenchymal cells which down regulate the expression of chondrocyte-specific type II collagen and up regulate a new set of genes including *GDF5*, *WNT4*, *WNT9A* and type I collagen [2, 7, 49, 78]. Elegant lineage tracing studies in mice indicate a role for the *GDF5* positive interzone cells in the formation of articular cartilage, synovial membrane, and associated joint structures during development. Just prior to cavitation of the joint, the interzone can be appreciated as a tripartite structure with a cell-dense intermediate layer and two outer layers with comparatively low cellularity [48, 89]. These authors suggest distinct fates for the two layers of the interzone. Cells in the outer zone contribute secondarily to the epiphyseal anlage chondrocytes that subsequently undergo endochondral ossification and replacement by bone while the intermediate zone forms the articular tissues, including cartilage. More recently, gene expression analyses of the intermediate and outer zones of murine embryonic interzone has provided additional evidence to support the view that cells in the interzone are the developmental progenitors of tissues in diarthrodial synovial joints [77].

Experiments with axolotl salamanders in our laboratory were the first to indicate that interzone cells have the potential to repair articular cartilage lesions [79, 80]. My

experiments, described in Chapter 2, support these findings and further demonstrate that the skeletal microenvironment supports interzone cells and promotes their ability to repair critical sized bone defects. The repair tissue that bridged the bone gap in these studies matured to an anatomically organized structure resembling an intact joint with an interzone layer positioned in between two cartilaginous zones of tissue. The newly formed cartilage included cells with morphological features very similar to both epiphyseal/articular and metaphyseal chondrocytes. In contrast, interzone tissue transplanted into a non-skeletal site failed to thrive and appeared to be rejected or resorbed.

The observation that interzone transplants placed in a random orientation within a skeletal defect develop into an accessory joint with the correct spatial patterning of the tissues is particularly interesting. It suggests that some form of cellular communication and regulation is occurring. One possibility is paracrine signals between skeletal cells of the recipient salamander and the transplanted interzone cells stimulating both self-renewal to maintain the interzone pool and chondrogenic differentiation to generate the cartilaginous tissues that form the new accessory joint. Moreover, this process might be governed by highly dynamic spatio-temporal patterns of gene expression, recapitulating embryogenic developmental events [95-97]. Unfortunately, technical challenges that limited our ability to culture primary amphibian cells precluded further studies with the axolotls.

In this chapter, we report establishing a mammalian *in vitro* co-culture model to examine a potential paracrine interaction between skeletal cells and the interzone.

Medium used to maintain cells in culture can be expected to accumulate the cells' secretome during incubation [98] and is referred to as conditioned medium. This medium 'conditioned' by the signal producing cells can be added exogenously to a second culture to assess an impact of cell-secreted factors on the signal receiving cells [99-105].

The experiments reported in this chapter were designed to test the hypothesis that paracrine signals derived from skeletal cells stimulate interzone cell proliferation employing skeletal cell-derived conditioned medium as the source of paracrine mitotic stimuli. The mitogenic potential of skeletal cells could differ with age of the individual from whom the cells were derived, with embryonic cells expected to exhibit a higher proliferative potential compared to those of adult origin [106]. This study also examines an effect of donor age on the ability of skeletal cells to induce proliferation of interzone cells.

Materials and methods

Isolation and culture of cells

Methods utilized for the isolation of equine tissue samples and the preparation of primary cell lines that were used in this project have been described previously [107]. Mares were bred by natural cover after estrous cycle synchronization with two doses of intramuscular synthetic prostaglandin F₂ α (500 μ g of cloprostenol sodium, Estrumate©) given 14 days apart. A stallion was placed in the pasture for 10 days with the mares. Serum progesterone levels of the mares were monitored daily leading up to the

approximate date of ovulation, which was called day 0 of gestation if the mare was determined to be pregnant. Gestational age was confirmed six days after the stallions were separated from the mares (16 days after the mares were programmed to ovulate) through a transrectal ultrasound examination to determine embryonic vesicle size [108].

Fetuses were recovered intact at 45 or 46 days of gestation from mares (one fetus per mare) while standing and sedated using a minimally invasive uterine lavage technique. Prior to collection, the mare's pregnancy status was reconfirmed by transrectal ultrasonography. The vulva and perineal area were cleaned aseptically, and 2 mg of synthetic prostaglandin E₂ paste (in 2.5 ml triacetin and 125 mg silicon dioxide gelling agent) instilled along the length of the cervical ostium after gentle and minimal digital dilation. One hour later, the mares were sedated with detomidine (10 – 16 µg/kg IV) and butorphanol (6 – 16 µg/kg IV). The cervical ostium was digitally dilated per vagina aseptically and a 28 mm OD endotracheal tube was positioned to the level of the internal ostium of the cervix. The uterus was lavaged following introduction of 2-3 liters of warmed sterile lactated Ringers' solution, including the gentle balloting of the fluid filled uterus per rectum. This readily displaced the embryo within its vesicle, which was then recovered into a sterile bag by gravity evacuation of the lavage fluid back through the tube. In all cases, great care was taken to ensure passage of the fetal membranes. Immediately after collection, fetuses were thoroughly rinsed in ice cold sterile Dulbecco's phosphate buffered saline (PBS; Gibco, Cat# 14190144) with 2% (v/v) amphotericin B (anti-mycotic, Gibco, Cat# 15290026) and 2% (v/v) penicillin/streptomycin (antibiotic; Gibco, Cat# 15070063). Each fetus was catalogued

and transported in a sterile container on ice for immediate tissue processing. After the procedure, each mare was given two doses of 500 µg of cloprostenol sodium (Estrumate©, synthetic prostaglandin F2α) as an intramuscular injection spaced 24 hours apart to facilitate complete uterine clearance. Mares also received a single dose of flunixin meglumine (1 mg/kg IV, non-steroidal anti-inflammatory).

All procedures were conducted in accordance with a University of Kentucky institutional animal care and use protocol (IACUC #2014-1215). The mares from which fetuses were collected did not suffer any observed post-harvest complications or health issues.

Fetal cell lines

Interzone cells and anlage chondrocytes were isolated from one forelimb and one hind limb of each fetus. Skin and developing soft tissues over the limb skeletal elements were carefully removed using a dissecting microscope and sterile instruments. Interzone cells were liberated from the cuboidal bone anlage of developing carpal and tarsal joints by digestion in 500 µl of commercial 0.25% trypsin EDTA solution (Gibco, Cat# 25200056) for 5-10 minutes with gentle agitation using a micropipette. The enzymatic activity of trypsin was then quenched with 1 ml Dulbecco's Modified Eagles Medium (DMEM, Gibco, Cat# 10569044) supplemented with 10% (v/v) heat inactivated fetal bovine serum (FBS), 1% (v/v) P/S, and 1% amphotericin B (FBS medium). The undigested tissue fragments and the cuboidal bones were allowed to settle by gravity for 3 minutes. The supernatant containing the suspended cells was then transferred to

a sterile 15 ml polypropylene tube, and centrifuged at 1000 rpm for 3 minutes. The resulting pellet was re-suspended in 5 ml of FBS medium, and plated in six well cell culture plates (Bio-Star, VWR Cat# 10062-892). Collagenase was not used in the isolation of interzone cells to prevent contamination from liberated anlage chondrocytes. Anlage chondrocytes were isolated from internal cubes dissected from distal metaphyseal anlage of the developing humerus and femur with careful attention to avoid inclusion of the epiphysis, diaphysis, or anlage surface. To further minimize the potential for cell contamination, the anlage cubes were incubated in 500 μ l of the commercial 0.25% trypsin EDTA solution for 5-10 minutes, followed by gravitational settling of the anlage cubes. This was followed by two rinses in sterile Dulbecco's phosphate buffered saline supplemented with 2% (v/v) P/S, and 2% (v/v) amphotericin B. Chondrocytes were then liberated from the matrix using 1 ml of 0.5% collagenase D (Worthington, Cat# CLS4; <http://www.worthington-biochem.com/cls/pl.html>) for 10-20 minutes with gentle agitation using a micropipette. Quenching of the collagenase enzyme activity, isolation and plating of primary anlage chondrocytes were performed in a similar fashion as described above for interzone cells. Fibroblasts were isolated from the truncal dermis targeting a region of skin located away from any skeletal structures. Care was taken during tissue dissection to ensure exclusion of epidermis and hypodermis. The subcutaneous dermal tissue was then finely minced, followed by digestion in 1 ml of the commercial 0.25% trypsin EDTA solution for 10-20 minutes with gentle agitation using a micropipette. Separation of undigested tissues, quenching of

enzyme activity, isolation, and plating of primary dermal fibroblasts were similar to the procedures described above for interzone and anlage chondrocytes.

Adult cell lines

Tissue samples were collected immediately postmortem from six young adult horses of mixed light breed heritage that were euthanized at 15-17 months of age for reasons unrelated to the current study (IACUC 00843A2005). Bone marrow aspirates were collected from the sternum using an 8 FrG Jamshidi needle and heparinized syringes [109]. The samples were stored on ice until processing, which involved direct plating in 1:1 FBS medium in T-75 tissue culture flasks (Bio-Star, VWR Cat# 82050-856). The cultures were rinsed with PBS over the course of the first few days of culture to facilitate removal of red blood cells and yield adherent cells.

Dermal fibroblasts were isolated from the dermal layer of skin at the tail base. Dermis was minced and transferred to tissue culture plates in FBS medium. Dermal tissue explants were maintained in FBS medium for several days to yield adherent dermal fibroblasts. The processing of bone marrow and dermal tissue samples were completed within three hours post-mortem.

Articular chondrocytes were isolated as previously described [110]. Briefly, articular cartilage of the femoro-tibial joint was shaved down to the calcified layer. Cartilage shavings were copiously rinsed in PBS with 2% antimycotic and antibiotic supplements as above. The shavings were minced, weighed, and digested for 22 hours in medium (OptiMEM [Gibco Cat # 51985091, 5% FBS, 1% antimycotic/antibiotic)

containing bacterial collagenase (Worthington) at 7.5 mg collagenase/g of cartilage. Primary chondrocytes released from the cartilage matrix were centrifuged, rinsed, counted, and plated into T-75 tissue culture flasks at a seeding density of 2.1×10^6 cells per flask.

A total of 6 primary cell lines isolated from five equine fetuses and five young adult horses were used for this study. Each biological replicate provided all three fetal or all three adult cell lines, respectively.

- | | | |
|---|---|--------------------|
| 1. Adult articular chondrocytes (AEC) | } | Skeletal cells |
| 2. Adult bone marrow derived cells (BM) | | |
| 3. Fetal anlage chondrocytes (FEC) | | |
| 4. Fetal interzone cells (IZ) | | |
| 5. Adult dermal fibroblasts (AEF) | } | Non-skeletal cells |
| 6. Fetal dermal fibroblasts (FEF) | | |

Conditioned medium preparation

The six primary cell lines isolated from skeletal and non-skeletal tissues of equine fetuses (n=5) and adult horses (n=5) were used for the preparation of conditioned medium. To prepare the conditioned medium, thawed P2 cells were passaged and plated at P3 into five T-75 tissue culture flasks at a seeding density of 500,000 cells per flask in FBS medium. Medium was replenished every 48 hours until the cells reached 70-80% confluence. The cells were then rinsed thrice with PBS, and incubated for 24 hours in 5 ml of DMEM supplemented with 1% (v/v) P/S, and 3 mg/ml of bovine serum

albumin (BSA; Sigma Cat# A9418; BSA Medium). This amount of BSA was calculated to be roughly equivalent to the amount of total protein in 10% FBS. In control experiments, 24 hours of conditioning was found to elicit a greater mitogenic response with adult dermal fibroblasts in comparison to medium conditioned for 72 hours (data not shown). At the end of the incubation period, the media from the five T-75 flasks were pooled for each cell type and each biological replicate, centrifuged, sterile filtered using a 0.2 μ M Polyethersulfone membrane filter (VWR, Cat # 28145-501), and stored at -80C in aliquots. For normalization, cells from each corresponding group of five T-75 flasks were trypsinized and counted, and the total cell count that generated the volume of conditioned medium was recorded and used throughout this study.

Co-culture

Background proliferation

To minimize background cell proliferation in the experimental system prior to assessing the mitogenic activity of the conditioned medium, a determination was made on growth arresting the P3 cells through FBS deprivation to the point where the rate of cell division approached zero but cell viability remained high. This was determined empirically for each cell line studied. P3 cells were plated in FBS medium for 24 hours after which the medium was replaced with BSA medium. The cells were maintained in this serum-deprived state, with viability and proliferation assessments performed as described below every 48 hours. BSA medium was also re-fed at 48 hour intervals. The

functional ability of the serum starved cells to respond to mitogenic stimuli was then evaluated by re-feeding with FBS medium.

Sample size was determined by power analysis. Power calculations were performed using data from a pilot study (Table 3.1) to assess interzone cell proliferation in response to conditioned medium from fetal skeletal and non-skeletal cell lines (n=2) using the following equation:

$$\phi = \sqrt{\frac{r}{MSE} \sum \frac{\tau_i^2}{t}}$$

where r is the number of randomized complete blocks, t is the number of treatments, MSE is the mean squared error and τ_i^2 is the square of the differences of each block and the overall mean for the treatment. The estimated sample size required to achieve a power of 0.80 was two. The number of biological and technical replicates used in this study is outlined in Table 3.2 and 3.3.

Differential production of mitogens

The first part of the experiments reported in this chapter compared the level of interzone cell proliferation stimulated by conditioned medium derived from six different skeletal and non-skeletal primary cell lines. The different preparations of conditioned medium were prepared as described above and considered as the source of paracrine signals. Interzone cells were kept constant as the responder cells. A summary of biological and technical replicates used is presented in Table 3.2.

Medium type	Mean \pm SD
Negative control (BSA medium)	3.42 \pm 0.57
Positive control (FBS medium)	78.58 \pm 4.05
Fetal anlage chondrocyte conditioned medium (FEC – CM)	48.96 \pm 0.88
Fetal dermal fibroblast conditioned medium (FEF – CM)	41.84 \pm 4.32
Fetal interzone cell conditioned medium (IZ – CM)	44.96 \pm 0.85

Table 3.1: Table showing the mean and standard deviation of percent change in proliferation of interzone cells in control and conditioned media from fetal dermal fibroblast (FEF-CM), Fetal anlage chondrocytes (FEC-CM), and Fetal interzone cells (IZ-CM).

Medium type	Biological replicates (n)	Technical replicates (n)
Fetal dermal fibroblast conditioned medium (FEF-CM)	5	6
Fetal anlage chondrocyte conditioned medium (FEC-CM)	5	6
Fetal interzone cell conditioned medium (IZ-CM)	5	6
Adult dermal fibroblast conditioned medium (AEF-CM)	5	6
Adult articular chondrocyte conditioned medium (AEC-CM)	5	6
Bone marrow derived cell conditioned medium (BM-CM)	5	6
Positive control	5	3
Negative control	5	3

Table 3.2: Differential production of mitogens – Description of biological and technical replicates in experimental and control groups. Biological replicates here represent the equine fetuses or adult horses from which primary cells were isolated and the individual wells of the 24 well culture plate represent the technical replicates. The sample size was determined by power analysis.

Interzone cells at P3 were plated in 24 well plates in FBS medium at a seeding density of 50,000 cells per well to yield an adherent monolayer. Following 24 hours of culture, the medium was replaced with BSA medium for 5 days (experimental time point for interzone cells) to minimize the level of background proliferation. On day 5, the interzone cell monolayers were re-fed with either conditioned medium derived from one of the experimental cell lines, BSA medium as a negative control, or FBS medium as a positive control.

Differential cellular response to the same level of mitogenic stimuli

The second set of the experiments reported in this chapter focused on determining whether any of the cell types exhibit a differential response to the same level of mitogenic stimulation. As such, the six primary cell lines isolated from equine fetuses and adult horses were evaluated independently as responders, while the stimuli from conditioned medium prepared from fetal anlage chondrocytes was held constant. A summary of the biological and technical replicates is outlined in Table 3.3. Plating and co-culture for all the cell lines were performed as described above.

Cell type	Biological replicates (n)	Technical replicates (n)
Fetal dermal fibroblasts (FEF)	5	8
Fetal anlage chondrocytes (FEC)	5	8
Interzone cells (IZ)	5	8
Adult dermal fibroblasts (AEF)	5	8
Adult articular chondrocytes (AEC)	5	8
Adult bone marrow stromal cells (BM)	5	8
Positive control	5	4
Negative control	5	4

Table 3.3: Differential cellular response to the same level of mitogenic stimuli – Description of biological and technical replicates in experimental and control groups. Biological replicates here represent the equine fetuses or adult horses from which primary cells were isolated and the individual wells of the 24 well culture plate represent the technical replicates. The sample size was determined by power analysis.

Assessment of cell viability

Cell viability was assessed using a commercial LIVE/DEAD® Viability/Cytotoxicity Kit for mammalian cells (ThermoFisher Scientific, Cat# L3224) according to the manufacturer’s protocol. Briefly, adherent cells in 24 well plates were washed twice with PBS to remove residual serum esterase activity. The cytoplasm of live cells stains with Calcein AM (1 µM), while nuclei of dead cells stain with ethidium homodimer-1 (2 µM). All cell nuclei were counterstained with Hoechst 3342 (5 mg/ml) (ThermoFisher Scientific, Cat# 3570). The total number of cell nuclei and the dead cell nuclei per field were counted using automated imaging software (NIS elements 4.0, Nikon Instruments Inc.) and the percent viability was calculated as the number of live cells per 100 cells total. The counts were recorded in 3 distinct fields and averaged for each well.

Assessment of cell proliferation

Levels of cell proliferation were quantified by measuring the incorporation of 5-ethynyl-2'-deoxyuridine (EdU) following a pulse labeling. EdU is a thymidine analog that is efficiently incorporated into newly synthesized DNA and can be fluorescently labeled to visualize those cells that have progressed through the synthesis (S) phase of the cell cycle. EdU incorporation and subsequent visualization were performed as described previously [111]. Briefly, cells were labeled with a 24 hour pulse of EdU (Jena Bioscience, Cat# CLK N001-25) at a concentration of 8 μ M. The cells were then fixed in 4% paraformaldehyde in PBS prior to permeabilization with 0.1% Triton-X followed by detection. For detection of the EdU label, the cells were incubated for 30 minutes in 100 mM Tris, 4 mM CuSO₄ (Sigma, Cat# 451657), 100 μ M Biotin conjugated azide in DMSO (Jena Bioscience, Cat# CLK-AZ104P4-25), and 100 mM ascorbic acid (Sigma, Cat# 451657). The staining mix was prepared fresh for each assay and was used for staining cells immediately after the addition of ascorbic acid. The EdU label was visualized with streptavidin-conjugated Texas Red (Vector Biolabs, Cat# SA 5006). The cells were counterstained with DAPI (4', 6-diamidino-2-phenylindole; Life Technologies, Cat# D1306).

The total number of cell nuclei and the number of proliferating cells (EdU labeled) were counted using automated imaging software (NIS elements 4.0, Nikon Instruments Inc.) by fluorescence microscopy. The rate of proliferation was calculated

as the number of EdU labeled cells as a percent of the total number of cells in each field. The percent proliferation was calculated for 3 fields per well and the values averaged.

Statistical analysis

Data from the viability and proliferation assays were independently evaluated by one-way analysis of variance. Medium type (conditioned and control media) was the factor being tested at the following levels – Conditioned medium from Fetal dermal fibroblasts (FEF-CM), Fetal anlage chondrocytes (FEC-CM), Fetal interzone cells (IZ-CM), Adult dermal fibroblasts (AEF-CM), Adult articular chondrocytes (AEC-CM) and Bone marrow derived cells (BM-CM), negative control (BSA medium), and positive control (FBS medium). Pair-wise comparisons were made between the different levels with a Bonferroni *post hoc* correction for multiple comparisons.

Differences were considered statistically significant if the corrected p-value was <0.005. Age of the donor from which primary cells were isolated was evaluated as an additional factor. Residual plots, histograms of residuals and Q-Q plot of residuals were evaluated to ensure that the normality assumptions were not violated.

Results

Background proliferation – The amount of time in BSA medium to achieve a minimal level of background proliferation in culture was identified for each cell line empirically.

They are as follows:

- | | | |
|------------------------------------|---|-------|
| 1. Adult articular chondrocytes | } | Day 3 |
| 2. Adult bone marrow derived cells | | |
| 3. Fetal anlage chondrocytes | } | Day 5 |
| 4. Fetal interzone cells | | |
| 5. Fetal dermal fibroblasts | | |
| 6. Adult dermal fibroblasts | } | Day 7 |

The cell lines were then evaluated for 10 days after re-feeding with FBS medium. In each case, the 48 hours post-treatment exhibited the maximum percentage of proliferating cells likely due to synchronization of the cell cycle. Cell viability was supported by re-feeding with FBS medium, but remained above 94% even in cells maintained in BSA medium. Figure 3.1 illustrates data from interzone cells, but is representative of all six cell lines.

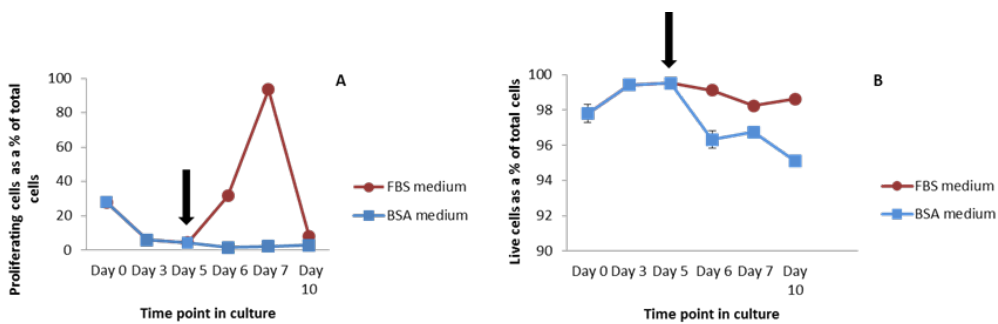


Figure 3.1: Time course study to identify point of minimal background proliferation for interzone cells - Change in cell proliferation (A) and viability (B) of interzone cells after feeding with FBS medium (red) on day 5 (arrow) compared to those maintained in the BSA medium (blue) throughout culture.

Differential production of mitogens

Proliferation

The level of proliferation was determined by measuring the number of cells that incorporated the EdU label as a percent of the total number of cells. Figure 3.2 shows representative images of proliferating interzone cells (48 hours post-treatment) in response to medium conditioned by the different fetal cell lines. Figure 3.3A and 3.3B demonstrate the overall change in percent proliferation in each experimental group over the time course of the study and specifically 48 hours post-treatment respectively. The percent proliferation trend in the fetal cell conditioned media was as follows: FBS medium > Fetal dermal fibroblast CM = Fetal anlage chondrocyte CM > Interzone cell CM > BSA medium. Interzone cells in the positive control medium exhibited the highest percent proliferation, approaching 100% in all the experiments. In contrast, the interzone cells in the negative control group had the smallest number of positively stained cells and lowest rate of proliferation. All conditioned media groups generated a significantly higher mitogenic response in interzone cells relative to the negative control medium. There was no significant difference in the percent proliferation values of interzone cells in fetal dermal fibroblast (FEF – CM) and anlage chondrocyte (FEC – CM). However, some variation was observed in the mitogenic induction ability within the FEC CM group compared to other groups (Figure 3.3 and Table 3.4). Interestingly, interzone cell conditioned media (IZ – CM) was the least mitogenic among all the groups, but still stimulated cell proliferation at a level significantly higher than the negative control medium ($p < 0.001$).

Interzone cells cultured with conditioned medium from all three types of adult cells exhibited significantly higher mitogenic activity than the negative control medium (Figure 3.4 and Table 3.4). Interzone cells in positive control and negative control medium showed the maximum and minimum percent proliferation values respectively. The bone marrow derived cell conditioned medium (BM – CM) showed significantly higher mitogenic potential compared to adult chondrocyte (AEC – CM) and dermal fibroblast (AEF – CM) conditioned medium. The difference in percent proliferation values of interzone cells in AEC – CM and AEF – CM did not reach statistical significance ($p=0.0883$).

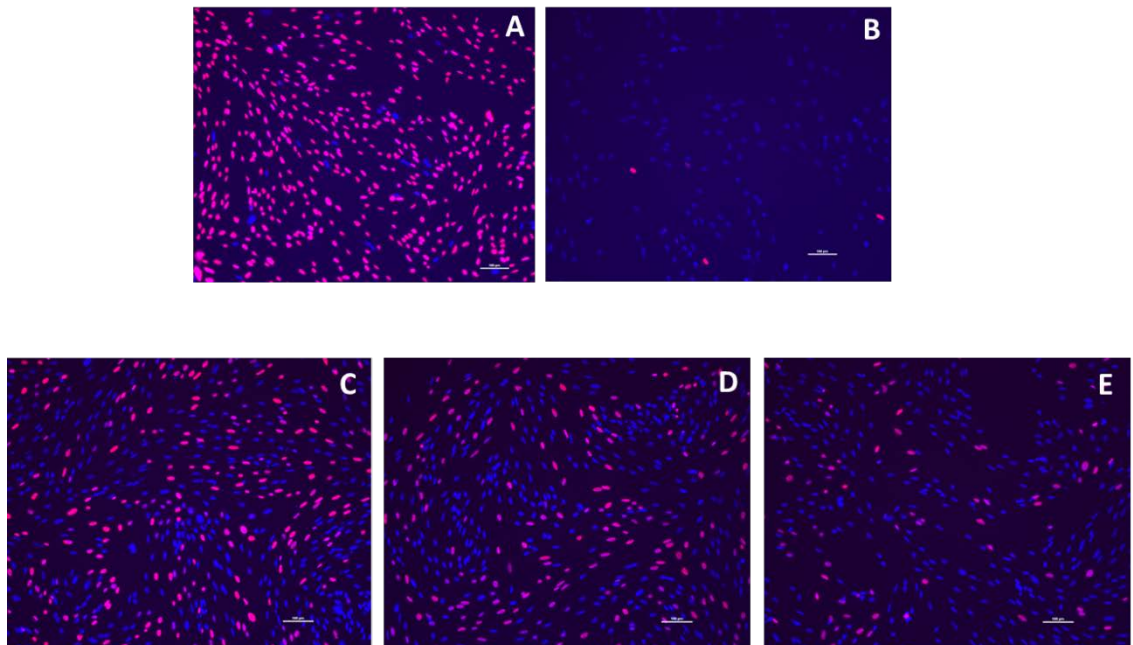


Figure 3.2: Panel (10x) showing the proliferation of interzone cells in response to fetal conditioned medium: Edu – labeled proliferating cell nuclei (pink) and non-proliferating cell nuclei (blue) in positive control/FBS medium (A), negative control/BSA medium (B), Fetal dermal fibroblast (C), Fetal anlage chondrocyte (D), and fetal interzone (E) conditioned media.

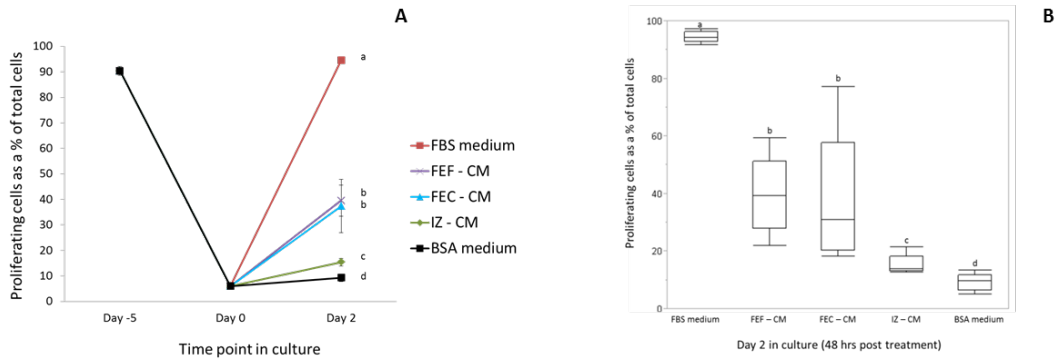


Figure 3.3: Percent change in proliferation of interzone cells in response to control and fetal cell derived conditioned media over the time course of the experiment as a line graph (A) and at 48 hours post-treatment as a box and whisker plot (B) Different letters indicate significant difference between treatment means from one-way ANOVA ($p < 0.005$). FEF-CM: Fetal dermal fibroblasts, FEC-CM: Fetal anlage chondrocytes, IZ-CM: Fetal interzone cells conditioned media, negative control (BSA medium) and positive control (FBS medium).

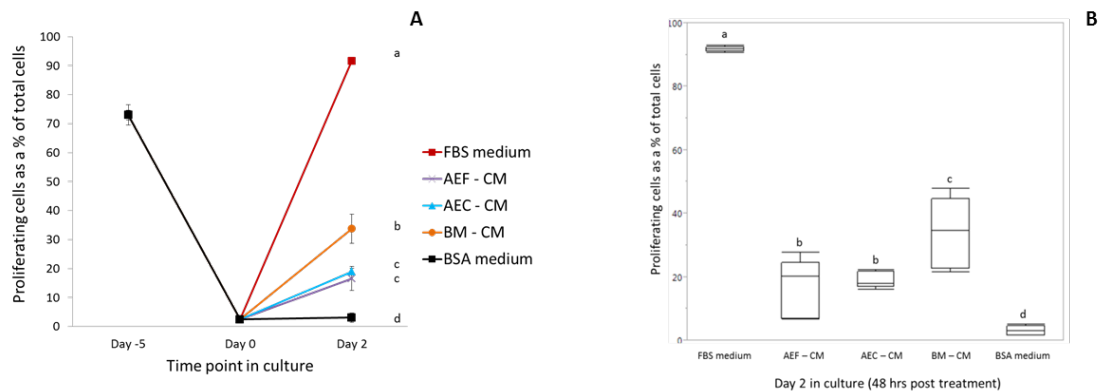


Figure 3.4: Percent change in proliferation of interzone cells in response to control and adult cell derived conditioned media over the time course of the experiment as a line graph (A) and at 48 hours post-treatment as a box and whisker plot (B) Different letters indicate significant difference between treatment means from one-way ANOVA ($p < 0.005$). AEF-CM: Adult dermal fibroblasts, AEC-CM: Adult articular chondrocytes and BM-CM: Bone marrow derived cells conditioned media, negative control (BSA medium) and positive control (FBS medium).

Medium type	Mean \pm SE
FBS medium (Fetal)	94.49 \pm 0.90
FEF - CM	39.52 \pm 6.08
FEC - CM	37.40 \pm 10.49
IZ - CM	15.37 \pm 1.56
BSA medium (Fetal)	9.27 \pm 1.36
FBS medium (Adult)	91.73 \pm 0.35
AEF - CM	16.60 \pm 4.14
AEC - CM	18.97 \pm 1.15
BM - CM	33.76 \pm 5.02
BSA medium (Adult)	3.09 \pm 0.64

Table 3.4: Table showing the mean and standard error values of percent change in proliferation in control and all experimental groups tested. These data are presented graphically in Figure 3.3 and 3.4. FEF-CM: Fetal dermal fibroblasts, FEC-CM: Fetal anlage chondrocytes, IZ-CM: Fetal interzone cells, AEF-CM: Adult dermal fibroblasts, AEC-CM: Adult articular chondrocytes and BM-CM: Bone marrow derived cells conditioned media, negative control (BSA medium) and positive control (FBS medium).

Viability

Cell viability was assessed by counting the number of live cells and was expressed as a percent of the total number of cells. Interzone cells in the different fetal cell conditioned media and positive control medium showed significantly greater viability (>99%) relative to those in the negative control serum-free medium, which still retained cell viability at more than 95% (Figure 3.5, 3.6 and Table 3.5). Interzone cells in the adult cell conditioned medium and positive control medium were significantly more viable compared to negative control medium. In the experimental groups, there was

some variation in the percent viability (Figure 3.7 and Table 3.5). However, it is worth noting that the lowest percent viability observed in our study was 94% indicating that a large majority of the cells remained viable within the time frame studied despite removal of FBS or another supplemental source of growth factors.

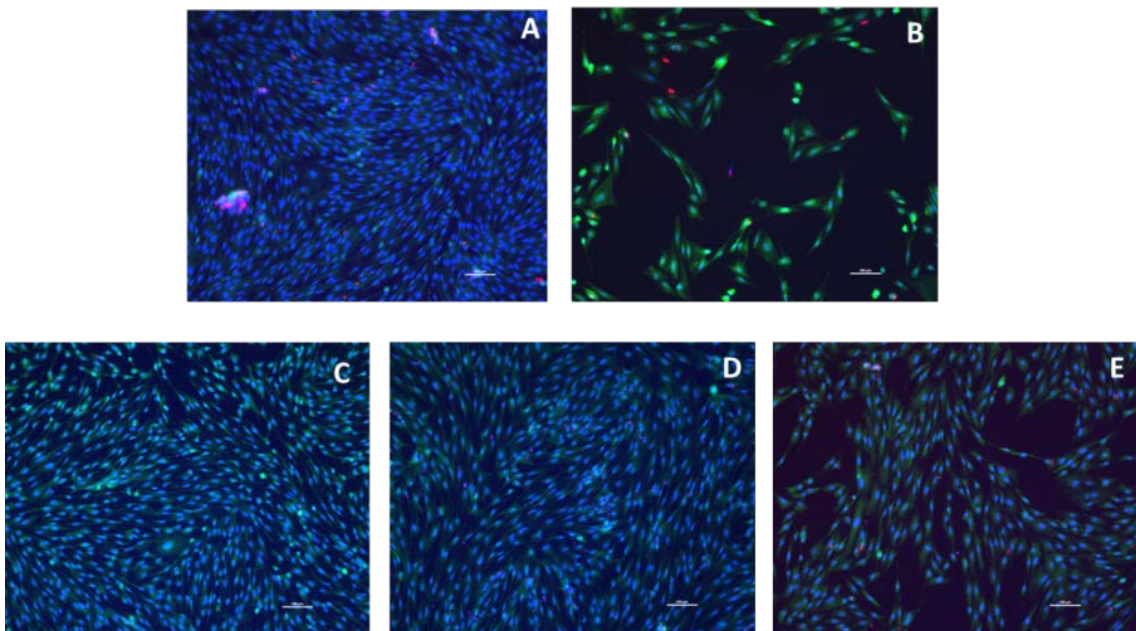


Figure 3.5: Panel (10x) showing the change in viability of interzone cells in response to positive control/FBS medium (A), negative control/BSA medium (B), Fetal dermal fibroblast (C), Fetal anlage chondrocyte (D), and fetal interzone (E) conditioned media. Cytoplasm of live cells appears green and dead cell nuclei stain red. All cells were counterstained with DAPI nuclear stain (blue).

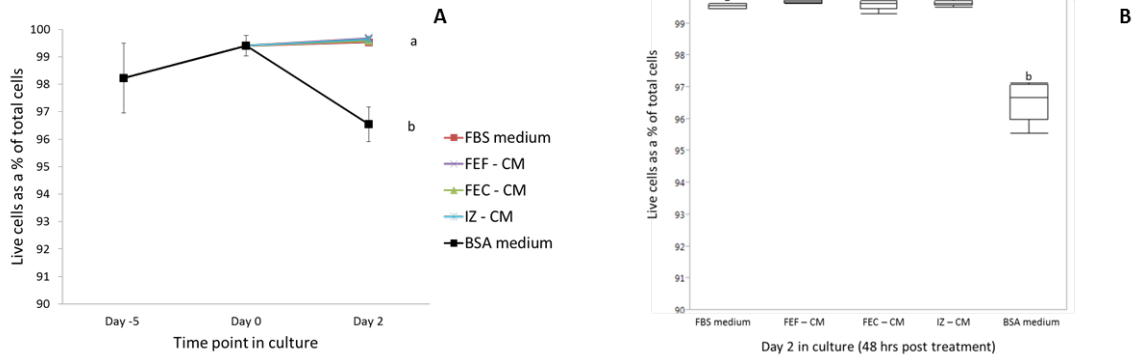


Figure 3.6: Percent viability of interzone cells in response to control and fetal cell derived conditioned media over the time course of the experiment as a line graph (A) and at 48 hours post-treatment as a box and whisker plot (B) Different letters indicate significant difference between treatment means from one-way ANOVA ($p < 0.005$). FEF-CM: Fetal dermal fibroblasts, FEC-CM: Fetal anlage chondrocytes, IZ-CM: Fetal interzone cells conditioned media, negative control (BSA medium) and positive control (FBS medium).

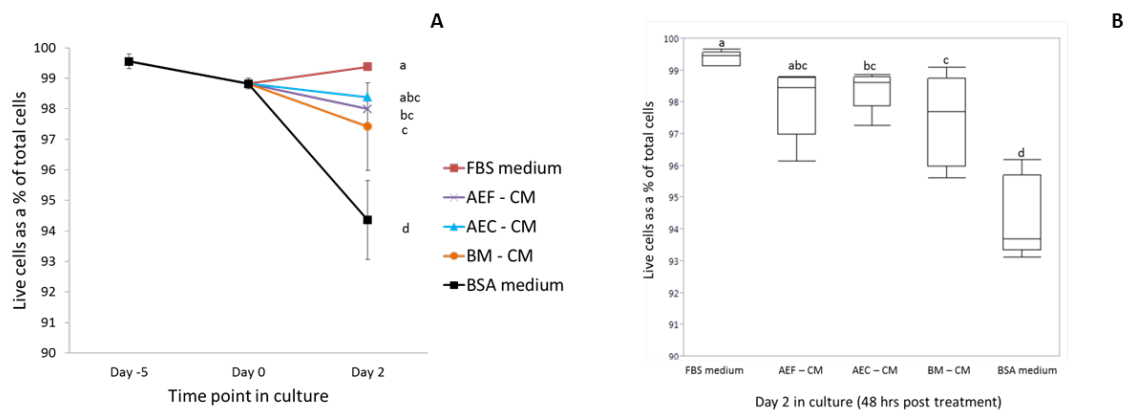


Figure 3.7: Percent viability of interzone cells in response to control and adult cell derived conditioned media over the time course of the experiment as a line graph (A) and at 48 hours post-treatment as a box and whisker plot (B) Different letters indicate significant difference between treatment means from one-way ANOVA ($p < 0.005$). AEF-CM: Adult dermal fibroblasts, AEC-CM: Adult articular chondrocytes and BM-CM: Bone marrow derived cells conditioned media, negative control (BSA medium) and positive control (FBS medium).

Medium type	Mean \pm SE
FBS medium (Fetal)	99.54 \pm 0.08
FEF - CM	99.67 \pm 0.05
FEC - CM	99.58 \pm 0.17
IZ - CM	99.63 \pm 0.09
BSA medium (Fetal)	96.55 \pm 0.63
FBS medium (Adult)	99.37 \pm 0.23
AEF - CM	97.99 \pm 1.11
AEC - CM	98.38 \pm 0.64
BM - CM	97.42 \pm 1.44
BSA medium (Adult)	94.36 \pm 1.29

Table 3.5: Table showing the mean and standard error values of percent viability in control and all experimental groups tested. These data have been presented graphically in Figure 3.6 and 3.7. FEF-CM: Fetal dermal fibroblasts, FEC-CM: Fetal anlage chondrocytes, IZ-CM: Fetal interzone cells, AEF-CM: Adult dermal fibroblasts, AEC-CM: Adult articular chondrocytes and BM-CM: Bone marrow derived cells conditioned media, negative control (BSA medium) and positive control (FBS medium).

Differential cellular response to the same level of mitogenic stimuli

Proliferation

The different cell lines demonstrated a positive but variable mitogenic response when exposed to the same conditioned medium. Fetal dermal fibroblasts showed a significantly higher response compared to skeletal cell types. Fetal anlage chondrocytes showed significantly lower percent proliferation relative to other fetal cell types (Figure 3.8A). The adult skeletal cell types showed lower percent proliferation relative to the non-skeletal dermal fibroblasts which demonstrated the greatest response to mitogenic stimuli comparable to that from serum containing FBS medium (Figure 3.8B).

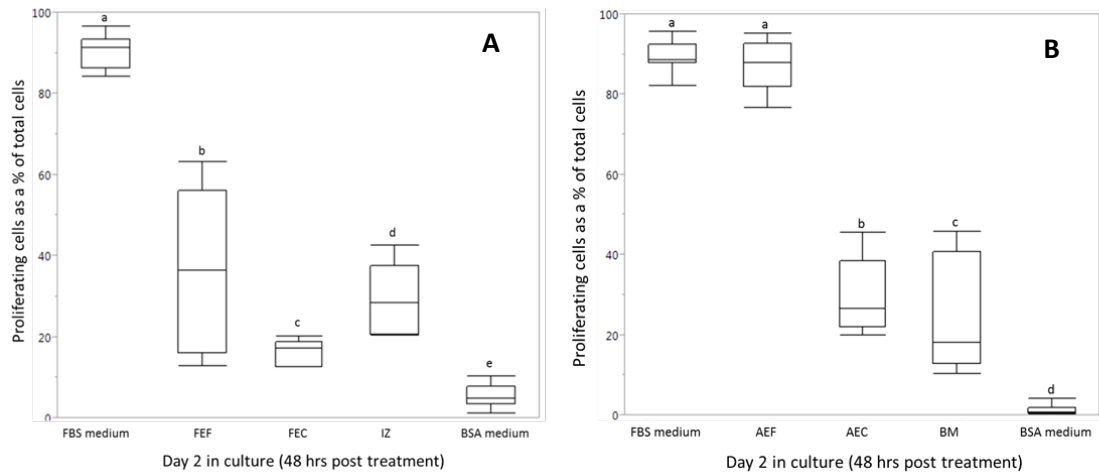


Figure 3.8: Box and whiskers plot representing the percent change in proliferation of fetal (A) and adult (B) cell types tested in response to fetal anlage chondrocyte conditioned medium at 48 hours post-treatment. Different letters indicate significant difference between treatment means from one-way ANOVA ($p < 0.005$). FEF: Fetal dermal fibroblasts, FEC: Fetal anlage chondrocytes, IZ: Fetal interzone cells, AEF: Adult dermal fibroblasts, AEC: Adult articular chondrocytes and BM: Bone marrow derived cells, negative control (BSA medium) and positive control (FBS medium).

Discussion

In this study, we examined how conditioned media, and thus, secreted paracrine signals from different cell lines, affected the proliferation and viability of interzone cells in co-culture. A change in the rate of proliferation could be a function of the difference in the mitogenic stimuli that the cells are exposed to as well as how the same stimulus is perceived by different cell types. Therefore, we assessed how the skeletal and non-skeletal cell types respond differentially to the same mitogenic stimuli. Additionally, we characterized an effect of donor age by comparing mitogenic potential of media conditioned by cells derived from equine fetuses and adult horses. The findings from

this study support the hypothesis that skeletal cell-derived paracrine signals have a mitogenic effect on interzone cells.

All experimental groups of conditioned media elicited a mitogenic response in interzone cells which fell between that from the positive and negative control media. In the fetal group, FEC - CM and FEF - CM showed a significantly higher mitogenic potential compared to IZ - CM. Among the adult cell conditioned media, BM - CM elicited a significantly higher response relative to AEC - CM and AEF - CM. The amount of paracrine signals delivered to the interzone cells in this study was normalized by using a uniform period of incubation and volume of conditioned medium throughout the study. However, normalization was performed based on the cells that were trypsinized and counted from the tissue culture flasks after collection of conditioned medium. This could contribute to the variation in mitogenic response that we observed in some of the experimental groups. Medium conditioned by both fetal and adult dermal fibroblasts elicited a robust mitogenic response in interzone cells, paralleling that of the corresponding chondrocyte-derived conditioned medium. Moreover, both fetal and adult dermal fibroblasts appear to be highly sensitive to mitogenic stimuli from fetal anlage chondrocytes compared to all other cell types. These findings along with the fact that fibroblasts readily propagate in adherent monolayer culture suggest that they could be more primed for proliferation signals [112-114].

Additionally, differential production of mitogenic factors by fetal versus adult cells was evaluated. Conditioned media derived from fetal chondrocytes were significantly more mitogenic (with a mean percent proliferation of 38 ± 2.33) compared to those

from adult chondrocytes (19 ± 0.92) (p value = 0.0035). Conditioned media derived from fetal fibroblasts (40 ± 1.42) elicited significantly higher mitogenic response relative to adult fibroblasts (17 ± 3.45) (p value = 0.0008). Our data indicate that paracrine stimuli from fetal cells have a significantly higher mitogenic ability or are secreted in higher quantities compared to those from adult cells.

The conditioned medium system that we utilized in this study is a widely used indirect co-culture model for studying paracrine interactions between distinct cell populations. It provides several advantages over other co-culture models including the ability to control the period of incubation and the volume of conditioned medium, and thus the quantity of paracrine signals delivered to the cells. Additionally, the distinct physical locations of the cells allow tracking of the phenotypic and genotypic changes in the signal receiving cell and the directionality of signaling pathways [98, 115-118]. We found this co-culture model to be useful for assessing the mitogenic potential of paracrine signals from all the cell types tested.

The data summarized above suggests a paracrine signaling between the interzone cells and the skeletal microenvironment which induce these cells to proliferate in culture. In the transplantation studies in the axolotl salamander (discussed in Chapter 2), cells within the new interzone layer of the accessory joint stain positively by GFP immunostaining indicating that they are derived directly from the transplanted interzone tissue. Our *in vitro* findings support a model whereby the transplanted interzone cells proliferate to maintain an interzone pool, in response to paracrine signals from the skeletal environment of the bone diaphysis. Further mechanistic studies will

be valuable in elucidating the signaling pathways and specific signaling molecules that are involved in regulating this paracrine interaction between interzone cells and their environment. Many of the processes and regulatory pathways involved in development are recapitulated during repair. Although the precise origin, fate and role of interzone cells in joint development is still unclear, a multitude of growth factors, signaling proteins and transcription factors have been shown to be involved in interzone cell specification and its function as the progenitors of joint tissues [47, 50, 78]. These could be potential candidates as regulators of cellular paracrine interactions between interzone and its environment.

Studies reported in this chapter were aimed at evaluating an effect of microenvironmental paracrine factors on interzone cell proliferation. However, cell proliferation is not an independent event in development, and may actually occur closely with the fundamental processes of cell differentiation and migration, often involving some degree of overlap. In the developing embryo, the unspecialized progenitor cells proliferate and increase in number, and subsequently differentiate into specialized cells. There is concurrent physical migration of the cells to the appropriate anatomical location which is essential for patterning of the embryo. This is regulated by both internal factors as well as external signals from the microenvironment. These cellular and secreted signals play a vital role in mediating the communication between cells [95-97, 119, 120]. The accessory joint that formed in the tibial CSD with the interzone transplants was spatially patterned with cartilaginous structures that showed cellular morphologies resembling those of epiphyseal/articular and metaphyseal

chondrocytes. GFP immunostaining confirmed their origin from the original interzone transplant tissue. These findings suggest that interzone cells could be differentiating into multiple cell types with the paracrine signals from the skeletal microenvironment acting as differentiation cues. Experiments in the following chapter focus on evaluating an effect of skeletal paracrine signals on chondrogenic differentiation of interzone cells.

Chapter 4

Effect of skeletal paracrine signals on the chondrogenic differentiation of interzone cells

Introduction

Articular cartilage injuries do not heal completely in mammals, often resulting in progressive joint degeneration, and are associated with significant joint dysfunction and disability. Current regenerative approaches in attempts to restore cartilage integrity in lesioned areas involve the use of stem or mesenchymal cells co-delivered with the appropriate extracellular matrix and trophic signaling molecules in order to 'engineer' a normal hyaline cartilage repair tissue. Several adult multipotent cells and embryonic stem cells have been explored as potential sources for cell-based joint therapy [8, 13, 14, 20, 121-123]. Interzone cells have attracted attention since they represent the normal progenitor of diarthrodial joints during development, forming the articular cartilage, synovial membrane and associated joint structures [48, 77, 89]. They have also been implicated in the repair of experimentally generated cartilage lesions in axolotl salamanders as described in Chapter 2 and reported previously [79, 80]. In addition, interzone cells remain viable when transplanted into a critical size skeletal defect and form a *de novo* joint. This accessory joint exhibits accurate spatial patterning as seen in a normal diarthrodial joint with an interzone positioned between two cartilaginous columns that include cells morphologically resembling both epiphyseal/articular and metaphyseal chondrocytes. At the time of the original surgery, interzone transplants were placed in random orientation in the axolotl salamanders.

However, approximately 7 months later, the cells that comprised the new accessory joint formed at the transplant site in the tibia diaphysis exhibited tissue organization resembling that of an intact joint. These findings suggest two things. First, that the axolotl interzone cells have an ability of self-renewal and multipotent differentiation that is characteristic of 'stem cells' [124, 125]. Second, that a local level of regulation and crosstalk exists between the transplanted interzone cells and the skeletal microenvironment. The end result was the *de novo* joint with accurate anatomical orientation and organization of tissue types. In contrast, the interzone cells placed in a non-skeletal site have limited viability and do not appear to differentiate into other cell types suggesting an absence of supportive trophic signals in the non-skeletal microenvironment. Taken together, these data suggest a vital role of the skeletal microenvironment in contributing to and regulating the interzone-mediated repair of both a large joint lesion [79] and critical sized diaphyseal defect ([80] and Chapter 2).

Many of the processes and mechanisms of tissue repair resemble events that occur during normal embryogenesis. Undifferentiated progenitor cells in the developing embryo proceed through the processes of proliferation, migration, and differentiation to give rise to diverse and multiple cell types in the body [95-97, 119, 120]. Chondrogenic differentiation is a critical process in the development of the embryonic skeleton. Chondrocytes are derived from mesodermal skeletal progenitor cells that proceed through successive steps of lineage commitment and differentiation to become highly specialized tissues including bone and several different types of cartilage. Chondrocyte fate decisions and functions are tightly regulated in a spatial and temporal

manner by numerous extrinsic and intrinsic regulatory factors. While many of the molecular and biomechanical mechanisms that govern chondrocyte differentiation continue to be areas of active research, it is clear that changing the type and strength of these extracellular signals allow diversity in the ultimate outcome. Differentiation of chondrocytes from embryonic precursor cells is also associated with expression of two genes that encode major cartilage matrix components - type II collagen (*COL2*) and aggrecan (*ACAN*) core protein, both of which represent traditional biomarkers for cartilage [71, 126, 127].

Based on our observations from the transplantation studies in axolotl salamanders described in Chapter 2, fate of the transplanted interzone cells appears to depend on the cellular environment, likely reflecting at least in part differences in paracrine signals. A better understanding of these signals may prove relevant when considering interzone cells as a potential new cell type for tissue-engineering in cartilage repair. In this chapter, we employed a mammalian co-culture model to test the hypothesis that skeletal cell-derived paracrine signals induce interzone cells to differentiate along a chondrogenic lineage, an effect mediated at least in part by soluble paracrine factors originating from the skeletal cells. Conditioned media were generated and normalized as described previously in Chapter 3, but interzone cells were maintained in high density pellet cultures to promote chondrogenic differentiation [128, 129].

Materials and methods

Isolation and culture of cells

Collection and isolation of primary cells from fetal and adult tissues were performed as described in Chapter 3. A total of six primary cell lines isolated from five equine fetuses and five young adult horses were used. This sample set included four cell types derived from skeletal tissues along with fibroblasts from skin as a control:

- | | | |
|---|---|--------------------|
| 1. Adult articular chondrocytes (AEC) | } | Skeletal cells |
| 2. Adult bone marrow derived cells (BM) | | |
| 3. Fetal anlage chondrocytes (FEC) | | |
| 4. Fetal interzone cells (IZ) | | |
| 5. Adult dermal fibroblasts (AEF) | } | Non-skeletal cells |
| 6. Fetal dermal fibroblasts (FEF) | | |

In addition, a sample of articular cartilage and dermis harvested from an age matched horse were snap frozen in liquid nitrogen for the subsequent isolation of total RNA to be used as control samples for gene expression analyses.

Co-culture

Media conditioned by fetal and adult primary cell lines of both skeletal and non-skeletal tissue origins were the source of paracrine signals. Interzone cells in high

density pellet cultures were used as the signal responders in all experiments as outlined in Table 4.1.

Medium type	Biological replicates (n)	Technical replicates (n)	Gene expression analyses	Histological analyses
Fetal anlage chondrocytes (FEC - CM)	5	10	6	4
Fetal dermal fibroblasts (FEF - CM)	5	10	6	4
Fetal interzone cells (IZ - CM)	5	10	6	4
Adult articular chondrocytes (AEC - CM)	5	10	6	4
Adult Bone marrow derived cells (BM - CM)	5	10	6	4
Adult dermal fibroblasts (AEF - CM)	5	10	6	4
Positive control (Chondrogenic induction medium)	5	9	6	3
Negative control (Basal medium)	5	9	6	3

Table 4.1: Description of biological and technical replicates in experimental and control groups. FEF-CM: Fetal dermal fibroblasts, FEC-CM: Fetal anlage chondrocytes, IZ-CM: Fetal interzone cells, AEF-CM: Adult dermal fibroblasts, AEC-CM: Adult articular chondrocytes and BM-CM: Bone marrow derived cells conditioned media.

To generate P3 interzone cell pellets, thawed P2 cells were plated in complete medium (Dulbecco's Modified Eagles Medium [DMEM, Gibco, Cat# 10569044] supplemented with 10% (v/v) heat inactivated Fetal Bovine Serum, 1% (v/v) P/S, and 1% amphotericin B) with the medium being replenished every 48 hours. At 65-70% confluence, the cells were trypsinized, washed twice in serum free medium, and resuspended in the appropriate test conditioned medium or control medium at 500,000 cells per ml. One milliliter of cell suspension was then transferred to a 1.5 ml

polypropylene microcentrifuge tube and centrifuged at 500g for 3 minutes to generate a cell pellet as previously described [130-132]. After 48 hours, each pellet was transferred from the tube to an individual well of a 1% Poly (2-hydroxyethyl methacrylate) (polyHEMA; Sigma Cat# P3932) coated 24-well plate. The polyHEMA coating enabled anchorage-independent growth of the pellets by preventing adhesion of the pellets to the surface of the well. The pellets were maintained in the appropriate test conditioned medium or control medium for 21 days with re-feeding every 48 hours.

Conditioned Medium and Controls

Preparation, processing, and normalization of conditioned medium were performed as described in Chapter 3. A total of 100 ml of conditioned media was generated from each biological replicate at 5 ml per T-75 flask to obtain sufficient volume for maintaining pellets for 21 days in culture.

Chondrogenic induction medium was used as the positive control and comprised of DMEM, 1% penicillin/streptomycin, 1.25 mg/ml bovine serum albumin, 1x ITS-A growth supplement (Thermo Fisher Scientific, Cat# 51300044), 1x non-essential amino acids, 100 nM dexamethasone, 50 µg/ml ascorbate-2-phosphate, and 10 ng/ml rhTGFβ1 (EMD Millipore, Cat# GF111) [131-135]. To optimize the negative control medium, interzone cell pellets were incubated in defined media with different components of the chondrogenic induction medium as outlined in Table 4.2, followed by an assessment of chondrogenic differentiation by morphological examination and matrix proteoglycan staining. The objective was to identify a recipe that was as close as possible to the

positive control chondrogenic induction medium without actually inducing chondrogenesis.

	A	B	C	D
DMEM + 1%P/S	+	+	+	+
BSA	+	+	+	+
A2P		+	+	+
TGFβ1				+
Dexamethasone				+
ITS-A			+	+
NEAA		+	+	+

Table 4.2 outlining the composition of types of defined media used to identify the negative control medium. Group D is the chondrogenic induction/ positive control medium.

Histological examination

The interzone cell pellets cultured for 21 days in each experimental medium preparation were pooled and then randomly allocated to either histology or gene expression subgroups. For histological analyses, the pellets were fixed in 4% paraformaldehyde for 24 hours followed by pre-embedding in 2% agar/2.5% gelatin blocks at 2-3 pellets per block [136]. The blocks were then fixed in 4% paraformaldehyde for 24 hours prior to storage in 70% ethanol for histological processing. Paraffin-embedded blocks were sectioned at 5 μm and stained with either Hematoxylin and Eosin (H&E) to assess pellet architecture or Safranin-O for proteoglycan content and distribution as described below. Analysis of pellet

morphology and staining patterns were completed in consultation with a board certified pathologist (Dr. Jennifer Janes, personal communication).

Proteoglycan staining and quantification

Safranin-O is a stoichiometric cationic dye which in its orthochromatic form binds to the sulfate groups of proteoglycan molecules in a 1:1 fashion, making it semi-quantitative [137-139]. Thus, the intensity of staining or 'redness' is approximately proportional to the proteoglycan content assuming the overall negative charge distribution of proteoglycans is uniform across all samples. All sections were stained with 0.1% Safranin-O and a Fast Green counterstain in two batches to reduce inter-batch technical variation. Adult equine articular cartilage was included as a positive control calibration sample in both batches and randomly placed in each 30-slide rack. Mounted sections were imaged with a Nikon Eclipse Ti microscope at 10x in a darkened room to minimize ambient light.

The 'redness' values of Safranin-O stained sections were measured using ImageJ Fiji software (<https://imagej.nih.gov/ij/download.html>) with the same microscope exposure and brightness settings maintained for all measurements. Red balancing was performed to correct for the background from white microscope source light. The contrast level for each pellet after red balancing was fixed and the color image was split into its corresponding red, green, and blue channels, thus effectively eliminating the interference from the green and blue background. A histogram which linearly mapped the pixel values in the image to values ranging from 0 - 255 was generated for the red

channel for each image. The mean integrated density value which is a product of the area and the mean pixel value was computed for the red channel for each image and recorded for all samples.

Gene expression analysis

At the end of the 21 day culture period, pellets that had been randomly selected for gene expression analysis were rinsed with PBS and snap frozen in liquid nitrogen in batches of 3 pellets. These samples were stored at -80°C for subsequent total RNA extraction. Pellets were homogenized, starting while they were still frozen, in 2 ml of Qiazol® (Qiagen, Cat# 79306), a guanidinium thiocyanate-phenol-chloroform extraction reagent (3 pellets/2ml). Total RNA was isolated using a spin column-based kit with modifications as previously described [140]. RNA samples were purified by ethanol precipitation to remove any residual processing contaminants and quantified by fluorescence using the Qubit BR Assay or Qubit HS Assay (Life Technologies®, Cat# Q10210, Q32852). The removal of any potential contaminating genomic DNA followed by reverse transcription of total RNA to generate cDNA were performed using a commercially available kit (Maxima First Strand cDNA Synthesis Kit® for RT-qPCR with dsDNase, Life Technologies, Cat# K1672) according to the manufacturer's protocol. The resulting cDNA was uniformly diluted to 0.67ng/μl with nuclease-free water and stored at -20°C in 100 μl aliquots. The quantity of total RNA isolated from the pellet samples was a limiting variable in the number of transcripts that could be analyzed by RT-PCR. To maximize this number, we compared three low input quantities of RNA for their

feasibility and reproducibility in template amplification. 3 ng of template per reaction was identified as the lowest template amount that could be reliably amplified (data not shown). Commercially available, validated equine-specific TaqMan® primer probe sets, listed in Table 4.3, were used to quantitate steady state mRNA levels of *ACAN*, *COL1A1* and *COL2A1* genes. After evaluating four commercially available equine-specific endogenous control gene primer-probe sets, β 2 microglobulin (B2M) was selected as the endogenous control, because it exhibited the most uniform level of expression across the experimental groups as recommended in MIQE guidelines [141]. The reactions were performed in 384 well plates in a total reaction volume of 10 μ l. Nuclease-free water and a minus reverse transcriptase reaction served as the negative control samples. Positive control and calibrator samples were a single age-matched sample of dermis (Dermis) for the analysis of *COL1A1* expression and articular cartilage tissue (AAC) for the analysis of *ACAN* and *COL2A1* expression. All samples were analyzed in triplicate and randomly assigned to each plate to control for any plate effects. Reactions were performed on a robotic ViiA™ 7 Real-Time PCR System (Thermo Fisher Scientific). Reaction amplification efficiencies were evaluated using LinRegPCR [142] and then used to correct cycle threshold measurements for each sample. Relative expression values (RE; relative quantity, RQ) of the transcript targets were calculated using the $2^{-\Delta\Delta C_t}$ method [143].

Gene symbol	Gene name	Catalog #	Catalog ID	Amplicon length	Exons spanned	NCBI EquCab 2.0 Coordinates
<i>B2M</i>	Beta-2-microglobulin	4331182	Ec03468699_m1	70	1-2	Chr.1: 144492381 - 144497809
<i>COL2A1</i>	Collagen Type II alpha 1	4351372	Ec03467416_m1	73	52-53	Chr.6: 65629017 - 65660099
<i>COL1A1</i>	Collagen Type I alpha 1	4351372	Ec03469680_m1	138	9-10	Chr.11: 25913092 - 25929428
<i>ACAN</i>	Aggrecan core protein	4351372	Ec03469667_m1	72	1-2	Chr.1: 94344146 - 94381944

Table 4.3 listing the details of the TaqMan® primer probe sets used in the qPCR reactions.

Statistical analysis

Redness values and individual InRQ values from the qPCR data were independently evaluated by one-way analysis of variance. Medium type (conditioned and control media) was the factor being tested at the following levels - Conditioned medium from Fetal dermal fibroblasts (FEF-CM), Fetal anlage chondrocytes (FEC-CM), Fetal interzone cells (IZ-CM), Adult dermal fibroblasts (AEF-CM), Adult articular chondrocytes (AEC-CM) and Bone marrow derived cells (BM-CM) and negative (basal medium), and positive control (chondrogenic induction medium). Pair-wise comparisons were made between the different levels with Tukey's *post hoc* correction for multiple comparisons. Significance was defined at $p < 0.05$. Residual plots, histograms of residuals and Q-Q plot of residuals were evaluated to ensure that the normality assumptions were not violated.

Results

Controls

Figure 4.1 shows histological images of interzone pellets from the different defined media stained with Safranin O and a Fast Green counterstain to identify the optimal negative control medium. Proteoglycan molecules stain red with Safranin O, while a bluish green color from the Fast Green counterstain is observed when there is an absence of proteoglycan. Positive matrix staining was observed only in the fully constituted chondrogenic medium. Therefore, the media formulation used to culture Group C pellets, comprised of all components of the chondrogenic positive control medium minus *TGF β 1* and dexamethasone, was selected for negative controls. This medium was the closest in composition to the positive control medium, but did not demonstrate any evidence by histological assessment of chondrogenic differentiation.

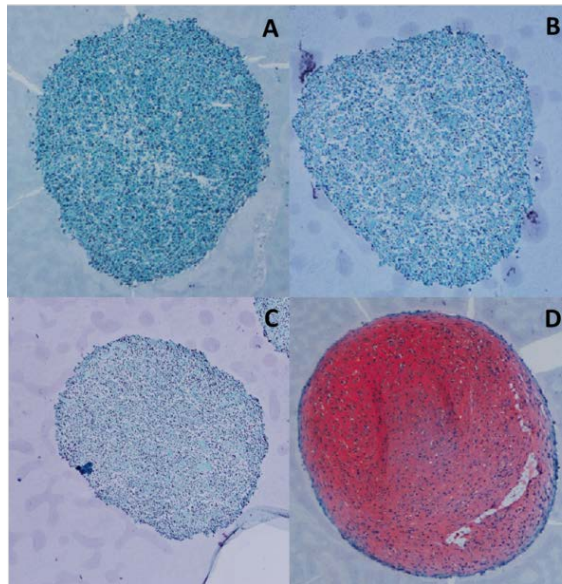


Figure 4.1 showing Safranin-O stained images of interzone pellets in defined media with selected components of chondrogenic induction medium outlined in Table 4.2 (A-C). Positive staining was observed only in the chondrogenic medium (D). All images are at 10x (objective lens) magnification.

Macroscopic assessment of pellets

Interzone pellets in the experimental and control groups maintained their shape and integrity throughout the period of culture. Pellets showed minimal variation in size with the positive and negative control pellets appearing slightly larger than others. Figure 4.2 shows their relative sizes on a 1 mm increment scale.

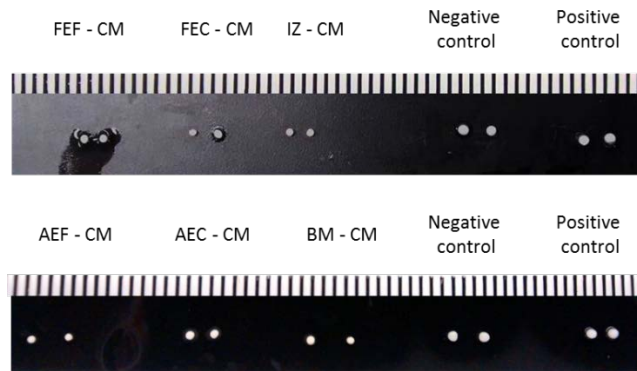


Figure 4.2 showing the relative sizes of pellets cultured in conditioned and control media. FEF-CM: Fetal dermal fibroblasts, FEC-CM: Fetal anlage chondrocytes, IZ-CM: Fetal interzone cells, AEF-CM: Adult dermal fibroblasts, AEC-CM: Adult articular chondrocytes and BM-CM: Bone marrow derived cells conditioned media.

Morphological examination of pellets

Figure 4.3 and 4.4 present representative images of pellets from control and all experimental groups of conditioned media, respectively. In the positive control chondrogenic medium, interzone cell pellets showed an outer cell-dense rim of spindle shaped cells with minimal cell matrix. This was followed by a middle zone of low cellularity (approximately 3-7 cell layers thick) comprising polygonal to spindle shaped cells with round to oval nuclei often found within lacunae, separated by a lightly basophilic matrix. The center of the pellet was composed of what appeared to be necrotic cells and debris within an acidophilic matrix. This pellet core was variably sized

across biological replicates. In contrast, this zonal appearance was absent to minimal in pellets maintained in the negative control medium. Pellets appeared irregular in shape and lacked a cell-dense outer rim. Spindle shaped to oval cells with round basophilic nuclei were observed distributed non-uniformly throughout the basophilic and sometimes fibrillar matrix of the pellets. Necrotic areas and debris with admixed polygonal cells were seen unevenly distributed in the negative control pellets.

Fetal cell lines

Fetal dermal fibroblast conditioned medium (FEF-CM): Pellets showed a single layer of spindle shaped cells along the outer rim. Islands of low to moderately acidophilic matrix with admixed oval to round cells were observed unevenly distributed throughout the pellet. All pellets showed focal areas of necrosis and cell debris.

Fetal anlage chondrocyte conditioned medium (FEC-CM): Streams of spindle shaped cells (approximately 2-5 cell layers thick) were observed along the periphery of all pellets. Some of the pellet samples comprised focal clusters of polygonal to round cells surrounded by a basophilic matrix. Areas of necrosis and cell debris were distributed throughout the pellet.

Fetal interzone cell conditioned medium (IZ-CM): Pellets were composed of paucicellular zones of lightly basophilic matrix with round to oval cells. Variably sized areas of necrotic cells and debris were distributed throughout the pellet. A zone of homogenous, acellular matrix was observed circumferentially bordering some of the pellets in this group.

Adult cell lines

Adult dermal fibroblast conditioned medium (AEF-CM): Pellets in this group showed a single layer of basophilic spindle cells arranged along the periphery. A zone of homogenous, acellular matrix was observed circumferentially under the outer rim in some samples. Variably sized areas of necrotic cells and debris were distributed throughout the pellets.

Adult articular chondrocyte conditioned medium (AEC-CM): Pellets were composed of an outer, densely cellular rim of spindle shaped cells with acidophilic cytoplasm. Necrotic cells and debris with admixed oval to round cells within a densely acidophilic matrix were distributed throughout the pellet. Pellets lacked a zonal organization.

Bone marrow derived cell conditioned medium (BM-CM): The architecture of pellets in this group was highly variable. All pellets showed an outer rim with spindle shaped cells. A thick rim of homogenous matrix populated by relatively few cells with round to oval nuclei and acidophilic cytoplasm was observed in some samples. Variably sized areas of necrosis and debris were observed towards the center of all pellets.

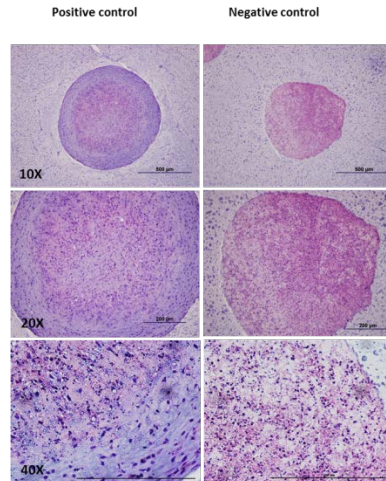


Figure 4.3: Panel showing hematoxylin and eosin stained sections of interzone pellets in positive and negative control media at different objective lens magnifications.

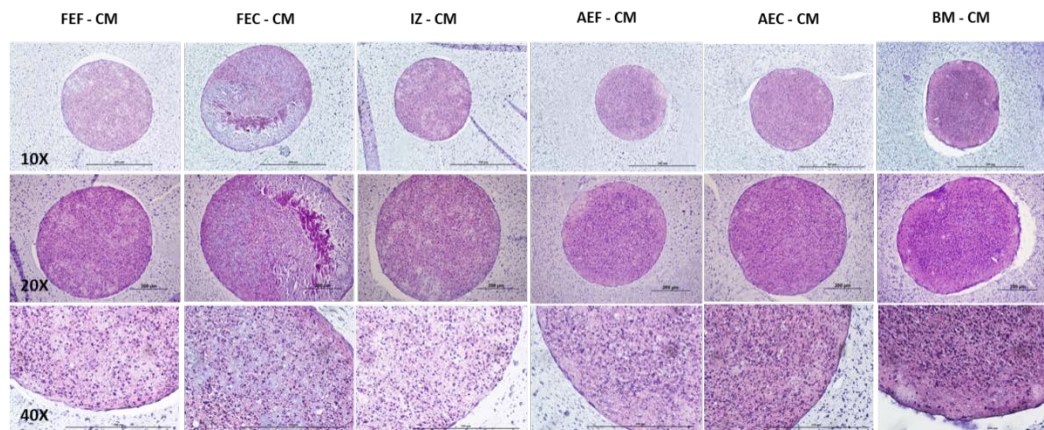


Figure 4.4: Panel showing hematoxylin and eosin stained sections of interzone pellets in conditioned media from FEF-CM: Fetal dermal fibroblasts, FEC-CM: Fetal anlage chondrocytes, IZ-CM: Fetal interzone cells, AEF-CM: Adult dermal fibroblasts, AEC-CM: Adult articular chondrocytes and BM-CM: Bone marrow derived cells at different objective lens magnifications as indicated at the left.

Proteoglycan staining and quantification

Staining was performed in two consecutive batches with all conditions being maintained uniform between batches. Figure 4.5 and 4.6 present representative images of pellets from control and all experimental groups of conditioned media, respectively.

The intensity of staining was quantified and recorded as the mean redness value as shown in Figure 4.7. Pellets in the positive control medium demonstrated significantly higher proteoglycan staining in comparison with the negative control and all experimental groups. The integrated density values were not significantly different between the conditioned media types.

Fetal cell lines

Pellets incubated in FEC-CM and IZ-CM demonstrated focal areas of marginally positive proteoglycan staining, however, there was considerable within-group variation in both groups. These islands of proteoglycan staining were composed of round to polygonal cells separated by lacunae. All pellets maintained in FEF-CM showed an absence of proteoglycan staining.

Adult cell lines

Pellets from AEC-CM and BM-CM demonstrated faint proteoglycan staining with round to oval cells, but the response was not uniform across all biological replicates of each group and did not reach statistical significance. Pellets in AEF-CM did not show any evidence of staining for matrix proteoglycans.

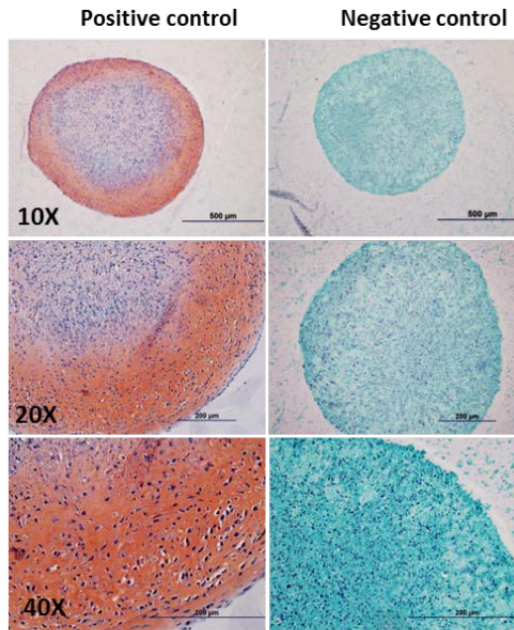


Figure 4.5: Panel showing Safranin O – Fast green stained sections of interzone pellets in positive and negative control media at different objective lens magnifications as indicated.

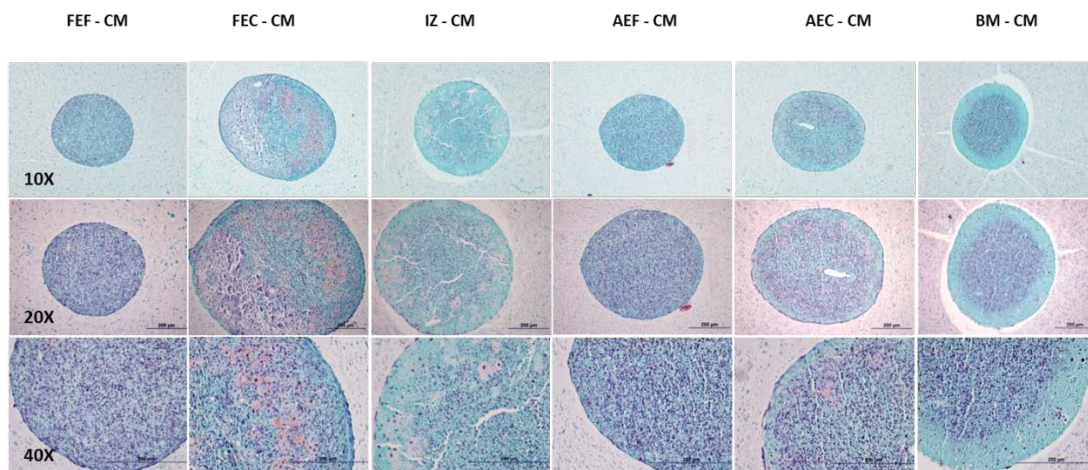


Figure 4.6: Panel showing Safranin O – Fast green stained sections of interzone pellets in conditioned media from FEF-CM: Fetal dermal fibroblasts, FEC-CM: Fetal anlage chondrocytes, IZ-CM: Fetal interzone cells, AEF-CM: Adult dermal fibroblasts, AEC-CM: Adult articular chondrocytes and BM-CM: Bone marrow derived cells at different objective lens magnifications as indicated at the left.

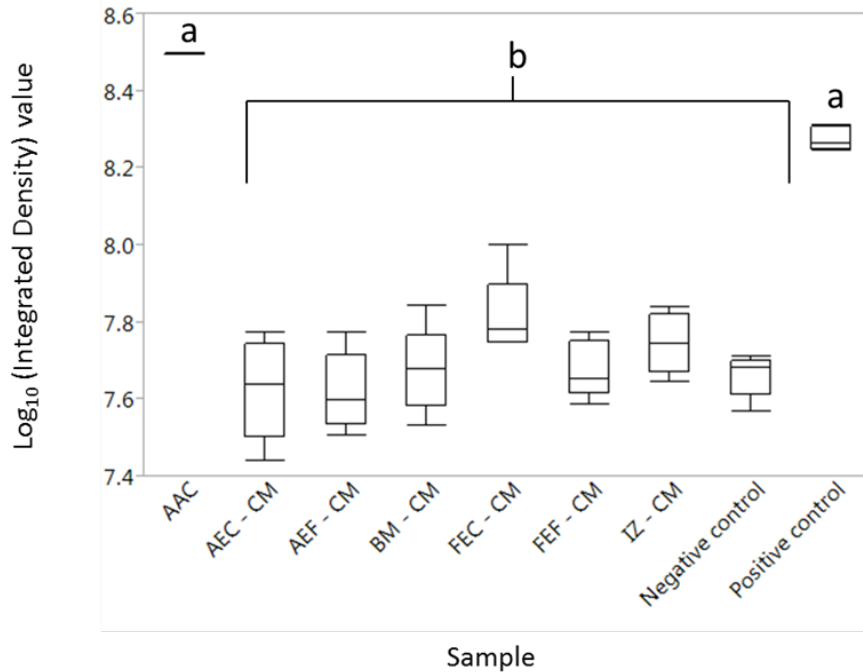


Figure 4.7: Semi-quantitative evaluation of proteoglycan staining – Box and whiskers plot depicting the \log_{10} of Integrated density values of pellets in control and conditioned media. FEC-CM: Fetal dermal fibroblasts, FEC-CM: Fetal anlage chondrocytes, IZ-CM: Fetal interzone cells, AEF-CM: Adult dermal fibroblasts, AEC-CM: Adult articular chondrocytes and BM-CM: Bone marrow derived cells conditioned media. AAC – Adult articular cartilage tissue PC – positive control medium, NC – negative control medium. Different letters indicate significant differences between groups.

Gene expression analysis

Aggrecan core protein (ACAN)

Articular cartilage tissue consistently expresses high levels of ACAN. As expected, ACAN mRNA expression was higher in articular cartilage tissue (AAC) compared to all other groups (Figure 4.8; Table 4.4) and was used as the calibrator sample. The cell pellets maintained in chondrogenic medium (positive control; PC) showed significantly higher levels of ACAN expression than all other media types, approaching that of AAC. Pellets from the fetal cell-derived conditioned media exhibited significantly greater expression levels relative to the negative control (NC) pellets. Interestingly, among the

types of conditioned media, the highest level of *ACAN* expression was seen in pellets in FEC-CM relative to negative control ($p < 0.001$).

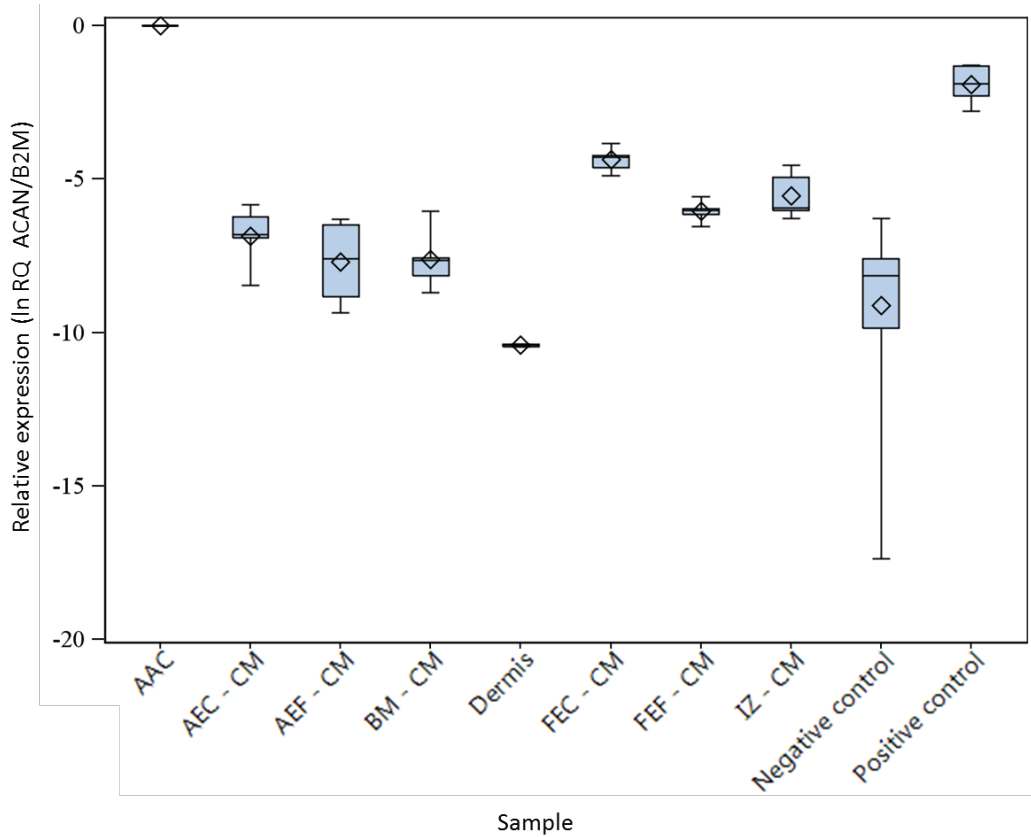


Figure 4.8: Box and whiskers plot illustrating steady state mRNA expression of *ACAN* in pellets from conditioned and control media relative to articular cartilage tissue (set to 0). Diamonds within the box plot represent the group mean. FEF-CM: Fetal dermal fibroblasts, FEC-CM: Fetal anlage chondrocytes, IZ-CM: Fetal interzone cells, AEF-CM: Adult dermal fibroblasts, AEC-CM: Adult articular chondrocytes and BM-CM: Bone marrow derived cells conditioned media. AAC – Adult articular cartilage tissue, PC – positive control medium, NC – negative control medium. Diamonds within the box plot represent the group mean.

Medium type/ACAN	AAC	AEC - CM	AEF - CM	BM - CM	Dermis	FEC - CM	FEF - CM	IZ - CM	NC	PC
AAC		0.0002	<.0001	<.0001	<.0001	0.0518	0.0015	0.0047	<.0001	0.8504
AEC - CM			0.9965	0.9985	0.1996	0.3023	0.9982	0.9453	0.2295	<.0001
AEF - CM				1	0.5622	0.0479	0.8046	0.4849	0.8193	<.0001
BM - CM					0.516	0.0601	0.8508	0.5455	0.7607	<.0001
Dermis						0.0015	0.0527	0.0196	0.9852	<.0001
FEC - CM							0.7919	0.9708	<.0001	0.1516
FEF - CM								1	0.0284	0.0008
IZ - CM									0.0056	0.0047
NC										<.0001
PC										

Table 4.4 listing the *p*-values of differences in ACAN expression as measured by steady state levels of mRNA in different media types. Significant differences are depicted by pink shading ($p < 0.05$ – Tukey’s post hoc correction). FEF-CM: Fetal dermal fibroblasts, FEC-CM: Fetal anlage chondrocytes, IZ-CM: Fetal interzone cells, AEF-CM: Adult dermal fibroblasts, AEC-CM: Adult articular chondrocytes and BM-CM: Bone marrow derived cells conditioned media. AAC – Adult articular cartilage tissue, PC – positive control medium, NC – negative control medium.

Type II collagen (COL2A1)

Expression patterns of *COL2A1* mRNA were similar to that of *ACAN* in all media and tissue types tested (Figure 4.9; Table 4.5). Steady state mRNA levels of *COL2A1* were significantly higher in AAC and positive control pellets in comparison with all other groups. In general, pellets in the fetal conditioned media exhibited higher levels of expression relative to the adult set. Interestingly, *COL2A1* mRNA levels were significantly higher in pellets maintained in FEC-CM ($p = 0.0082$) and IZ-CM ($p = 0.001$) relative to those in the negative control medium.

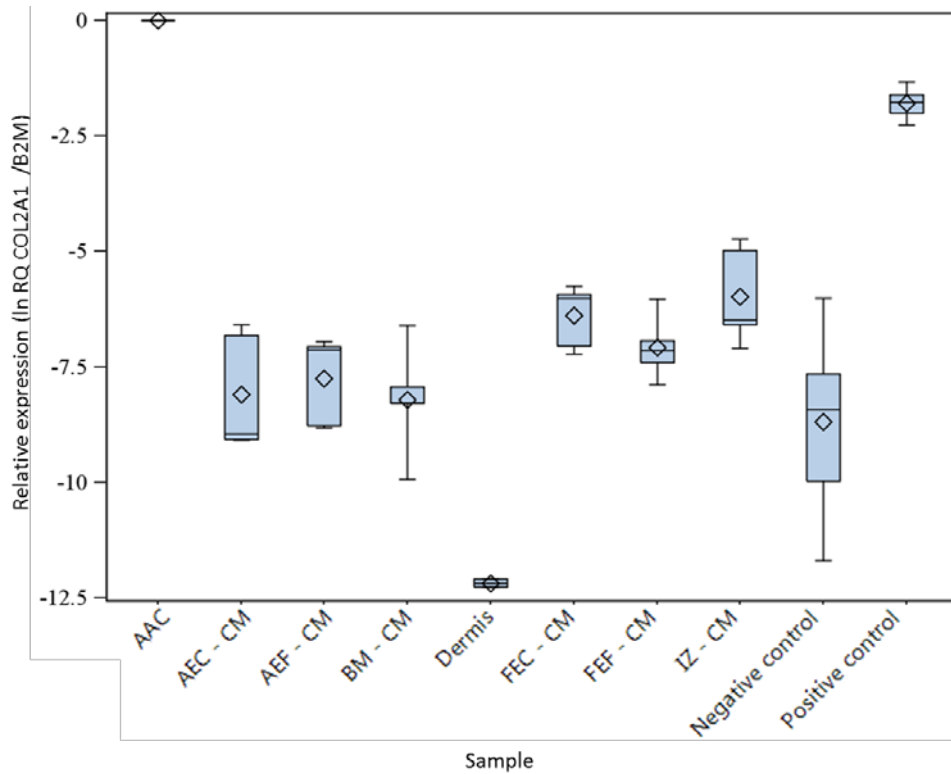


Figure 4.9: Box and whiskers plot illustrating steady state mRNA expression of COL2A1 in pellets from conditioned and control media relative to articular cartilage tissue (set to 0) which was used as the calibrator sample. Diamonds within the box plot represent the group mean. FEF-CM: Fetal dermal fibroblasts, FEC-CM: Fetal anlage chondrocytes, IZ-CM: Fetal interzone cells, AEF-CM: Adult dermal fibroblasts, AEC-CM: Adult articular chondrocytes and BM-CM: Bone marrow derived cells conditioned media. AAC – Adult articular cartilage tissue, PC – positive control medium, NC – negative control medium. Diamonds within the box plot represent the group mean.

Medium type/COL2A1	AAC	AEC - CM	AEF - CM	BM - CM	Dermis	FEC - CM	FEF - CM	IZ - CM	NC	PC
AAC		<.0001	<.0001	<.0001	<.0001	<.0001	<.0001	<.0001	<.0001	0.4615
AEC - CM			0.9999	1	0.0012	0.2532	0.8612	0.067	0.988	<.0001
AEF - CM				0.9993	0.0003	0.5689	0.9897	0.2145	0.8099	<.0001
BM - CM					0.0017	0.1868	0.7802	0.0454	0.9971	<.0001
Dermis						<.0001	<.0001	<.0001	0.0034	<.0001
FEC - CM							0.9876	0.9997	0.0082	<.0001
FEF - CM								0.8042	0.1609	<.0001
IZ - CM									0.001	<.0001
NC										<.0001
PC										

Table 4.5 listing the p-values of differences in COL2A1 expression as measured by steady state levels of mRNA in different media types. Significant differences are depicted by pink shading ($p < 0.05$ – Tukey’s post hoc correction). FEF-CM: Fetal dermal fibroblasts, FEC-CM: Fetal anlage chondrocytes, IZ-CM: Fetal interzone cells, AEF-CM: Adult dermal fibroblasts, AEC-CM: Adult articular chondrocytes and BM-CM: Bone marrow derived cells conditioned media. AAC – Adult articular cartilage tissue, PC – positive control medium, NC – negative control medium.

Type I collagen (COL1A1)

Expression of COL1A1 was variable in all groups, but relatively higher in the pellets maintained in fetal conditioned media than those in the adult conditioned media (Figure 4.10; Table 4.6). The level of expression in dermis was set to zero and was used as the calibrator sample. Pellets in FEC-CM showed significantly higher levels of expression compared to the negative control ($p=0.0182$).

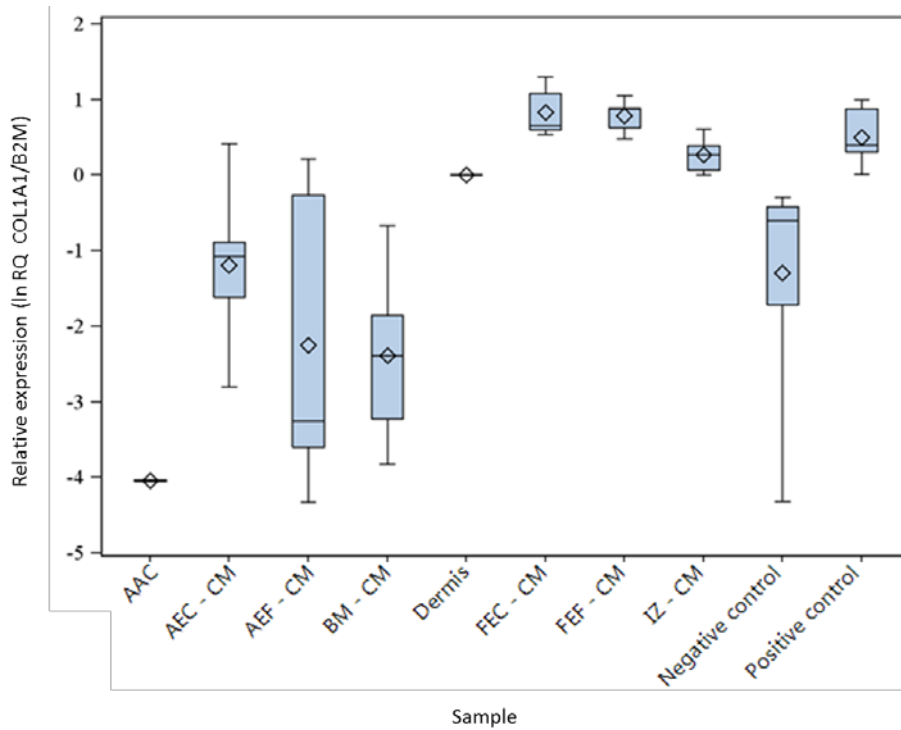


Figure 4.10: Box and whiskers plot illustrating steady state mRNA expression of COL1A1 in pellets from conditioned and control media relative to dermis tissue (set to 0) which was used as the calibrator sample. Diamonds within the box plot represent the group mean. FEF-CM: Fetal dermal fibroblasts, FEC-CM: Fetal anlage chondrocytes, IZ-CM: Fetal interzone cells, AEF-CM: Adult dermal fibroblasts, AEC-CM: Adult articular chondrocytes and BM-CM: Bone marrow derived cells conditioned media. AAC – Adult articular cartilage tissue, PC – positive control medium, NC – negative control medium. Diamonds within the box plot represent the group mean.

Medium type/Col1A1	AAC	AEC - CM	AEF - CM	BM - CM	Dermis	FEC - CM	FEF - CM	IZ - CM	NC	PC
AAC		0.0583	0.56	0.6687	0.0119	<.0001	<.0001	0.0005	0.0415	<.0001
AEC - CM			0.8349	0.7122	0.9286	0.0926	0.1086	0.4585	1	0.1159
AEF - CM				1	0.2555	0.0012	0.0014	0.0141	0.7975	0.0007
BM - CM					0.1867	0.0006	0.0007	0.0076	0.6443	0.0003
Dermis						0.9929	0.9953	1	0.8371	0.9997
FEC - CM							1	0.9968	0.0182	0.9999
FEF - CM								0.9983	0.0227	1
IZ - CM									0.1914	1
NC										0.0127
PC										

Table 4.6 listing the *p*-values of differences in COL1A1 expression as measured by steady state levels of mRNA in different media types. Significant differences are depicted by pink shading ($p < 0.05$ – Tukey’s post hoc correction). FEF-CM: Fetal dermal fibroblasts, FEC-CM: Fetal anlage chondrocytes, IZ-CM: Fetal interzone cells, AEF-CM: Adult dermal fibroblasts, AEC-CM: Adult articular chondrocytes and BM-CM: Bone marrow derived cells conditioned media. AAC – Adult articular cartilage tissue, PC – positive control medium, NC – negative control medium.

Discussion

The data from experiments described in this chapter suggests the production of paracrine signals by the skeletal tissue derived primary cell lines that induce chondrogenic differentiation in interzone cells. However, the magnitude of this effect with the methods used was limited. Interzone cell pellets cultured in skeletal cell derived conditioned media showed weak proteoglycan staining, however, the response was highly variable within all groups. Still, this response was greater than that observed in conditioned medium from fetal and adult fibroblasts. None of the interzone pellets cultured with fetal or adult fibroblast conditioned medium demonstrated any evidence of positive matrix proteoglycan staining.

The data from gene expression analysis were generally consistent with the results of matrix staining. Expression of the cartilage biomarker genes *ACAN* and *COL2A1* were higher in the pellets cultured with skeletal cell-derived conditioned media. As with the

Safranin-O staining, however, the magnitude was small relative to steady state mRNA levels observed in the positive controls. Within the experimental groups, pellets in the FEC-CM appeared to elicit the most robust chondrogenic differentiation response as evidenced by significantly higher expression of *ACAN* and *COL2A1* relative to negative controls. The expression of *COL1A1* in all groups of pellets is consistent with both an absence (negative control, FEF-CM, AEF-CM) and incomplete (conditioned medium from skeletal cell-derived conditioned medium, positive control) level of chondrogenic differentiation. Only adult articular cartilage tissue had negligible *COL1A1* steady state mRNA levels.

Based on the data presented in this chapter, the evidence for a robust chondrogenic induction response is limited. Possible reasons for this could be that the cells are not secreting any chondroinductive signals or, that the levels of paracrine chondroinductive signals accumulated in the conditioned media with the methods used could be insufficient to elicit a profound response. It is worth noting that these were functional assays and were not designed to characterize the quantity or integrity of factors known to have chondroinductive ability. The proliferation assays described in Chapter 3 were performed on interzone cells in monolayer culture while assessment of chondrogenic differentiation was performed on pellet cultures of interzone cells. These cell culture formats were adopted to ensure an optimal system for cells to respond to paracrine inductive signals in culture. However, the source of paracrine signals, namely the conditioned media was generated from cells in monolayer which could be biased towards proliferation and not chondrogenic differentiation. Traditionally, the

fundamental cellular processes of proliferation and differentiation are believed to have an inverse relationship, wherein cells initially undergo active cell division and as they start to differentiate, they down regulate the genes for proliferation [95, 106, 119, 144, 145]. Therefore, the conditioned medium could likely have been enriched for signaling proteins and growth factors involved in cell division and might be lacking chondroinductive signals. In addition, conditioned medium was generated by 24 hours of incubation with cells. While this was likely sufficient for the mitogenic stimuli from cells to accrue in the media, this short period of incubation might have limited the amount of chondrogenic signals elaborated by the cells. These could be possible reasons for the limited chondrogenic induction that we observed from all types of conditioned media in our experiments. It could also be that interzone cells are unresponsive to the paracrine signals present in the conditioned medium. Another likely explanation is that a chondrogenic effect, if any, is beyond the resolution that we can robustly measure using proteoglycan staining and steady state mRNA levels of *ACAN* and *COL2A1*. We observed considerable variation within the skeletal cell conditioned medium groups, among which the BM-CM group was the most variable. This could be a result of the diversity in the source of bone marrow derived cells as suggested by Cote et. al., 2016 [146].

The data presented in this chapter alone does not strongly support or refute a model whereby paracrine signaling from the cells in the skeletal tissue microenvironment induces interzone cells to undergo chondrogenic differentiation. Further experiments employing more sensitive experimental systems and assessment strategies are essential

in understanding the interaction between interzone cells and their skeletal environment. It would be worth assessing these paracrine interactions using an indirect coculture system whereby cells are physically separated by a semi-permeable membrane but share media and secreted signals [86, 98, 147]. This system could allow for a more real-time analysis of cellular interactions between the interzone cells and the skeletal microenvironment. We used cartilage biomarker expression, evaluated at both RNA and protein levels, to assess chondrogenic differentiation. Recent advances in high throughput sequencing platforms facilitate characterization of global patterns of gene expression in samples both quantitatively and qualitatively. This offers a valuable resource to identify the gene expression patterns unique to articular cartilage which could result in more sensitive strategies to assess chondrogenic differentiation. It would also be interesting to examine the differential gene expression patterns in interzone cells in monolayer versus high density pellet cultures. This information could be useful in identifying the molecular signals regulating interzone cell proliferation and chondrogenic differentiation and could contribute to additional mechanistic studies to elucidate these regulatory mechanisms. Much progress has been made in this regard facilitated by an RNA-seq dataset generated for cells in monolayer and pellet cultures using aliquots from the same primary cell preparations used in this study [107]. This dataset also represents an opportunity to identify additional biomarkers of chondrogenic differentiation that could allow us to reexamine our data for assessment of chondrogenic differentiation. These studies will be of relevance when considering interzone cells in cell-based therapeutic strategies for repair of the joint cartilage.

Chapter 5

Reflections and looking ahead to future studies

Reflections

Research efforts in this dissertation were directed towards understanding the cellular and molecular mechanisms of interzone-mediated repair of skeletal defects. Within this dissertation, results have been reported for experiments that have been performed to meet the following objectives 1) to examine the role of the microenvironment on the process of interzone-mediated repair, 2) to determine whether the fundamental cellular processes of proliferation and chondrogenic differentiation of interzone cells are regulated by extrinsic paracrine signals from their microenvironment.

With the advent of tissue engineering strategies for cartilage repair, adult and embryonic mesenchymal cells have been explored for their potential to repair articular cartilage and restore normal joint function [20, 101, 148-150]. Interzone cells have been implicated both in the development and repair of articular cartilage in studies described in previous chapters. Therefore, a complete understanding of the mechanisms of interzone-mediated repair, or more specifically the contribution of interzone cells versus environmental paracrine regulatory mechanisms, to this repair process is relevant with regard to their potential use as therapy cells for reengineering articular cartilage.

The data presented in chapter 2 evaluated the functionality of interzone cells in an *in vivo* model by comparing the outcomes of interzone transplantation in skeletal and

non-skeletal sites in axolotl salamanders. Repair was observed only in the skeletal environment whereas the transplanted cells could not be located in a majority of the samples in the non-skeletal site. The interpretation of these findings is that the skeletal environment selectively supports and influences the proliferation and differentiation of interzone cells. One possibility for this differential response could be a potential disparity in the quantity and duration of localized growth factor production between the two surgical sites. The large induced lesion in the tibial diaphysis could have experienced more local trauma from the surgical procedure and could be expected to take longer to heal. This offers an extended period of time when there is localized growth factor production which could also be stimulating the transplanted interzone cells. In contrast, the degree and duration of stimulation by localized growth factors in the non-skeletal site could be limited owing to lower trauma and rapid tissue repair. Further characterization of the repair response in this *in vivo* model was hampered by the absence of a reference genome for the axolotl salamander which could have enabled efficient lineage tracing of the transplanted cells. In addition, considerable challenges in culturing salamander cells, in an effort to isolate a homogenous cell population, prompted me to utilize an alternate *in vitro* model using equine primary cells. While having to reconsider and retool the experimental systems to test our hypothesis may have slowed the pace of this study to some extent, it was a valuable and enriching educational experience in experimental biology and discovery science.

In the research presented in Chapter 3, the hypothesis tested was that skeletal cell-derived paracrine factors play a vital role in regulating the proliferation of interzone

cells in an *in vitro* model and thus, contributing to the interzone-mediated repair process. Media conditioned by the primary cells and therefore, termed 'conditioned medium' was used to evaluate how skeletal and non-skeletal cells differ in the production and response to mitogenic signals. Our findings from this study supported the hypothesis. The interzone cells showed a robust mitogenic response with all conditioned media types. There are limitations to this study that need to be addressed in future studies. First, normalization of the medium was performed based on the number of cells which conditioned the media. Limitations associated with trypsinization and/or cell counting techniques could have affected the accuracy of normalization and contributed to the variation that we observed. Secondly, all *in vitro* models, especially methods used to prepare the conditioned media, are approximations of the actual biological system and the complex signaling pathways that regulate cellular processes in the body. The conditioned medium was used in an attempt to represent the soluble and stable paracrine signals that are constitutively secreted into the culture medium by cells. While employing this system has enabled an understanding of the effect of these paracrine mitogenic stimuli on interzone cells, it does not account for insoluble, transient or unstable proteins that are secreted in a regulated fashion which could also be contributing to tissue repair. Furthermore, the conditioned medium was supplemented with a significant quantity of bovine serum albumin (BSA) in order to maintain the total protein concentration uniform across experimental and control media. However, this may have interfered with characterization of the cell's secretome in the conditioned media using traditional protein quantification assays.

Studies in Chapter 4 used the same experimental system to evaluate a potential effect of environmental paracrine signals on the chondrogenic differentiation of interzone cells in high density pellet cultures. While our findings were suggestive of paracrine signaling between the skeletal cells and interzone cells that likely induces chondrogenic differentiation, the magnitude of differences were not compelling. There are several limitations with this study that would be worth considering during the design of any future studies. First, the medium conditioned by cells in monolayer may have been inadequate to assess chondrogenic differentiation as these may have been preferentially enriched for mitogenic paracrine signals and with only low levels of chondrogenic stimuli. However, there are considerable logistical challenges to using cells in three dimensional cultures to generate conditioned media such as high cell numbers required to condition the media and optimal culture conditions that would maintain cell viability while minimizing background differentiation, to name a few. The levels of chondroinductive signals secreted by cells during the short period of conditioning may have been insufficient to elicit a response at the resolution that we could efficiently measure by cartilage biomarker expression on a gene and protein level.

The data reported in this dissertation have contributed to the increasing pool of knowledge on the biology of interzone cells, suggesting that they are not autonomous; rather, their fate is influenced and regulated at least partly by external environmental cues. The work presented here represents a “piece of the puzzle” that ongoing research efforts in our laboratory and the orthopedic research community are working to put together. Additional studies are needed to elucidate the intricate signaling pathways

that are involved in cell-cell communication, which would be of relevance in consideration of interzone cells for cell-based repair strategies for articular cartilage.

Future studies

The studies described in this dissertation have led to an improved understanding of the functionality of interzone cells, with regard to their interaction with the microenvironment. However, shortfalls of the *in vitro* co-culture model used limit our ability to dissect the precise signaling cascades that mediate the crosstalk between interzone cells and their environment. Due to logistical challenges, the conditioned medium requires storage before use which limits our ability to examine soluble paracrine signals with short half-lives. In addition, it does not allow for assessment of reciprocal signaling between cells [100]. Furthermore, the *in vitro* system fails to simulate the complexity of interactions between multiple cell types that comprise a tissue and the regulatory molecules that govern these interactions which could function in a synergistic or antagonistic manner. These reflections are not meant to diminish the significance of this work, on the contrary, to emphasize the importance of expanding on it. It would be worth re-examining the paracrine and possibly other interactions in more refined direct or indirect coculture models. One promising model is an indirect coculture system employing membrane inserts which allows physical separation of the cells but permit sharing of media and signaling molecules between them [98, 147, 151, 152]. This is a better representation of the biological system as cells are in constant communication with their neighbors during the entire culture period and it accounts for

the transient paracrine protein factors that have a regulated secretory pathway. It also enables characterization of a reciprocal interaction between both participating cell types. Employing mixed cultures of skeletal cells would be useful in reproducing the complexity of the biological system and enabling a better understanding of these cellular interactions. More sensitive matrices for assessment of chondrogenic differentiation need to be developed and optimized. With the advent of high throughput sequencing technology, analysis of global gene expression patterns of large sample sets can be performed with relative ease. This could be a valuable resource in identifying additional biomarkers for articular cartilage and interzone. Efforts in this regard are already underway in our laboratory being facilitated by an RNA-seq data set generated from equine cartilage and interzone at relevant developmental stages [107]. Establishing a transcriptome signature for interzone cells would also be valuable for lineage tracing experiments to elucidate the origin and fate of interzone cells in development and repair.

Additionally, questions remain with regard to what are the specific paracrine signals that induce proliferation and the limited chondrogenic differentiation of interzone cells in culture. As discussed above, analyzing the conditioned medium using traditional protein detection and quantification methods to identify secreted paracrine proteins, which are often present in pico or nanogram quantities, was hindered by the significant amount of BSA (3 mg/ml) in our conditioned medium. Employing a serum-free and protein-free medium in future studies will help minimize this interference from BSA and enable detection and quantification of the cell secretome in the conditioned

medium. Further mechanistic studies are needed to parse out the precise signaling pathways orchestrating this cell-cell communication. Identification of such signaling molecule(s) that can induce interzone cells to differentiate into and maintain an articular cartilage phenotype could open several avenues for cartilage tissue repair. Advances in molecular biology have enabled access to tools for manipulation of specific molecular signals using knock out, knock down or over-expression strategies in mice. Utilizing these approaches to gain a better understanding of the role of paracrine signals in interzone cell biology would be valuable. Furthermore, with the technology on IPS cells infiltrating many aspects of cell biology and medical applications [153], identifying a master regulatory switch that can drive stable chondrogenic differentiation in interzone cells can have massive implications in the field of orthopedic regenerative medicine. One could envision a point in the future when reprogramming patient-derived somatic cells to induce an interzone cell phenotype capable of producing a durable and functional hyaline cartilage repair tissue to replace injured cartilage is a reality.

One of the unique features of the axolotl salamander model is the retention of interzone in the intraarticular space through adulthood. In mammals, the interzone can no longer be appreciated once the joint undergoes cavitation, an event that occurs within the first trimester of gestation. Lineage tracing studies in mice have suggested that interzone is incorporated into the articular tissues during development [48, 49]. In our transplantation studies in the axolotl salamander, the interzone placed in the diaphyseal bone defect appears to proliferate and differentiate into multiple cartilage

types based on histological examination and GFP immunostaining. These observations are suggestive of some degree of 'stemness' as self-renewal and multipotency are characteristic attributes of stem cells [124, 125, 154]. This leads us to the interesting question of whether there could be a reserve interzone-derived stem cell population in postnatal mammalian joints with potential regenerative capacity but which are maintained in a quiescent state through adulthood. Identifying the molecular signal(s) that can potentially activate these cells to reenter the stem cell life cycle could hold exciting prospects for cartilage repair. In fact, several studies have suggested the presence of chondroprogenitor cells in the superficial zone of articular cartilage in human, bovine and equine models [42, 155-158]. However, comparisons between these studies is challenging due to a lack of uniformity between stem cell surface markers across species and precise protocols to assess the nature of stem cells. Further studies to characterize the stemness of equine interzone cells would be valuable in addressing these questions.

During development, the growth and patterning of embryonic tissues is tightly regulated by dynamic patterns of expression of intrinsic and extrinsic signals which often act as morphogens. Their concentration gradients set the positional information for recruitment and differentiation of cells [159]. In our studies in the axolotl salamander, the accessory joint that formed in the critical sized defect followed accurate spatial patterning although the interzone cells were transplanted with no consideration of orientation. In addition, a zonal organization could be appreciated in interzone cell pellets that were induced to differentiate along a chondrogenic lineage

(Chapter 4; Figure 4.3 and 4.5 – positive control). These observations in the *in vivo* and *in vitro* models are reminiscent of the controlled processes of growth and pattern formation in the developing embryo. Further studies are necessary to understand why and how interzone cells achieve this spatial patterning. What are the intrinsic and/or extrinsic regulatory mechanisms that govern this process? Do interzone cells retain a memory of their polarity even when removed from their environment? Characterization of the zonal organization of induced interzone pellets would be valuable in order to help address these questions. A recent lineage tracing study using knockin *GDF5*-CreER mice suggests a role for *GDF5* in the recruitment and differentiation of interzone cells in the developing joint. The authors propose that spatio-temporal patterns of *GDF5* expression determine the lineage of interzone cells populating the *GDF5* domain [78]. With additional studies emphasizing the importance of *GDF5* in joint formation [47, 50, 77], it is tempting to speculate that *GDF5* could be a potential master switch regulating the fate and function of interzone cells.

The experiments reported in this dissertation examine a potential effect of skeletal cells on interzone cells. However, as in the biological system, this could be a bi-directional interaction. Additional studies are necessary to understand how interzone cells communicate with its microenvironment and how these external stimuli affect the behavior of interzone cells both *in vitro* and *in vivo*. These could be performed employing an indirect or direct coculture system as discussed above. Finally, while *in vitro* models are essential in understanding the behavior of cells and their regulation, it is important to translate this knowledge for clinical use using *in vivo* models. There have

been significant advances in the field of regenerative medicine involving tissue engineering approaches in the last few years [105, 160, 161]. This offers the possibility of generating a repair tissue incorporating interzone cells co-delivered with the appropriate biomaterial scaffold and/or microenvironmental signaling molecules. Engineering a functional cartilage repair tissue using these emergent strategies and further evaluation of its functionality in an *in vivo* mammalian model should be a long-term goal in translational research.

Appendix

List of abbreviations

Abbreviation	Definition
AAC	Adult articular cartilage
ACAN	Aggrecan
ACI	Autologous chondrocyte implantation
AEC	Adult equine articular chondrocytes
AEF	Adult equine dermal fibroblasts
BM	Adult equine bone marrow derived cells
BMP	Bone morphogenetic protein
BSA	Bovine serum albumin
CD	Cluster of differentiation
CM	Conditioned medium
COL	Collagen
CSD	Critical sized defect
DAPI	4',6-Diamidino-2-Phenylindole, Dihydrochloride
DMEM	Dulbecco's Modified Eagle Medium
ECM	Extracellular matrix
EDTA	Ethylenediaminetetraacetic acid
EdU	5-ethynyl-2'-deoxyuridine
FBS	Fetal bovine serum
FEC	Fetal equine anlage chondrocytes
FEF	Fetal equine dermal fibroblasts
FGF	Fibroblast growth factor
GDF	Growth and differentiation factor
GFP	Green Fluorescent protein
GLI	Glioma-Associated Oncogene Homolog
H&E	Hematoxylin and Eosin
HRP	Horseradish peroxidase
IGF	Insulin-like growth factor
IZ	Fetal equine interzone cells
MACI	Matrix-assisted autologous chondrocyte implantation
PBS	Phosphate buffered saline
polyHEMA	Poly(2-hydroxyethyl methacrylate)
SOX	SRY box
TGF	Transforming growth factor
WNT	Wingless-related integration site

References

1. Alford JW, Cole BJ. Cartilage restoration, part 1: basic science, historical perspective, patient evaluation, and treatment options. *Am J Sports Med* 2005; 33: 295-306.
2. Archer CW, Dowthwaite GP, Francis-West P. Development of synovial joints. *Birth Defects Research Part C: Embryo Today: Reviews* 2003; 69: 144-155.
3. Bernhard JC, Vunjak-Novakovic G. Should we use cells, biomaterials, or tissue engineering for cartilage regeneration? *Stem Cell Res Ther* 2016; 7: 56.
4. Hunziker EB. Articular cartilage repair: basic science and clinical progress. A review of the current status and prospects. *Osteoarthritis and Cartilage* 2002; 10: 432-463.
5. Hunziker EB. The elusive path to cartilage regeneration. *Advanced Materials* 2009; 21: 3419-3424.
6. Lories RJ, Luyten FP. Overview of Joint and Cartilage Biology. In: *Genetics of Bone Biology and Skeletal Disease*, Thakker RV, Whyte MP, Eisman J, Igarashi T Eds.: Elsevier Science 2012:35-51.
7. Pacifici M, Koyama E, Iwamoto M. Mechanisms of synovial joint and articular cartilage formation: recent advances, but many lingering mysteries. *Birth Defects Research Part C: Embryo Today: Reviews* 2005; 75: 237-248.
8. Beris AE, Lykissas MG, Papageorgiou CD, Georgoulis AD. Advances in articular cartilage repair. *Injury* 2005; 36 Suppl 4: S14-23.
9. Cokelaere S, Malda J, van Weeren R. Cartilage defect repair in horses: Current strategies and recent developments in regenerative medicine of the equine joint with emphasis on the surgical approach. *The Veterinary Journal* 2016; 214: 61-71.
10. Hunziker EB. Articular cartilage repair: are the intrinsic biological constraints undermining this process insuperable? *Osteoarthritis Cartilage* 1999; 7: 15-28.
11. Redman SN, Oldfield SF, Archer CW. Current strategies for articular cartilage repair. *Eur Cell Mater* 2005; 9: 23-32; discussion 23-32.
12. Correa D, Lietman SA. Articular cartilage repair: Current needs, methods and research directions. *Semin Cell Dev Biol* 2016.
13. Diekman BO, Guilak F. Stem cell-based therapies for osteoarthritis: challenges and opportunities. *Curr Opin Rheumatol* 2013; 25: 119-126.
14. Mauck RL, Burdick JA. Engineering Cartilage Tissue. *Tissue engineering* 2011: 493-520.
15. Buckwalter JA, Mankin HJ, Grodzinsky AJ. Articular cartilage and osteoarthritis. *Instr Course Lect* 2005; 54: 465-480.
16. Pearle AD, Warren RF, Rodeo SA. Basic science of articular cartilage and osteoarthritis. *Clin Sports Med* 2005; 24: 1-12.
17. Huber M, Trattng S, Lintner F. Anatomy, biochemistry, and physiology of articular cartilage. *Invest Radiol* 2000; 35: 573-580.
18. Poole CA. Articular cartilage chondrons: form, function and failure. *J Anat* 1997; 191 (Pt 1): 1-13.
19. Sophia Fox AJ, Bedi A, Rodeo SA. The Basic Science of Articular Cartilage: Structure, Composition, and Function. *Sports Health* 2009; 1: 461-468.
20. Temenoff JS, Mikos AG. Review: tissue engineering for regeneration of articular cartilage. *Biomaterials* 2000; 21: 431-440.
21. Esko JD, Kimata K, Lindahl U. Proteoglycans and sulfated glycosaminoglycans. 2009.

22. Hunziker EB, Quinn TM, Hauselmann HJ. Quantitative structural organization of normal adult human articular cartilage. *Osteoarthritis Cartilage* 2002; 10: 564-572.
23. Suri P, Morgenroth DC, Hunter DJ. Epidemiology of osteoarthritis and associated comorbidities. *PM R* 2012; 4: S10-19.
24. Sovani S, Grogan SP. Osteoarthritis Detection, Pathophysiology, and Current/Future Treatment Strategies. *Orthopaedic Nursing* 2013; 32: 25-36.
25. Felson DT, Neogi T. Osteoarthritis: is it a disease of cartilage or of bone? *Arthritis Rheum* 2004; 50: 341-344.
26. Felson DT, Lawrence RC, Dieppe PA, Hirsch R, Helmick CG, Jordan JM, et al. Osteoarthritis: new insights. Part 1: the disease and its risk factors. *Ann Intern Med* 2000; 133: 635-646.
27. Caron J, Genovese R. Principles and practices of joint disease treatment. Diagnosis and management of lameness in the horse. Philadelphia: WB Saunders Co 2003: 746-764.
28. McIlwraith CW, Frisbie DD, Kawcak CE. The horse as a model of naturally occurring osteoarthritis. *Bone Joint Res* 2012; 1: 297-309.
29. Ruta DJ, Villarreal AD, Richardson DR. Orthopedic Surgical Options for Joint Cartilage Repair and Restoration. *Phys Med Rehabil Clin N Am* 2016; 27: 1019-1042.
30. Brittberg M, Lindahl A, Nilsson A, Ohlsson C, Isaksson O, Peterson L. Treatment of deep cartilage defects in the knee with autologous chondrocyte transplantation. *New England Journal of Medicine* 1994; 331: 889-895.
31. Litzke L-F, Wagner E, Baumgaertner W, Hetzel U, Josimović-Alasević O, Libera J. Repair of extensive articular cartilage defects in horses by autologous chondrocyte transplantation. *Annals of Biomedical Engineering* 2004; 32: 57-69.
32. Nixon AJ, Begum L, Mohammed HO, Huibregtse B, O'Callaghan MM, Matthews GL. Autologous chondrocyte implantation drives early chondrogenesis and organized repair in extensive full-and partial-thickness cartilage defects in an equine model. *Journal of Orthopaedic Research* 2011; 29: 1121-1130.
33. Beyzadeoglu T, Onal A, Ivkovic A. Matrix-induced autologous chondrocyte implantation for a large chondral defect in a professional football player: a case report. *J Med Case Rep* 2012; 6: 173.
34. Cherubino P, Grassi FA, Bulgheroni P, Ronga M. Autologous chondrocyte implantation using a bilayer collagen membrane: a preliminary report. *J Orthop Surg (Hong Kong)* 2003; 11: 10-15.
35. Clar H, Pascher A, Kastner N, Gruber G, Robl T, Windhager R. Matrix-assisted autologous chondrocyte implantation into a 14cm(2) cartilage defect, caused by steroid-induced osteonecrosis. *Knee* 2010; 17: 255-257.
36. Nehrer S, Domayer SE, Hirschfeld C, Stelzeneder D, Trattnig S, Dorotka R. Matrix-Associated and Autologous Chondrocyte Transplantation in the Ankle: Clinical and MRI Follow-up after 2 to 11 Years. *Cartilage* 2011; 2: 81-91.
37. Nixon A, Rickey E, Butler T, Scimeca M, Moran N, Matthews G. A chondrocyte infiltrated collagen type I/III membrane (MACI® implant) improves cartilage healing in the equine patellofemoral joint model. *Osteoarthritis and Cartilage* 2015; 23: 648-660.
38. Laporta TF, Richter A, Sgaglione NA, Grande DA. Clinical relevance of scaffolds for cartilage engineering. *Orthop Clin North Am* 2012; 43: 245-254.
39. Hui JH, Buhary KS, Chowdhary A. Implantation of orthobiologic, biodegradable scaffolds in osteochondral repair. *Orthop Clin North Am* 2012; 43: 255-261.

40. Fermor HL, Russell SL, Williams S, Fisher J, Ingham E. Development and characterisation of a decellularised bovine osteochondral biomaterial for cartilage repair. *J Mater Sci Mater Med* 2015; 26: 186.
41. Douthwaite GP, Bishop JC, Redman SN, Khan IM, Rooney P, Evans DJ, et al. The surface of articular cartilage contains a progenitor cell population. *Journal of cell science* 2004; 117: 889-897.
42. Hattori S, Oxford C, Reddi AH. Identification of superficial zone articular chondrocyte stem/progenitor cells. *Biochemical and biophysical research communications* 2007; 358: 99-103.
43. Jayasuriya CT, Chen Q. Potential benefits and limitations of utilizing chondroprogenitors in cell-based cartilage therapy. *Connect Tissue Res* 2015; 56: 265-271.
44. Jones EA, Crawford A, English A, Henshaw K, Mundy J, Corscadden D, et al. Synovial fluid mesenchymal stem cells in health and early osteoarthritis: Detection and functional evaluation at the single-cell level. *Arthritis & Rheumatism* 2008; 58: 1731-1740.
45. Richardson SM, Kalamegam G, Pushparaj PN, Matta C, Memic A, Khademhosseini A, et al. Mesenchymal stem cells in regenerative medicine: Focus on articular cartilage and intervertebral disc regeneration. *Methods* 2016; 99: 69-80.
46. Vinatier C, Bouffi C, Merceron C, Gordeladze J, Brondello J-M, Jorgensen C, et al. Cartilage tissue engineering: towards a biomaterial-assisted mesenchymal stem cell therapy. *Current stem cell research & therapy* 2009; 4: 318-329.
47. Decker RS, Koyama E, Pacifici M. Genesis and morphogenesis of limb synovial joints and articular cartilage. *Matrix Biol* 2014; 39: 5-10.
48. Koyama E, Shibukawa Y, Nagayama M, Sugito H, Young B, Yuasa T, et al. A distinct cohort of progenitor cells participates in synovial joint and articular cartilage formation during mouse limb skeletogenesis. *Developmental biology* 2008; 316: 62-73.
49. Pacifici M, Koyama E, Shibukawa Y, Wu C, Tamamura Y, Enomoto-Iwamoto M, et al. Cellular and molecular mechanisms of synovial joint and articular cartilage formation. *Annals of the New York Academy of Sciences* 2006; 1068: 74-86.
50. Decker RS. Articular cartilage and joint development from embryogenesis to adulthood. *Semin Cell Dev Biol* 2016.
51. Lenas P, Moos Jr M, Luyten FP. Developmental engineering: a new paradigm for the design and manufacturing of cell-based products. Part I: from three-dimensional cell growth to biomimetics of in vivo development. *Tissue Engineering Part B: Reviews* 2009; 15: 381-394.
52. Ozpolat BD, Zapata M, Fruge JD, Coote J, Lee J, Muneoka K, et al. Regeneration of the elbow joint in the developing chick embryo recapitulates development. *Developmental biology* 2012; 372: 229-238.
53. Karsenty G, Wagner EF. Reaching a genetic and molecular understanding of skeletal development. *Developmental cell* 2002; 2: 389-406.
54. Tuan RS. Biology of Developmental and Regenerative Skeletogenesis. *Clinical Orthopaedics and Related Research* 2004; 427: S105-S117.
55. Liu CF, Samsa WE, Zhou G, Lefebvre V. Transcriptional control of chondrocyte specification and differentiation. *Semin Cell Dev Biol* 2016.
56. Lefebvre V, Bhattaram P. Chapter Eight-Vertebrate Skeletogenesis. *Current topics in developmental biology* 2010; 90: 291-317.
57. DeLise A, Fischer L, Tuan R. Cellular interactions and signaling in cartilage development. *Osteoarthritis and Cartilage* 2000; 8: 309-334.

58. Gimble JM, Morgan C, Kelly K, Wu X, Dandapani V, Wang CS, et al. Bone morphogenetic proteins inhibit adipocyte differentiation by bone marrow stromal cells. *J Cell Biochem* 1995; 58: 393-402.
59. Reddi AH. Bone morphogenetic proteins: an unconventional approach to isolation of first mammalian morphogens. *Cytokine & growth factor reviews* 1997; 8: 11-20.
60. Granjeiro J, Oliveira R, Bustos-Valenzuela J, Sogayar M, Taga R. Bone morphogenetic proteins: from structure to clinical use. *Brazilian journal of medical and biological research* 2005; 38: 1463-1473.
61. Storm EE, Kingsley DM. GDF5 coordinates bone and joint formation during digit development. *Dev Biol* 1999; 209: 11-27.
62. Sun ZB, Zhang YK, Yang SH, Jia J, Ye SN, Chen D, et al. Growth differentiation factor 5 modulation of chondrogenesis of self-assembled constructs involves gap junction-mediated intercellular communication. *Development Growth & Differentiation* 2012; 54: 809-817.
63. Buxton P, Edwards C, Archer CW, Francis-West P. Growth/differentiation factor-5 (GDF-5) and skeletal development. *The Journal of Bone and Joint Surgery (American)* 2001; 83: S23-S30.
64. Reddi AH. Regulation of cartilage and bone differentiation by bone morphogenetic proteins. *Curr Opin Cell Biol* 1992; 4: 850-855.
65. Wrana JL. Signaling by the TGFbeta superfamily. *Cold Spring Harb Perspect Biol* 2013; 5: a011197.
66. Danišovič L, Varga I, Polák Š. Growth factors and chondrogenic differentiation of mesenchymal stem cells. *Tissue and Cell* 2012; 44: 69-73.
67. Sekiya I, Larson BL, Vuoristo JT, Reger RL, Prockop DJ. Comparison of effect of BMP-2, -4, and -6 on in vitro cartilage formation of human adult stem cells from bone marrow stroma. *Cell Tissue Res* 2005; 320: 269-276.
68. Van der Kraan P, Davidson EB, Blom A, Van den Berg W. TGF-beta signaling in chondrocyte terminal differentiation and osteoarthritis: modulation and integration of signaling pathways through receptor-Smads. *Osteoarthritis and Cartilage* 2009; 17: 1539-1545.
69. Green JD, Tollemar V, Dougherty M, Yan Z, Yin L, Ye J, et al. Multifaceted signaling regulators of chondrogenesis: Implications in cartilage regeneration and tissue engineering. *Genes Dis* 2015; 2: 307-327.
70. Guo X, Day TF, Jiang X, Garrett-Beal L, Topol L, Yang Y. Wnt/beta-catenin signaling is sufficient and necessary for synovial joint formation. *Genes Dev* 2004; 18: 2404-2417.
71. Liu Z, Ren Y, Mirando AJ, Wang C, Zuscik MJ, O'Keefe RJ, et al. Notch signaling in postnatal joint chondrocytes, but not subchondral osteoblasts, is required for articular cartilage and joint maintenance. *Osteoarthritis Cartilage* 2016; 24: 740-751.
72. Oldershaw RA, Tew SR, Russell AM, Meade K, Hawkins R, McKay TR, et al. Notch signaling through Jagged-1 is necessary to initiate chondrogenesis in human bone marrow stromal cells but must be switched off to complete chondrogenesis. *Stem Cells* 2008; 26: 666-674.
73. Hellingman CA, Koevoet W, Kops N, Farrell E, Jahr H, Liu W, et al. Fibroblast growth factor receptors in in vitro and in vivo chondrogenesis: relating tissue engineering using adult mesenchymal stem cells to embryonic development. *Tissue Eng Part A* 2010; 16: 545-556.

74. Jenner F, van Osch GJ, Weninger W, Geyer S, Stout T, van Weeren R, et al. The embryogenesis of the equine femorotibial joint: The equine interzone. *Equine Vet J* 2015; 47: 620-622.
75. Holder N. An experimental investigation into the early development of the chick elbow joint. *Journal of embryology and experimental morphology* 1977; 39: 115-127.
76. Hyde G, Dover S, Aszodi A, Wallis GA, Boot-Handford RP. Lineage tracing using *matrilin-1* gene expression reveals that articular chondrocytes exist as the joint interzone forms. *Developmental biology* 2007; 304: 825-833.
77. Jenner F, A IJ, Cleary M, Heijnsman D, Narcisi R, van der Spek PJ, et al. Differential gene expression of the intermediate and outer interzone layers of developing articular cartilage in murine embryos. *Stem Cells Dev* 2014; 23: 1883-1898.
78. Shwartz Y, Viukov S, Krief S, Zelzer E. Joint Development Involves a Continuous Influx of Gdf5-Positive Cells. *Cell Rep* 2016; 15: 2577-2587.
79. Cosden RS, Lattermann C, Romine S, Gao J, Voss SR, MacLeod JN. Intrinsic repair of full-thickness articular cartilage defects in the axolotl salamander. *Osteoarthritis Cartilage* 2011; 19: 200-205.
80. Cosden-Decker RS, Bickett MM, Lattermann C, MacLeod JN. Structural and functional analysis of intra-articular interzone tissue in axolotl salamanders. *Osteoarthritis Cartilage* 2012; 20: 1347-1356.
81. Ateshian GA. The role of interstitial fluid pressurization in articular cartilage lubrication. *J Biomech* 2009; 42: 1163-1176.
82. Namba RS, Meuli M, Sullivan KM, Le AX, Adzick NS. Spontaneous repair of superficial defects in articular cartilage in a fetal lamb model. *J Bone Joint Surg Am* 1998; 80: 4-10.
83. Wagner W, Reichl J, Wehrmann M, Zenner HP. Neonatal rat cartilage has the capacity for tissue regeneration. *Wound Repair Regen* 2001; 9: 531-536.
84. Marcacci M, Filardo G, Kon E. Treatment of cartilage lesions: What works and why? *Injury* 2013; 44: S11-S15.
85. Nishida T, Kubota S, Kojima S, Kuboki T, Nakao K, Kushibiki T, et al. Regeneration of defects in articular cartilage in rat knee joints by CCN2 (connective tissue growth factor). *J Bone Miner Res* 2004; 19: 1308-1319.
86. Perera JR, Gikas PD, Bentley G. The present state of treatments for articular cartilage defects in the knee. *Ann R Coll Surg Engl* 2012; 94: 381-387.
87. van Osch GJ, Brittberg M, Dennis JE, Bastiaansen-Jenniskens YM, Erben RG, Konttinen YT, et al. Cartilage repair: past and future--lessons for regenerative medicine. *J Cell Mol Med* 2009; 13: 792-810.
88. van Weeren PR, Back W. Musculoskeletal Disease in Aged Horses and Its Management. *Vet Clin North Am Equine Pract* 2016; 32: 229-247.
89. Ito MM, Kida MY. Morphological and biochemical re-evaluation of the process of cavitation in the rat knee joint: cellular and cell strata alterations in the interzone. *Journal of anatomy* 2000; 197: 659-679.
90. Armstrong J, Duhon S, Malacinski G. Raising the axolotl in captivity. *Developmental biology of the axolotl* 1989: 220-227.
91. Brighton CT. The biology of fracture repair. *Instructional course lectures* 1983; 33: 60-82.
92. Marsell R, Einhorn TA. The biology of fracture healing. *Injury* 2011; 42: 551-555.
93. Kinefuchi K, Kushida Y, Touma M, Hosono M. Limited immune diversity in Urodela: chronic transplantation responses occur even with family-disparate xenografts. *Zoological science* 2013; 30: 577-584.

94. Nedelkovska H, Robert J. Comparative Study of Skin Graft Tolerance and Rejection in the Frog *Xenopus laevis*, INTECH Open Access Publisher 2011.
95. Basson MA. Signaling in cell differentiation and morphogenesis. *Cold Spring Harbor perspectives in biology* 2012; 4: a008151.
96. Morriss-Kay G, Sokolova N. Embryonic development and pattern formation. *The FASEB Journal* 1996; 10: 961-968.
97. Zuniga A. Next generation limb development and evolution: old questions, new perspectives. *Development* 2015; 142: 3810-3820.
98. Janardhanan S, Wang MO, Fisher JP. Coculture strategies in bone tissue engineering: the impact of culture conditions on pluripotent stem cell populations. *Tissue Eng Part B Rev* 2012; 18: 312-321.
99. Boucek Jr RJ, Steele J, Jacobs JP, Steele P, Asante-Korang A, Quintessenza J, et al. Ex Vivo Paracrine Properties of Cardiac Tissue: Effects of Chronic Heart Failure. *The Journal of Heart and Lung Transplantation*.
100. Domenech M, Yu H, Warrick J, Badders NM, Meyvantsson I, Alexander CM, et al. Cellular observations enabled by microculture: paracrine signaling and population demographics. *Integr Biol (Camb)* 2009; 1: 267-274.
101. Hwang NS, Varghese S, Puleo C, Zhang Z, Elisseeff J. Morphogenetic signals from chondrocytes promote chondrogenic and osteogenic differentiation of mesenchymal stem cells. *J Cell Physiol* 2007; 212: 281-284.
102. Jikko A, Kato Y, Hiranuma H, Fuchihata H. Inhibition of chondrocyte terminal differentiation and matrix calcification by soluble factors released by articular chondrocytes. *Calcif Tissue Int* 1999; 65: 276-279.
103. Potapova IA, Gaudette GR, Brink PR, Robinson RB, Rosen MR, Cohen IS, et al. Mesenchymal stem cells support migration, extracellular matrix invasion, proliferation, and survival of endothelial cells in vitro. *Stem Cells* 2007; 25: 1761-1768.
104. Ruiz EJ, Oeztuerk-Winder F, Ventura JJ. A paracrine network regulates the cross-talk between human lung stem cells and the stroma. *Nat Commun* 2014; 5: 3175.
105. Thornemo M. Cartilage Tissue Engineering; the search for chondrogenic progenitor cells and associated signalling pathways 2009.
106. Strehl R, Schumacher K, de Vries U, Minuth WW. Proliferating cells versus differentiated cells in tissue engineering. *Tissue Eng* 2002; 8: 37-42.
107. Adam EN, Janes JG, Lowney RS, Lambert J, Stromberg A, MacLeod JN. Comparative Chondrogenic Potential of Equine Fetal Progenitor Cells and Adult Adipose- and Bone Marrow Derived Cells (in preparation).
108. Betteridge K, Eaglesome M, Mitchell D, Flood P, Beriault R. Development of horse embryos up to twenty two days after ovulation: observations on fresh specimens. *Journal of anatomy* 1982; 135: 191.
109. Kisiday JD, Goodrich LR, McIlwraith CW, Frisbie DD. Effects of equine bone marrow aspirate volume on isolation, proliferation, and differentiation potential of mesenchymal stem cells. *American journal of veterinary research* 2013; 74: 801-807.
110. Stewart MC, Saunders KM, Burton-Wurster N, Macleod JN. Phenotypic stability of articular chondrocytes in vitro: the effects of culture models, bone morphogenetic protein 2, and serum supplementation. *J Bone Miner Res* 2000; 15: 166-174.
111. Salic A, Mitchison TJ. A chemical method for fast and sensitive detection of DNA synthesis in vivo. *Proceedings of the National Academy of Sciences* 2008; 105: 2415-2420.
112. Kalluri R, Zeisberg M. Fibroblasts in cancer. *Nature Reviews Cancer* 2006; 6: 392-401.

113. Rhim JS, Dritschilo A. Neoplastic transformation in human cell culture: mechanisms of carcinogenesis. Volume 25, Springer Science & Business Media 2012.
114. Vasil'ev IUM, Gel'fand IM. Neoplastic and normal cells in culture. Volume 8, CUP Archive 1981.
115. Miki Y, Ono K, Hata S, Suzuki T, Kumamoto H, Sasano H. The advantages of co-culture over mono cell culture in simulating in vivo environment. *J Steroid Biochem Mol Biol* 2012; 131: 68-75.
116. Prasadam I, van Gennip S, Friis T, Shi W, Crawford R, Xiao Y. ERK-1/2 and p38 in the regulation of hypertrophic changes of normal articular cartilage chondrocytes induced by osteoarthritic subchondral osteoblasts. *Arthritis Rheum* 2010; 62: 1349-1360.
117. van Buul GM, Villafuertes E, Bos PK, Waarsing JH, Kops N, Narcisi R, et al. Mesenchymal stem cells secrete factors that inhibit inflammatory processes in short-term osteoarthritic synovium and cartilage explant culture. *Osteoarthritis Cartilage* 2012; 20: 1186-1196.
118. Xu L, Wang Q, Xu F, Ye Z, Zhou Y, Tan WS. Mesenchymal stem cells downregulate articular chondrocyte differentiation in noncontact coculture systems: implications in cartilage tissue regeneration. *Stem Cells Dev* 2013; 22: 1657-1669.
119. Cooper GM. *Cell Proliferation in Development and Differentiation*. 2000.
120. Hubbard EJA, Greenstein D. *Introduction to the germ line*. 2005.
121. De Bari C, Dell'Accio F. Mesenchymal stem cells in rheumatology: a regenerative approach to joint repair. *Clinical Science* 2007; 113: 339-348.
122. Deans RJ, Moseley AB. Mesenchymal stem cells: biology and potential clinical uses. *Experimental hematology* 2000; 28: 875-884.
123. Kessler MW, Ackerman G, Dines JS, Grande D. Emerging technologies and fourth generation issues in cartilage repair. *Sports Med Arthrosc* 2008; 16: 246-254.
124. Blanpain C, Lowry WE, Geoghegan A, Polak L, Fuchs E. Self-renewal, multipotency, and the existence of two cell populations within an epithelial stem cell niche. *Cell* 2004; 118: 635-648.
125. Sprio AE, Di Scipio F, Raimondo S, Salamone P, Pagliari F, Pagliari S, et al. Self-renewal and multipotency coexist in a long-term cultured adult rat dental pulp stem cell line: an exception to the rule? *Stem cells and development* 2012; 21: 3278-3288.
126. Hall BK. Earliest evidence of cartilage and bone development in embryonic life. *Clin Orthop Relat Res* 1987: 255-272.
127. von der Mark K, Conrad G. Cartilage cell differentiation: review. *Clinical orthopaedics and related research* 1979; 139: 185-205.
128. Bosnakovski D, Mizuno M, Kim G, Takagi S, Okumura M, Fujinaga T. Chondrogenic differentiation of bovine bone marrow mesenchymal stem cells (MSCs) in different hydrogels: influence of collagen type II extracellular matrix on MSC chondrogenesis. *Biotechnology and bioengineering* 2006; 93: 1152-1163.
129. Zhang L, Su P, Xu C, Yang J, Yu W, Huang D. Chondrogenic differentiation of human mesenchymal stem cells: a comparison between micromass and pellet culture systems. *Biotechnol Lett* 2010; 32: 1339-1346.
130. Watts AE, Ackerman-Yost JC, Nixon AJ. A Comparison of Three-Dimensional Culture Systems to Evaluate In Vitro Chondrogenesis of Equine Bone Marrow-Derived Mesenchymal Stem Cells. *Tissue Eng Part A* 2013; 19: 2275-2283.
131. Barberini DJ, Freitas NPP, Magnoni MS, Maia L, Listoni AJ, Heckler MC, et al. Equine mesenchymal stem cells from bone marrow, adipose tissue and umbilical cord:

- immunophenotypic characterization and differentiation potential. *Stem cell research & therapy* 2014; 5: 1.
132. Giovannini S, Brehm W, Mainil-Varlet P, Nestic D. Multilineage differentiation potential of equine blood-derived fibroblast-like cells. *Differentiation* 2008; 76: 118-129.
 133. Watts AE, Ackerman-Yost JC, Nixon AJ. A comparison of three-dimensional culture systems to evaluate in vitro chondrogenesis of equine bone marrow-derived mesenchymal stem cells. *Tissue Engineering Part A* 2013; 19: 2275-2283.
 134. Worster AA, Nixon AJ, Brower-Toland BD, Williams J. Effect of transforming growth factor β 1 on chondrogenic differentiation of cultured equine mesenchymal stem cells. *American journal of veterinary research* 2000; 61: 1003-1010.
 135. Jakobsen RB, Ostrup E, Zhang X, Mikkelsen TS, Brinchmann JE. Analysis of the effects of five factors relevant to in vitro chondrogenesis of human mesenchymal stem cells using factorial design and high throughput mRNA-profiling. *PLoS One* 2014; 9: e96615.
 136. Jones MV, Calabresi PA. Agar-gelatin for embedding tissues prior to paraffin processing. *Biotechniques* 2007; 42: 569.
 137. Jubb RW, Eggert FM. Staining of demineralized cartilage. II. Quantitation of articular cartilage proteoglycan after fixation and rapid demineralization. *Histochemistry* 1981; 73: 391-396.
 138. Kiviranta I, Jurvelin J, Tammi M, Saamanen AM, Helminen HJ. Microspectrophotometric quantitation of glycosaminoglycans in articular cartilage sections stained with Safranin O. *Histochemistry* 1985; 82: 249-255.
 139. Rosenberg L. Chemical basis for the histological use of safranin O in the study of articular cartilage. *J Bone Joint Surg Am* 1971; 53: 69-82.
 140. Mienaltowski MJ, Huang L, Bathke AC, Stromberg AJ, MacLeod JN. Transcriptional comparisons between equine articular repair tissue, neonatal cartilage, cultured chondrocytes and mesenchymal stromal cells. *Brief Funct Genomics* 2010; 9: 238-250.
 141. Bustin SA, Benes V, Garson J, Hellemans J, Huggett J, Kubista M, et al. The need for transparency and good practices in the qPCR literature. *Nature methods* 2013; 10: 1063-1067.
 142. Ramakers C, Ruijter JM, Deprez RHL, Moorman AF. Assumption-free analysis of quantitative real-time polymerase chain reaction (PCR) data. *Neuroscience letters* 2003; 339: 62-66.
 143. Livak KJ, Schmittgen TD. Analysis of relative gene expression data using real-time quantitative PCR and the 2- $\Delta\Delta$ CT method. *methods* 2001; 25: 402-408.
 144. Agathocleous M, Harris WA. Metabolism in physiological cell proliferation and differentiation. *Trends in cell biology* 2013; 23: 484-492.
 145. Ruijtenberg S, van den Heuvel S. Coordinating cell proliferation and differentiation: Antagonism between cell cycle regulators and cell type-specific gene expression. *Cell Cycle* 2016; 15: 196-212.
 146. Cote AJ, McLeod CM, Farrell MJ, McClanahan PD, Dunagin MC, Raj A, et al. Single-cell differences in matrix gene expression do not predict matrix deposition. *Nature communications* 2016; 7.
 147. Qu C, Puttonen KA, Lindeberg H, Ruponen M, Hovatta O, Koistinaho J, et al. Chondrogenic differentiation of human pluripotent stem cells in chondrocyte co-culture. *Int J Biochem Cell Biol* 2013; 45: 1802-1812.
 148. Adeniran-Catlett AE, Beguin E, Bozal FK, Murthy SK. Suspension-based differentiation of adult mesenchymal stem cells toward chondrogenic lineage. *Connect Tissue Res* 2016; 57: 466-475.

149. Coates EE, Fisher JP. Engineering Superficial Zone Chondrocytes from Mesenchymal Stem Cells. *Tissue Eng Part C Methods* 2014.
150. Wang SJ, Jiang D, Zhang ZZ, Huang AB, Qi YS, Wang HJ, et al. Chondrogenic Potential of Peripheral Blood Derived Mesenchymal Stem Cells Seeded on Demineralized Cancellous Bone Scaffolds. *Sci Rep* 2016; 6: 36400.
151. Pereira RC, Costa-Pinto AR, Frias AM, Neves NM, Azevedo HS, Reis RL. In vitro chondrogenic commitment of human Wharton's jelly stem cells by co-culture with human articular chondrocytes. *J Tissue Eng Regen Med* 2015.
152. Hendriks J, Riesle J, van Blitterswijk CA. Co-culture in cartilage tissue engineering. *J Tissue Eng Regen Med* 2007; 1: 170-178.
153. Nagata N, Yamanaka S. Perspectives for induced pluripotent stem cell technology: new insights into human physiology involved in somatic mosaicism. *Circ Res* 2014; 114: 505-510.
154. He S, Nakada D, Morrison SJ. Mechanisms of stem cell self-renewal. *Annu Rev Cell Dev Biol* 2009; 25: 377-406.
155. Frisbie DD, McCarthy HE, Archer CW, Barrett MF, McIlwraith CW. Evaluation of articular cartilage progenitor cells for the repair of articular defects in an equine model. *J Bone Joint Surg Am* 2015; 97: 484-493.
156. Jiang Y, Tuan RS. Origin and function of cartilage stem/progenitor cells in osteoarthritis. *Nat Rev Rheumatol* 2015; 11: 206-212.
157. Karlsson C, Lindahl A. Articular cartilage stem cell signalling. *Arthritis Res Ther* 2009; 11: 121.
158. Williams R, Khan IM, Richardson K, Nelson L, McCarthy HE, Anabalsi T, et al. Identification and clonal characterisation of a progenitor cell sub-population in normal human articular cartilage. *PLoS One* 2010; 5: e13246.
159. Tabata T, Takei Y. Morphogens, their identification and regulation. *Development* 2004; 131: 703-712.
160. Toh WS, Spector M, Lee EH, Cao T. Biomaterial-mediated delivery of microenvironmental cues for repair and regeneration of articular cartilage. *Molecular Pharmaceutics* 2011.
161. Yoon DM, Fisher JP. Chondrocyte signaling and artificial matrices for articular cartilage engineering. In: *Tissue Engineering*: Springer 2007:67-86.

VITA

Parvathy Thampi

Place of Birth: Kerala, India

EDUCATION

2011 – Present	Department of Veterinary Science, University of Kentucky Lexington, KY, USA
2011	M.V.Sc. (M.S.) – Veterinary Pathology, Centre of Excellence in Pathology, Kerala Veterinary and Animal Sciences University, Kerala, India
2009	B.V.Sc. – Veterinary Medicine, Kerala Agricultural University, Kerala, India

PROFESSIONAL POSITIONS

2011 – Present	Graduate Research Assistant, Department of Veterinary Science, University of Kentucky, Lexington, KY
2009 – 2011	Junior Research Fellow, Centre of Excellence in Pathology, Kerala Veterinary and Animal Sciences University, Kerala, India
2011	Visiting Graduate Student, Sree Chitra Tirunal Institute for Medical Sciences and Technology, Trivandrum, Kerala, India
2008 – 2009	Veterinary Intern, Animal Husbandry Department, Government of Kerala, India

SCHOLASTIC AND PROFESSIONAL HONORS

First place, 3 minute thesis presentation, Department of Veterinary Science, University
of Kentucky, 2016

Kentucky Opportunity Fellowship, 2014 and 2015

Lyman T. Johnson Academic Year Fellowship, 2011, 2012, and 2013

Dr. N. P. Panicker Memorial Award for highest GPA in M.V.Sc. program, 2012

First place, Oral presentation, South Zone Conference of Indian Association of Veterinary Pathologists (IAVP), Tamilnadu, India, 2011
Junior Research Fellowship, Kerala Veterinary and Animal Sciences University, 2009 and 2010

PROFESSIONAL PUBLICATIONS

Peer – reviewed journal articles

1. Thampi, P., Nair, D., Lalithakunjamma, R., Vijayan, N., Venugopal, S., and Ramachandra, U. Pathological effects of processed bovine pericardial scaffolds – a comparative in vivo evaluation. *Artif Organs*, 2013, 37(7):600-605

Manuscripts under preparation

1. Thampi, P., Liu, J., Zeng, Z., and MacLeod, J. N. Changes in the appendicular skeleton of axolotl salamanders during metamorphosis
2. Thampi, P., Ruspi, B., Wood, C.L., Janse, S., Roemmele, E., Janes, J.G., Adam, E.N., Lowney, R.S and MacLeod, J. N. Effect of skeletal paracrine signals on the proliferation and differentiation of equine interzone cells

Peer – reviewed abstracts

1. Thampi, P., Liu, J., Zeng, Z., and MacLeod, J. N. Determining cDNA sequences for targeted axolotl salamander genes using assembled RNA-seq reads. Plant and Animal Genome Conference, January, 2015, San Diego, CA. Abstract # 16316

Oral presentations

1. Thampi, P. 3 minute thesis presentation (First place), March, 2016, Department of Veterinary Science, University of Kentucky, Lexington, KY
2. Thampi, P. Leiomyosarcoma in hen. Oral presentation, South Zone Conference of Indian Association of Veterinary Pathologists (IAVP) and National Symposium on, “Pathobiology of Poultry and Laboratory Animal Diseases”, April, 2011, Veterinary College and Research Institute, Namakkal, India

Parvathy Thampi